Characterization of inflammatory bowel disease in transgenic mice

Dissertation

zur Erlangung des Doktorgrades
der Mathematisch-Naturwissenschaftlichen Fakultät
der Christian-Albrechts-Universität
zu Kiel

vorgelegt von

Nina Adam

Kiel, Mai 2010

Referent: Prof. Dr. Stefan Rose-John

Ko-Referent:

Tag der mündlichen Prüfung:

Table of contents

Abbreviations

A	adenine
Amp	ampicillin
aa	amino acid
AOM	azoxymethane
bp	basepair
BSA	bovine serum albumin
C	cytosine or celsius
CNTF	ciliary neurotrophic factor
cDNA	complementary DNA
cm	centimeter
cm^2	square centimeter
Da	dalton
DMSO	dimethl sulfoxide
DNA	desoxyribonucleic acid
dNTP	desoxynucleotide triphosphate
E.coli	*Escherichia coli*
FACS	fluorescence activated cell sorting
FCS	fetal calf serum
Fig	figure
G	guanine
g	gram or gravity
H_2SO_4	sulfuric acid
IgG	immunglobulin G
IL	interleukin
IL-6R	interleukin-6 receptor
JAK	janus kinase
LB_{amp}	LB medium with 50 µg/ml ampicillin
l	liter
LIF	leukemia-inhibitory factor
LIFR	LIF receptor
M	molar
m	murine
mA	milliampère
µg	microgram

µl	microliter
µM	micromolar
mg	milligram
ml	milliliter
mM	millimolar
min	minute
NaOH	sodium hydroxide
ng	nanogram
nm	nanometer
PE	phycoerythrin
PBS	phosphate buffered saline
PCR	polymerase chain reaction
pH	pH (potentia Hydrogenii)-value
P/S	penicillin/streptomycin
RNA	ribonucleic acid
RNase	ribonuclease
rpm	rounds per minute
RT	room temperature
SDS	sodium dodecyl sulfate
sec	second(s)
sIL-6R	soluble interleukin-6 receptor
sgp130Fc	soluble gp130Fc
T	thymine
Tab.	table
Taq	*Thermophilus aquaticus*
TEMED	N,N,N´,N´- tetramethylethylenediamine
T_M	primer-annealing temperature
TNF	tumor necrosis factor
Tris	tris-(Hydroxymethyl)-aminomethane
tRNA	transfer RNA
U	unit(s)
V	volt
v/v	volume per volume
w/v	weight per volume

1 Introduction

1.1 Interleukin-6 and the gp130 cytokine family

Cytokines are small soluble proteins, which are secreted by and act on a variety of different cell types. They are grouped into different families based on structural features. The Interleukin-6 family cytokines are characterized by four α-helices. They comprise of Interleukin-6 (IL-6), Interleukin-11 (IL-11), Interleukin-27 (IL-27), Interleukin-31 (IL-31), ciliary's neurotrophic factor (CNTF), leukemia inhibitory factor (LIF), oncostatin M (OSM), cardiotrophin-1 (CT-1), cardiotrophin-like cytokine (CLC) and neuropoietin (NPN) (Taga and Kishimoto 1997; Derouet et al. 2004; Dillon et al. 2004; Pflanz et al. 2004). IL-6 type cytokines bind to plasma membrane receptor complexes containing the common signal transducing protein gp130. gp130 as well as LIFR and OSMR are ß-receptors and activated through binding of their cytokine ligands. Some cytokines such as IL-6, IL-11, LIF, CLC or CNTF first bind to their specific α-receptor before binding to gp130 which finally activates the e.g. IL-6 specific signal. Signal transduction involves activation of JAK (Janus kinase) tyrosine kinase family members, leading to activation of STAT (signal tranducers and activators of transcription) transcription factors or activation of MAPK (mitogen-activated protein kinase) cascade. All cytokines of this family can activate target genes which are involved in differentiation, survival, apoptosis and proliferation, have pro- as well as anti-inflammatory properties and play major roles in hematopoiesis, acute phase response and immune responses of the organism (Heinrich et al. 2003).

The first identified cytokine of the Interleukin-6 family is IL-6 itself. It is a pleiotropic cytokine and was originally isolated as B cell differentiation factor (BSF-2) that induced final maturation of B cells into antibody producing cells (Hirano et al. 1985; Hirano et al. 1986). IL-6 plays a central role in differentiation and growth of different cell types as for example keratinocytes, macrophages, B cells, T cells or neuronal cells. Moreover, IL-6 induces expression of various acute phase response genes, acts as hepatocyte stimulating factor and is important for the maintenance of numerous inflammatory diseases such as Crohn's disease, Castleman's disease, osteoporosis, sepsis or rheumatoid arthritis (Naka et al. 2002).

1.2 Interleukin-6 signaling

On target cells IL-6 first binds to the Interleukin-6 receptor α (IL-6Rα). The complex of IL-6 and IL-6Rα associates with gp130 which dimerizes and initiates intracellular signaling (Fig. 1-1 A, Taga and Kishimoto 1997; Heinrich et al. 1998). Almost all cells express gp130, but IL-6Rα is only present on some cells including hepatocytes, neutrophils, monocytes, macrophages and T-lymphocytes. This so-called classic signaling pathway is activated during early inflammation as well as infection responses and leads to the expression of different acute-phase proteins. A soluble form of the IL-6R (sIL-6R) can be generated by differential splicing or proteolytic cleavage of membrane-anchored IL-6R by the metalloproteases A Disintegrin And Metalloprotease 10 (ADAM10) or ADAM17, also known as TNF-α converting enzyme (TACE, Lust et al. 1992; Rose-John and Heinrich 1994; Mullberg et al. 2000). sIL-6R together with IL-6 forms a complex which directly binds to gp130 and activates intracellular signaling (Fig. 1-1 B).

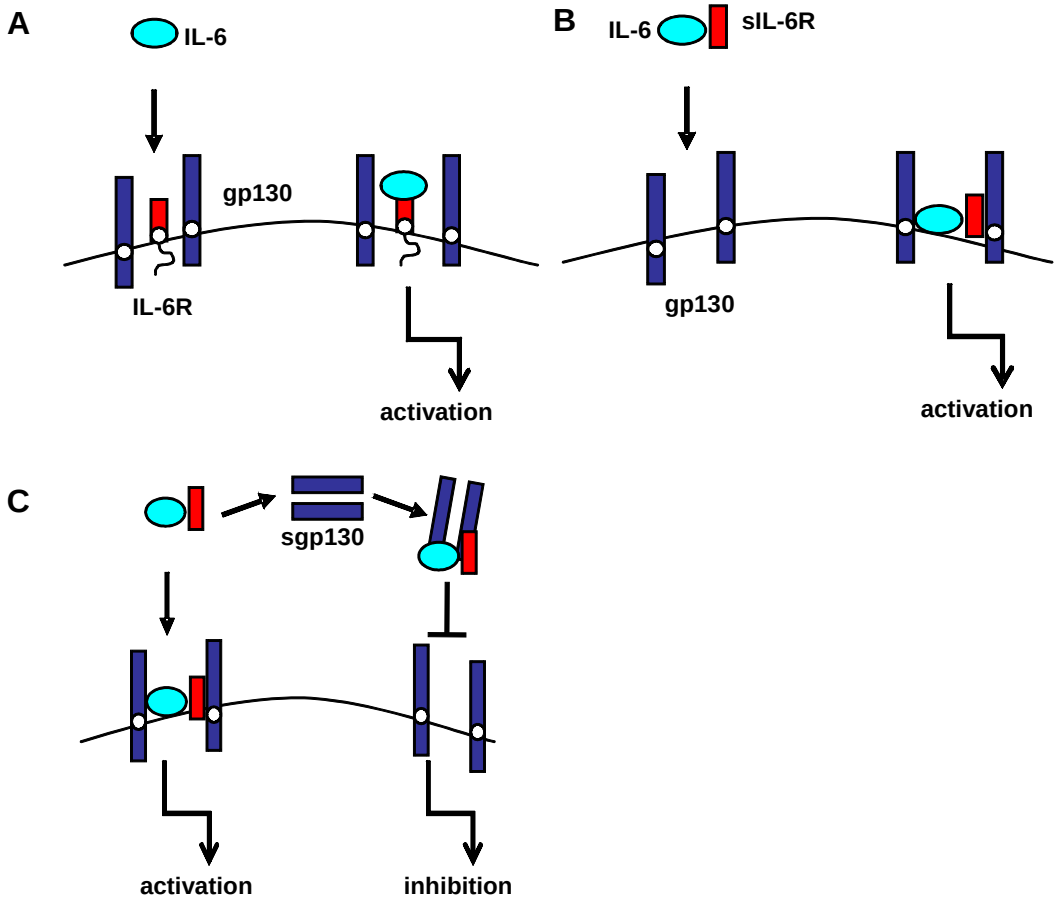

Fig. 1-1: The different IL-6 signaling pathways (A) Classic IL-6 signaling, (B) IL-6 trans-signaling, (C) Inhibition of IL-6 trans-signaling using sgp130. Modified from Scheller et al. 2006.

This pathway, termed trans-signaling, can stimulate cells which only express gp130 and lack the α-receptor. However, activity of the IL-6/sIL-6R complex is limited by the presence of a soluble form of gp130 (sgp130). Soluble gp130 can compete with membrane-bound gp130 for binding to IL-6/sIL-6R complex (Fig. 1-1 C). Therefore, sgp130 inhibits IL-6 trans-signaling but not the classical pathway (Muller-Newen et al. 1998; Jostock et al. 2001). IL-6 trans-signaling plays a key role in the pathophysiology of chronic inflammatory disorders and several types of cancer (Rose-John and Heinrich 1994; Peters et al. 1998; Mullberg et al. 2000).

In both pathways ligand-induced dimerization of gp130 leads to autophosphorylation of JAK kinases which stimulates the phosphorylation of five tyrosine residues of gp130. This subsequently induces recruitment of signaling proteins via SH2 domains, such as SHP2 (Src homology 2-containing tyrosine phosphatase) or STAT1 and STAT3 (signal transducers and activators of transcription 1 and 3). Upon phosphorylation, STAT1 or STAT3 dimerize and translocate into the nucleus to induce expression of IL-6 target genes. Alternatively, SHP-2 is phosphorylated and activates the Ras-Raf-MAPK signaling pathway via its interaction with the GRB2/SOS (Growth factor receptor-bound protein 2/Son of Sevenless) complex which finally induces expression of gp130 target genes (Holgado-Madruga et al. 1996; Schiemann et al. 1997; Gu et al. 1998).

IL-6 signaling is tightly regulated by different mechanisms: (i) Degradation of receptor-ligand complex via internalization and ubiquitin-proteasome pathway leads to cessation of signaling (Thiel et al. 1998). (ii) Dephosphorylation of cytokine receptors or JAKs by several protein tyrosine phosphatases (Irie-Sasaki et al. 2001) and (iii) binding of SOCS proteins to phosphorylated tyrosines of gp130 inhibit cytokine signaling (Nicholson et al. 1999; Schmitz et al. 2000).

1.3 The TNF-α converting enzyme TACE/ADAM17

Several membrane proteins are cleaved at the plasma membrane to release soluble ectodomains which have different functions (Blobel 2005; Murphy 2008; Pruessmeyer and Ludwig 2009). For example, membrane bound growth factors and cytokines are solubilized upon shedding. One very important sheddase family is the “A Disintegrin And Metalloprotease” or ADAM family. ADAMs are widely expressed in eukaryotes with 38 family members in humans (Edwards et al. 2008). They are characterized by presence of a metalloprotease, a disintegrin, a cysteine-rich, an

EGF-like, a transmembrane and a cytoplasmic domain. TACE (TNF-α converting enzyme), also termed ADAM17, is a member of this family and was discovered in 1997 as sheddase which cleaves the pro-inflammatory cytokine tumor necrosis-factor α (TNF-α, Black et al. 1997; Moss et al. 1997). Moreover, ADAM17 is involved in shedding of IL-6R, L-selectin and ligands ot the EGFR (see Fig. 1-2, Peschon et al. 1998; Horiuchi et al. 2005; Sahin and Blobel 2007).

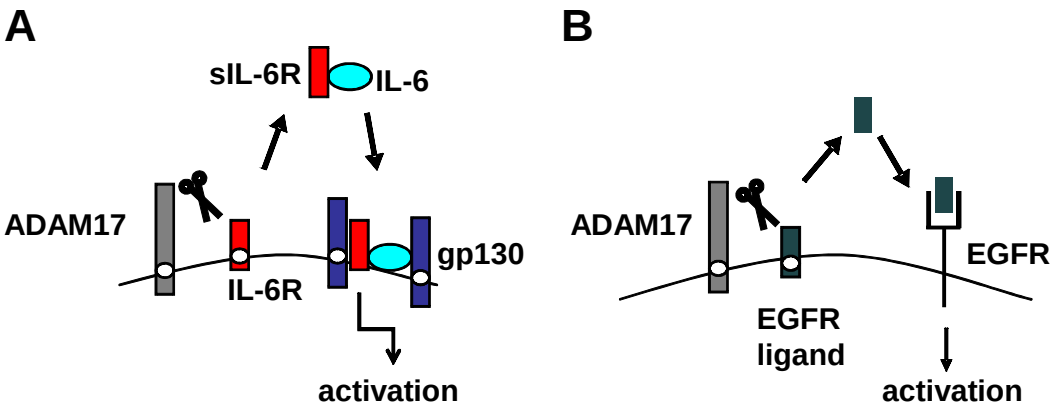

Fig. 1-2: ADAM17 mediated shedding (A) Shedding of IL-6R. (B) Shedding of EGFR ligands. Modified from Jones et al. 2005 and Blobel 2005.

However, complete analysis of the *in vivo* function of ADAM17 has been hampered by the fact that ADAM17 knock-out (KO) mice are not viable (Peschon et al. 1998). Their phenotype is reminiscent to that of mice lacking TGF-α. These mice have open eyelids, curly vibrissae, and dense, irregular pigmentation patterns of pelage hair. Since TGF-α is a ligand of EGFR and is released from the cell surface by ADAM17, it seems that ectodomain shedding is important for EGFR signaling (Peschon et al. 1998).

Due to lethality of complete knock-out, conditional ADAM17 knock-out mice have been generated which allow the analysis of the *in vivo* function of ADAM17.

For example, ADAM17$^{flox/flox}$/Mx1-Cre mice allow the excision of a floxed exon by intraperitoneal injection of Polyinosinic-Polycytidylic Acid (pIpC). pIpC-induced recombination occurs in various organs with different efficiency with almost complete recombination in bone marrow, liver and spleen. ADAM17$^{flox/flox}$/Mx1-Cre mice were tested in the murine model for endotoxin shock which can be induced by LPS and is dependent on soluble TNF-α. These mice showed a strong protection from endotoxin-induced lethality with lower levels of TNF-α in serum compared to wildtype (wt) mice. To further narrow the cell type in which ADAM17 is required for endotoxin shock, ADAM17$^{flox/flox}$/LysM-Cre mice were generated to inactivate ADAM17 only in

myeloid cells since these cells are critical for LPS-induced shock. ADAM17$^{flox/flox}$/LysM-Cre mice were subjected to LPS and showed a protection to endotoxin shock. These findings verified that ADAM17 is a principle enzyme responsible for shedding of TNF-α from myeloid cells during endotoxin shock (Horiuchi et al. 2007).

Furthermore, conditional ADAM17-deficient mice in which a Cre recombinase is under the control of the Sox-9 promoter were generated. Sox-9 is an essential transcription factor for skeletal development and is expressed in chondrogenic cells as well as in pancreas, heart, lung, brain and skin, but not in hematopoietic cells. ADAM17$^{flox/flox}$/Sox-9-Cre mice have defects in bone metabolism, hematopoiesis, skin development, growth and fertility (Horiuchi et al. 2009). This study showed that ADAM17 is involved in bone metabolism and hematopoiesis.

In another approach, mice with ADAM17 deficiency in all leukocytes have been used (Long et al. 2010). Analysis of shedding in these mice revealed that release of TNF-alpha, $TNFR_I$ and $TNFR_{II}$ as well as L-selectin is impaired. Moreover, these ADAM17-deficient mice were protected from *E.coli* induced peritonitis by having reduced systemic pro-inflammatory cytokine levels and bacterial burden as compared to wildtype mice (Long et al. 2010).

In addition, conditional ADAM17 knock-out mice were also generated in endothelial cells or smooth muscle cells. Therefore, floxed ADAM17 was removed by Tie2-Cre in endothelial cells or by smooth muscle (sm) Cre in smooth muscle cells and pericytes. These conditional ADAM17 knock-out mice showed no developmental defects. However, pathological neovascularization and growth of heterotopically injected tumor cells was reduced in ADAM17$^{flox/flox}$/Tie2-Cre, but not in ADAM17$^{flox/flox}$/sm-Cre mice. Furthermore, a lack of ADAM17 in endothelial cells decreased *ex vivo* chord formation which was restored by addition of the ADAM17 substrate HB-EGF (heparin-binding epidermal growth factor-like growth factor). These results show that ADAM17 is involved in pathological neovascularization *in vivo* (Weskamp et al. 2010).

All of the conditional ADAM17 knock-out mice described above provide insights into the *in vivo* function of ADAM17, however the analyses were restricted to a single tissue. In contrast, a mouse strain carrying a natural deletion of ADAM17 was discovered recently. This strain, called wave with open eyelid (woe) mouse, has various defects as for example wavy fur, open eyelids at birth as well as an enlarged

heart and oesophagus. It was shown that the ADAM17 gene is mutated leading to an aberrant ADAM17 splicing, diminished ADAM17 protein expression and, thereby, to a reduced shedding of ADAM17 substrates. Therefore, this strain provides an opportunity for studying the role of ADAM17 throughout postnatal development and homeostasis (Hassemer et al. 2010).

In our group hypomorphic ADAM17 knock-out mice in all tissues were generated using a novel strategy named exon induced translational stop (EXITS). This strategy was based upon the usage of a new exon between exon11 and 12 of the murine ADAM17 gene. The targeting vector contained exon11 of ADAM17 flanked by two loxP sites. Within the exon11 a cryptic donor and acceptor splice site was inserted which generate an additional, artificial exon11a. Alternative use of the artificial exon11a leads to premature disruption of ADAM17 protein translation due to the in-frame stop codon in exon11a (see Fig. 1-3) and reduction of ADAM17 protein to five to ten percent of wildtype level.

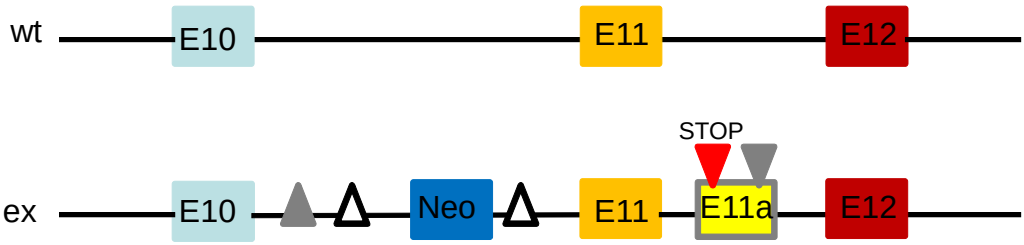

Fig.1-3: Strategy for generation of conditional ADAM17 knock-out mice. Mice were generated using exon induced translational stop codon (EXITS). A new exon (E11a) was inserted between exon 11 and 12 which started with an in-frame translational stop-codon. About 95% of the ADAM17 mRNA contained the new exon. Closed triangle: loxP sites, open triangle: FLP recombinase sites. Neo: neomycin resistance cassette.

The hypomorphic ADAM17$^{ex/ex}$ mice are viable and show eye, heart and skin defects as well as compromised shedding of different ADAM17 substrates (Chalaris et al. accepted). Although ADAM17 is known to be involved in inflammation and cancer, there is still less comprehensive understanding of its exact function and, therefore, hypomorphic ADAM17$^{ex/ex}$ mice represent an informative model to study the *in vivo* function of ADAM17 in all tissues.

1.4 Inflammatory bowel disease

Inflammatory bowel diseases (IBD), such as Crohn's disease and ulcerative colitis, are characterized by chronic inflammation of the intestinal tissue and by subsequent progressive destruction of mucosal integrity (Auernhammer et al. 2005). IBD mainly develops between the second to fourth decade of life (Cho and Weaver 2007).

Patients typically suffer from frequent and chronically relapsing flares resulting in diarrhea, abdominal pain, rectal bleeding and malnutrition (Cho and Weaver 2007). Crohn's disease occurs commonly in the ileum, but can also affect the whole gut, whereas ulcerative colitis always involves the rectum (Podolsky 2002). The pathogenesis of IBD is complex. Genetic, immunological and environmental factors are involved (Cho and Weaver 2007). Genome-wide screens led to the identification of genes that contribute to disease susceptibility. Alterations in genes of the immune system such as NOD2, IL-23R and ATG16L1 are specific to patients with Crohn's disease, but are not observed in those with ulcerative colitis (Hugot et al. 2001; Ogura et al. 2001; Hampe et al. 2002). NOD2 polymorphisms were the first definitive risk factors identified for Crohn's disease (Hugot et al. 2001). NOD2 is a pattern recognition receptor and functions as an intracellular sensor for bacterial peptidoglycan. The polymorphisms of NOD2 led to a dysregulated host response to luminal bacteria. Accordingly, the discovery of the association of NOD2 polymorphism with susceptibility to Crohn's disease supported the hypothesis that Crohn's disease results from a genetically dysregulated host response to luminal bacteria (Cho and Weaver 2007). Furthermore, a nonsynonymous single nucleotide polymorphism (SNP) in ATG16L1 gene was discovered which is also associated with the increased risk for Crohn's disease (Hampe et al. 2007). Mutations affecting autophagy factors, which are involved in restricting microbial growth within the host tissue (Amano et al. 2006), resulted in reduced pathogen clearance and more intracellular growth of bacterial pathogens (Xavier and Podolsky 2007). SNPs were also found in genes responsible for ulcerative colitis including STAT3 or XBP1 (Franke et al. 2008; Kaser et al. 2008).

Furthermore, many inflammatory mediators, such as chemokines and cytokines, are dysregulated. Patients suffering from Crohn's disease displayed increased IL-6 levels in the serum (Mitsuyama et al. 1991) as well as elevated sIL-6R levels (Mitsuyama et al. 1995). Soluble IL-6R is released by neutrophils and macrophages through shedding of IL-6R from the cell surface. This mechanism is induced by either apoptosis (Rose-John and Heinrich 1994), acute phase protein CRP in macrophages (Jones et al. 1999), by bacterial toxin (Walev et al. 1996) or by microbial metalloproteinases in human monocytes (Vollmer et al. 1996). Thereby, IL-6 can bind to sIL-6R to form the IL-6/sIL-6R complex. As T cells which are also activated during Crohn's disease (Rose-John et al. 2009) express membrane bound gp130, the IL-6/sIL-6R complex can bind to gp130 to activate the expression and nuclear

translocation of STAT3. Thus, anti-apoptotic genes are expressed which leads to an increased resistance to apoptosis and a perpetuation of intestinal inflammation (see Fig. 1-4).

Latest studies have underlined the importance of STAT3 in intestinal inflammation. Mice deficient in STAT3 develop only mild colitis (Alonzi et al. 2004), whereas disease was more severe in mice with a hyperactivated form of STAT3 (Jenkins et al. 2005). Furthermore, Samp1/YIT mice which develop spontaneous intestinal inflammation showed a strong expression of phosphorylated STAT3 during course of colitis (Mitsuyama et al. 2006). This indicates a crucial role of STAT3 in the development of intestinal inflammation.

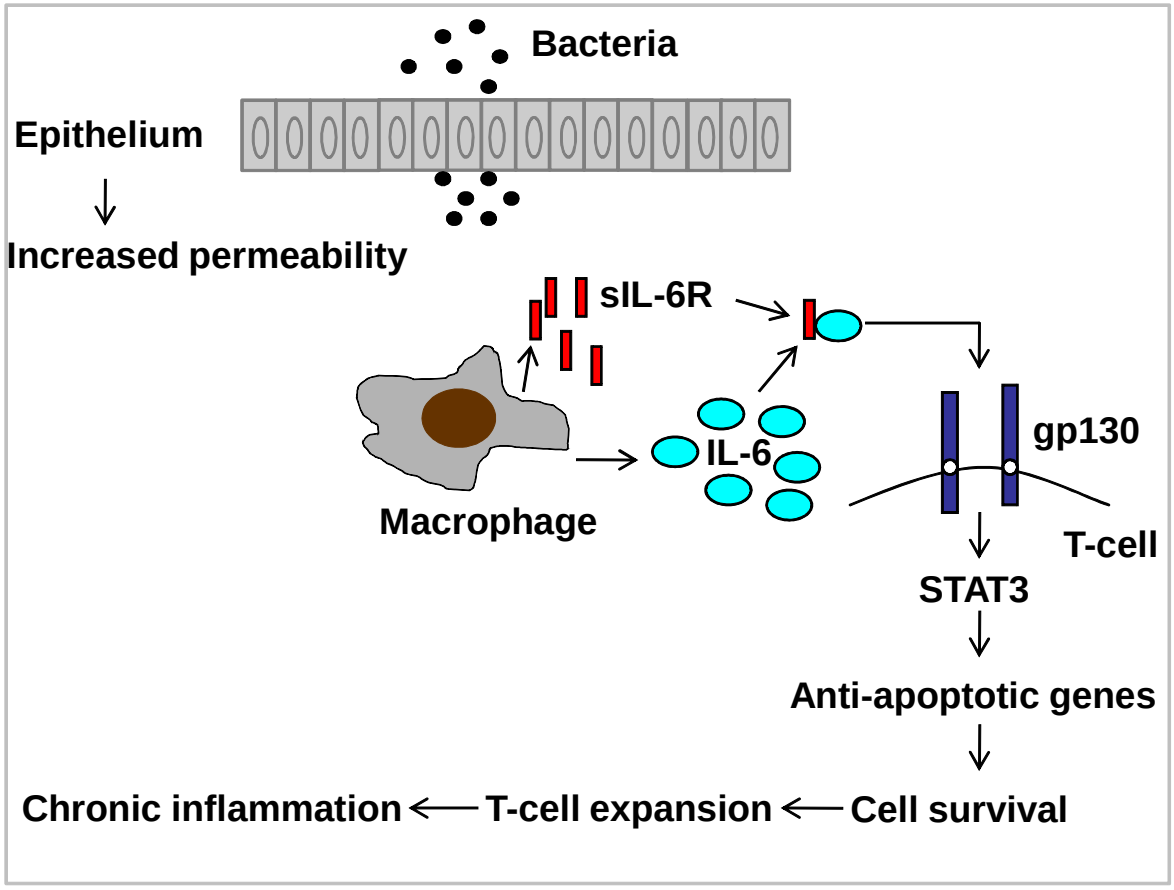

Fig. 1-4: Schematic model of IL-6 trans-signaling in inflammatory bowel diesease. Modified from Atraya and Neurath, 2005 and Rose-John et al., 2009.

In several other published studies the functional role of IL-6 and STAT3 in inflammation associated colon cancer was analyzed (Bollrath et al. 2009; Grivennikov et al. 2009; Matsumoto et al. 2010).

Grivennikov et al. reported that IL-6 knockout mice develop less tumors, but display a higher inflammatory score than wildtype animals. IL-6 knock-out mice had increased apoptosis and less cellular proliferation. The group of Bollrath *et al.* showed that a

genetic hyperactivation of STAT3 leads to an increased tumor incidence together with a resistance to colitis. Both groups could verify that the severity of inflammation was dramatically increased in mice with a deletion of STAT3 in intestinal epithelial cells. Furthermore, STAT3 activation is increased during colitis associated premalignant cancer (CApC) or chronic colitis (CC) in Balb/c mice (Matsumoto et al. 2010).

From these studies two different functions for IL-6 are obvious. On the one hand, IL-6 in complex with sIL-6R is responsible for the apoptotic resistance of T cells which leads to the progression of the disease. On the other hand, IL-6 together with membrane bound IL-6R plays a role in the regenerative response of intestinal epithelial cells to cellular damage.

Since IL-6 trans-signaling seems to be involved in progression of IBD, it was elucidated if the disease can be ameliorated by blocking IL-6 trans-signaling alone. In a TNBS-induced colitis model, IL-6 as well as IL-6/sIL-6R complex was blocked by using anti-IL-6R antibody, whereas injection of recombinant sgp130Fc interfered with IL-6 trans-signaling. It was shown that inflammation was decreased compared to control mice (Atreya et al. 2000). Mice treated with antil-IL6R antibody showed less weight loss than untreated mice and normal colon architecture. Furthermore, the colitis score indicated that mice treated with sgp130Fc or anti-IL-6R antibody displayed less inflammation than control mice. Interestingly, treatment of patients with Crohn’s disease using anti-IL-6R antibody successfully prevented and treated inflammation (Ito 2005).

1.5 Mouse models of intestinal inflammation

Animal models of intestinal inflammation are indispensable for the understanding of inflammatory bowel disease. The most widely used chemically induced models of intestinal inflammation are trinitro benzene sulfonic acid (TNBS), oxazolone or dextran sodium sulfate (DSS) colitis (Wirtz et al. 2007). TNBS as well as oxazolone are haptenating substances in ethanol and are given intrarectal to different susceptible strains. Ethanol breaks the mucosal barrier integrity, whereas TNBS and oxazolone induce a T cell mediated response against hapten-modified autologous proteins or luminal antigens. Contrary, DSS is applied in drinking water of mice and induces an acute colitis characterized by bloody diarrhea, ulcerations and infiltrations with granulocytes (Okayasu et al. 1990). DSS is directly toxic to gut epithelial cells of

the basal crypts and, therefore, affects the integrity of the mucosal barrier (Wirtz et al. 2007). As T and B cell deficient mice also develop severe intestinal inflammation after DSS administration, the adaptive immune system is not involved in this model (Dieleman et al. 1994). Hence, the DSS-induced colitis model is useful to study the contribution of innate immune mechanisms to colitis.

1.6 Aim of the work

The metalloprotease ADAM17 is responsible for limited proteolysis of more than 40 substrates (Pruessmeyer and Ludwig 2009) and known to be involved in different inflammatory disorders. Since conditional ADAM17 knock-out mice only show the consequence of its ablation in a single tissue, transgenic mice with dramatically reduced ADAM17 levels in all cells were generated in our group (Chalaris et al. accepted). These mice completely lost the ability to shed L-selectin, TNF- R_{II} and TNF-α from the cell surface. Are these transgenic mice protected from excessive inflammatory responses and, therefore, from IBD?

To elucidate this issue the inflammatory response in ADAM17$^{ex/ex}$ mice was analyzed using a DSS-colitis model.

Furthermore, other signaling pathways such as IL-6 trans-signaling are involved in inflammatory disorders e.g. IBD. Blocking this pathway with sgp130Fc as well as anti-IL-6R antibody showed reduced levels of inflammation in a TNBS-induced colitis model (Atreya et al. 2000). Surprisingly, IL-6 knock-out mice were highly inflamed after DSS-induced colitis (Grivennikov et al. 2009). Hence, it was interesting to analyze if C57BL/6N mice treated with sgp130Fc and anti-IL-6 antibody are protected from IBD in a DSS-induced colitis model.

Therefore, specific goals of this thesis were:
(i) to establish DSS-colitis model;
(ii) to monitor the specific intensity of inflammatory response to colitis in ADAM17 $^{ex/ex}$ mice as well as mice injected with sgp130Fc and anti-IL-6 antibody using several physiological parameters including weight loss, rectal bleeding, colonoscopy, tissue integrity as well as permeability, cellular proliferation, monitoring of cytokine as well as MPO levels and immigration of inflammatory cells.

2 Results

2.1 ADAM17$^{ex/ex}$ mice are highly susceptible to DSS-induced colitis

The metalloprotease ADAM17 is responsible for shedding of TNF-α, L-selectin as well as EGFR ligands. Hypomorphic ADAM17$^{ex/ex}$ mice were generated using the new EXITS strategy (see 1.3). The usage of the new exon E11a which contains a premature stop codon between exon 11 and exon 12 of the murine ADAM17 gene was tested in brain and liver tissue by RT-PCR (see Fig. 2-1 A, B). In wildtype mice a single band of 380bp was detected, whereas heterozygous ADAM17$^{wt/ex}$ mice showed an additional band of 550bp due to insertion of the new exon. In homozygous ADAM17$^{ex/ex}$ mice only the 550bp band could be detected. Interestingly, approximately 95% of all ADAM17 transcripts contain the modified exon E11a.

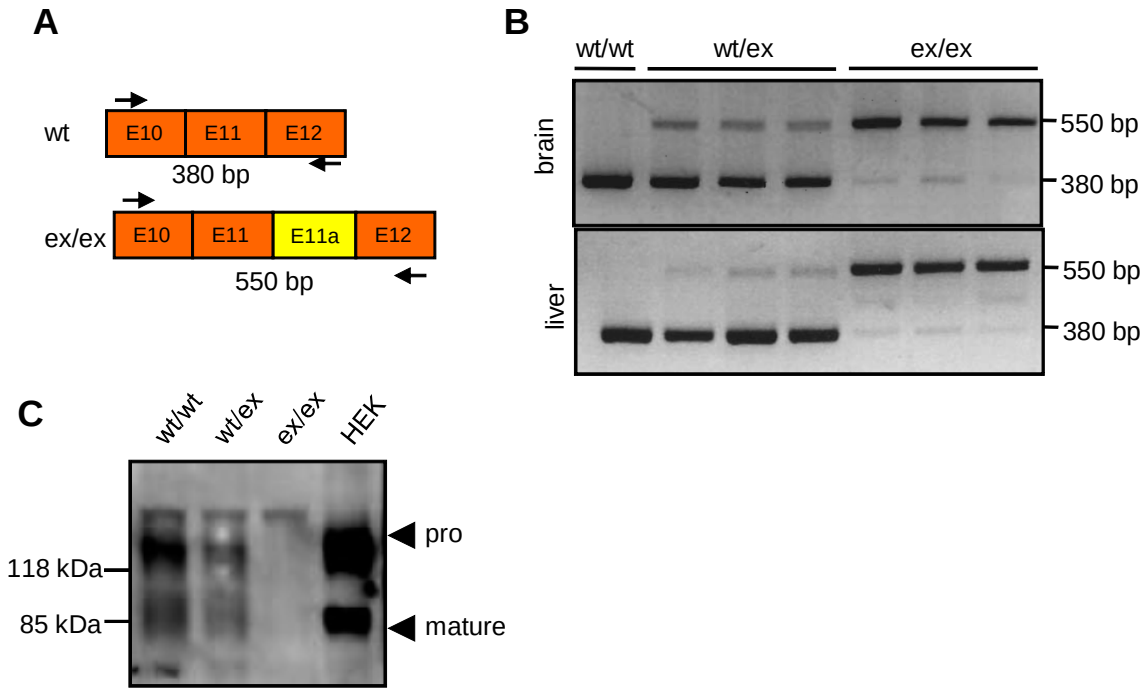

Fig. 2-1: Generation of hypomorphic ADAM17$^{ex/ex}$ mice. (A) RT-PCR analysis was performed with primers for exon10 (E10) and exon12 (E12) of the ADAM17 gene. (B) mRNA from brain and liver tissue was isolated and analyzed by RT-PCR. The 380bp wildtype fragment was detected in wildtype and heterozygous brain and liver samples, whereas the 550bp transcript containing the new exon (E11a) was only detectable in heterozygous and homozygous tissue samples. (C) ADAM17 Western blot of membrane fractions of mouse embryonic fibroblasts (MEFs). ADAM17 expression was detectable in wt and ADAM17$^{wt/ex}$ MEFs, but was absent in ADAM17$^{ex/ex}$ MEFs. HEK cells were used as positive control.

Furthermore, expression of ADAM17 in cell lysates of mouse embryonic fibroblasts (MEFs) was analyzed. No ADAM17 protein was detectable in MEFs from ADAM17$^{ex/ex}$ mice, whereas MEFs from wildtype and heterozygous ADAM17 mice expressed both the pro- as well as the mature form of ADAM17 (see Fig. 2-1 C).

ADAM17 protein expression was also undetectable in other tissues, whereas mRNA expression of ADAM17 was unchanged (data not shown). These results indicate that viable mice with undetectable levels of ADAM17 protein in all tissues were generated successfully.

Homozygous ADAM17$^{ex/ex}$ mice developed eye, heart and skin defects which represents the TGF-α knock-out mice phenotype. Furthermore, the release of known substrates of ADAM17 (Black et al. 1997; Moss et al. 1997) was analyzed. Therefore, splenic B cells were isolated from ADAM17$^{ex/ex}$, ADAM17$^{wt/ex}$ as well as wildtype mice and stimulated with the phorbol ester PMA which induces shedding of ADAM17 substrates (Arribas et al. 1996; Matthews et al. 2003). Wildtype and heterozygous ADAM17$^{wt/ex}$ mice showed a dramatic loss of L-selectin from the cell surface, whereas homozygous mice had the same L-selectin expression level before and after treatment with PMA (see Fig. 2-2 A).

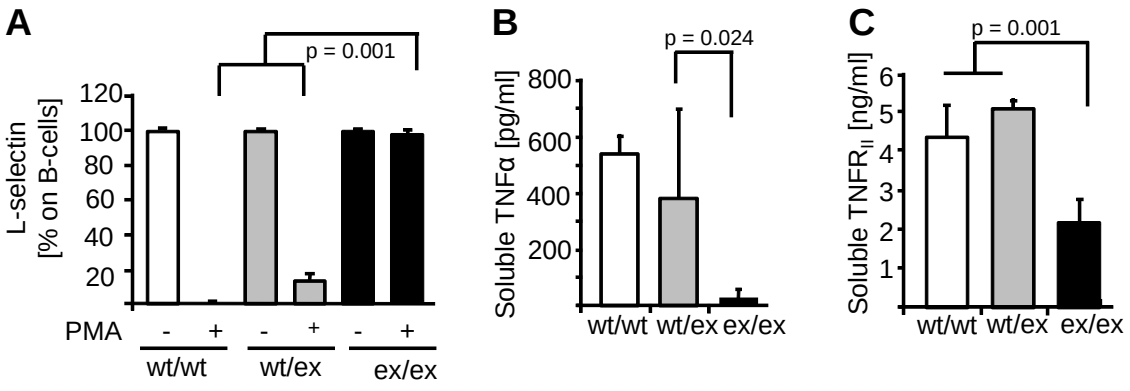

Fig. 2-2: Functional characterization of ADAM17$^{ex/ex}$ mice. (A) Isolated splenic B cells from wt (n=2), ADAM17$^{wt/ex}$ (n=3) and ADAM17$^{ex/ex}$ (n=4) mice were stimulated with PMA (100nM). Cells were double stained with anti-L-selectin and anti-B220 mAbs and analyzed by flow cytometry. Shedding of L-selectin was impaired in B cells derived from ADAM17$^{ex/ex}$ mice. (B and C) Isolated splenocytes from wildtype (n=2), ADAM17$^{wt/ex}$ (n=3) and ADAM17$^{ex/ex}$ (n=6) were stimulated with LPS. Supernatant was collected and TNF-α as well as $TNFR_{II}$ levels were determined by ELISA. Shedding of TNF-α and $TNFR_{II}$ was impaired in splenocytes from ADAM17$^{ex/ex}$ mice.

Furthermore, shedding of TNF-α as well as TNF-R_{II} was analyzed in splenocytes isolated from wildtype, heterozygous ADAM17$^{wt/ex}$ or homozygous ADAM17$^{ex/ex}$ mice after stimulation with lipopolysaccharide (LPS). LPS can also induce shedding of different ADAM17 substrates (Mullberg et al. 1995). As shown on Fig. 2-2 B, splenocytes from wt and heterozygous ADAM17$^{wt/ex}$ mice generated similar amounts of soluble TNF-α after LPS stimulation, whereas homozygous ADAM17$^{ex/ex}$ mice produced no soluble TNF-α. Same results were obtained for soluble $TNFR_{II}$ (see Fig.

2-2 C). Taken together, shedding of L-selectin, TNF-α and $TNFR_{II}$ is impaired in $ADAM17^{ex/ex}$ mice.

TNF-α is a pro-inflammatory cytokine and implicated in many diseases such as Crohn's disease or rheumatoid arthritis (Black et al. 1997, Moss et al. 1997). Moreover, EGFR ligands are known to be involved in STAT3 dependent cell proliferation (Sanderson et al. 2006). As these proteins are substrates of ADAM17, it was interesting to analyze if $ADAM17^{ex/ex}$ mice are resistant or more susceptible to DSS-induced colitis.

$ADAM17^{ex/ex}$ mice as well as heterozygous ADAM17 and wildtype mice were treated with 2% DSS in the drinking water for five days followed by five days of water. Disease severity was monitored daily by weight progression, hemoccult test and stool consistency. A group of six wildtype, seven heterozygous and eight homozygous animals were used. Interestingly, five of eight homozygous $ADAM17^{ex/ex}$ mice died during the DSS treatment and the residual animals lost about 20% of their weight (Fig. 2-3). In contrast to that, wildtype and heterozygous mice lost only little weight (5%) and all animals survived. Treated $ADAM17^{ex/ex}$ mice died mostly immediately after the DSS cycle showing that $ADAM17^{ex/ex}$ mice are highly susceptible to DSS-induced colitis (Fig. 2-3).

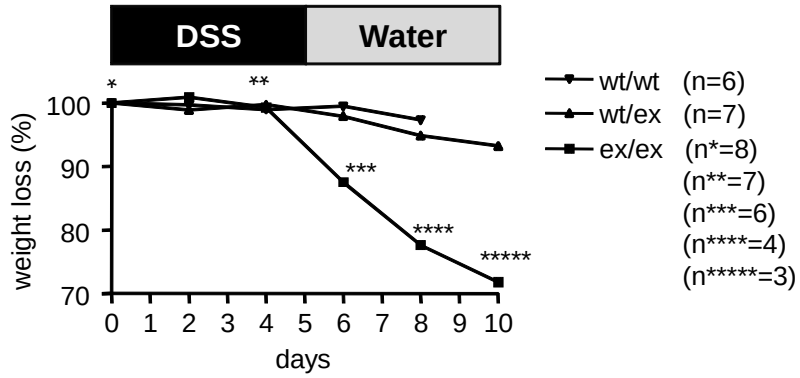

Fig. 2-3: Weight progression during DSS-induced colitis. 2% DSS was applied in drinking water for 5d followed by 5d of water. wt/wt: wildtype $ADAM17^{wt/wt}$ mice, wt/ex: heterozygous $ADAM17^{wt/ex}$ mice, ex/ex: homozygous $ADAM17^{ex/ex}$ mice. The numbers in brackets indicate the number of mice used for the experiment and asterisks show the number of remaining mice.

Disease severity was further assessed by colonoscopy. Under normal conditions, luminescence in the colon is maintained meaning other organs are still visible through the colon and mice are not vulnerable to contact bleeding. After DSS treatment the colons of wildtype and heterozygous mice showed normal architecture represented by maintained luminescence, absence of diarrhea and no bloody stool,

low hyperemia and no increased contact vulnerability. On the contrary, homozygous ADAM17$^{ex/ex}$ mice are highly inflamed as indicated by diarrhea, absence of luminescence, increased contact vulnerability, bloody stool and hyperemia (see Fig. 2-4 A). Thus, endoscopic score for ADAM17$^{ex/ex}$ mice is high, indicating strong inflammation (Fig. 2-4 B). Untreated animals were also examined to control colon architecture of wildtype, heterozygous and ADAM17$^{ex/ex}$ mice. Untreated mice showed no signs of inflammation as depicted in colonoscopy as well as in the endoscopic score.

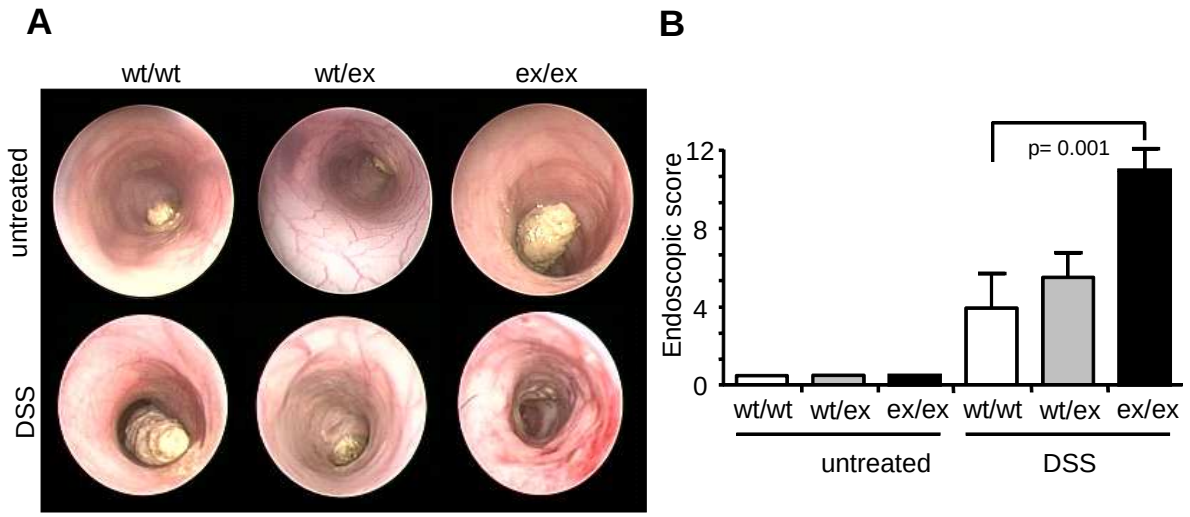

Fig. 2-4: Colonoscopy of untreated and treated wt, ADAM17$^{wt/ex}$ and ADAM17$^{ex/ex}$ mice. (A) Untreated mice are shown in the upper panel, treated mice in the lower panel. (B) Endoscopic score (MEICS) after DSS-treatment.

The Disease Activity Index (DAI) comprises of the combined score of rectal bleeding, weight loss and histology at day ten (see Fig. 2-5 A). As shown on Fig. 2-5 B, the DAI is significantly increased in ADAM17$^{ex/ex}$ mice compared to heterozygous or wildtype mice.

A

Score / Index	1	2	3
Bleeding	No bleeding	Detectable with HC test	visible
Weight loss	0-5%	5-10%	>10%
Histology	Epithelium lost, crypts intact	Partial crypt lost	Entire crypt lost

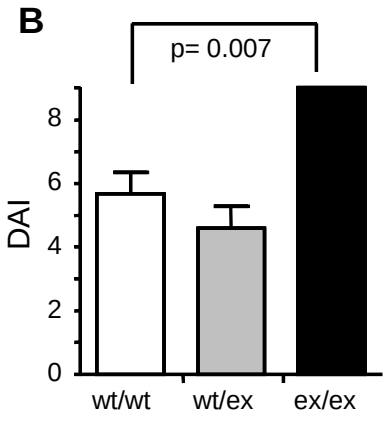

Fig. 2-5: DAI score after DSS-treatment. (A) Composition of DAI. (B) Index with values are shown as means ± SD.

Colon sections were immunostained with anti-ADAM17 antibody to localize ADAM17 protein in DSS-induced colitis. As shown on Fig. 2-6, ADAM17 protein was expressed in crypts of the colon of wildtype mice, but no expression was detected in ADAM17$^{ex/ex}$ mice.

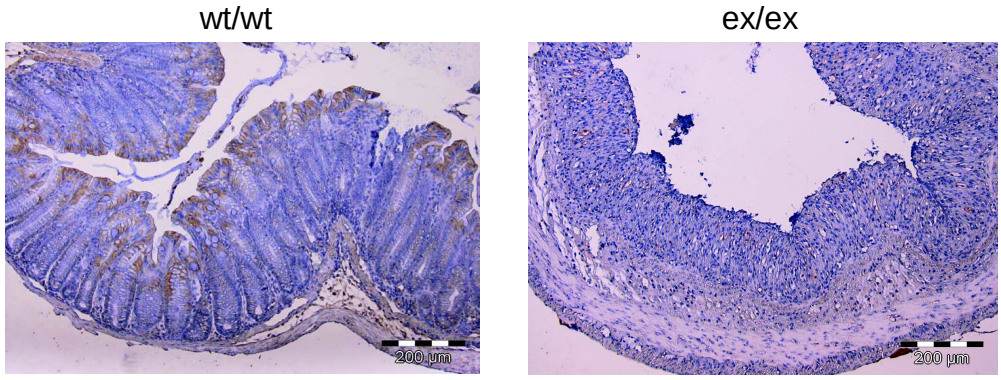

Fig. 2-6: ADAM17 protein expression in crypts of the colon of wt and ADAM17$^{ex/ex}$ mice. Colon sections were immunostained with anti-ADAM17 mAb labeled with peroxidase. Figure from Chalaris et al. accepted. Bars represent 200µm.

HE staining of the colon of mice treated with DSS revealed minor signs of inflammation in wt and heterozygous mice but strong signs in homozygous ADAM17 mice. In all three genotypes the epithelium was destroyed by DSS toxicity to gut epithelial cells. A clear difference was detected in the architecture of the crypts. In mildly inflamed mice like wt and heterozygous ADAM17 animals the crypts are almost intact. In highly inflamed ADAM17$^{ex/ex}$ mice the crypt structure was completely lost after day five and day ten (see Fig. 2-7). There are two possible causes why crypts are destroyed: (i) Apoptosis could be promoted or (ii) regenerative proliferation of epithelial cells might be impaired.

Interestingly, previous data point to the latter possibility as a similar damage was seen in mice with a targeted disruption of STAT3 in intestinal epithelial cells treated with AOM/DSS as reported recently (Bollrath et al. 2009; Grivennikov et al. 2009). This showed that STAT3 is important for survival and proliferation of intestinal epithelial cells (Bollrath et al. 2009).

To analyze the regenerative response of the gut epithelium during DSS-induced colitis, cell proliferation was measured via BrdU staining. Cells were labeled by intraperitoneal injection of BrdU two hours before sacrifice. As shown on Fig. 2-7, proliferating cells could only be detected in crypts of the gut of wildtype and heterozygous ADAM17 animals but not in ADAM17$^{ex/ex}$ mice. As mice lacking STAT3 fail to induce cell proliferation, the activation status of STAT3 in DSS treated mice

was examined. STAT3 is phosphorylated in wildtype and heterozygous mice, whereas no phoshorylated STAT3 could be detected in sections of ADAM17$^{ex/ex}$ mice (Fig. 2-7).

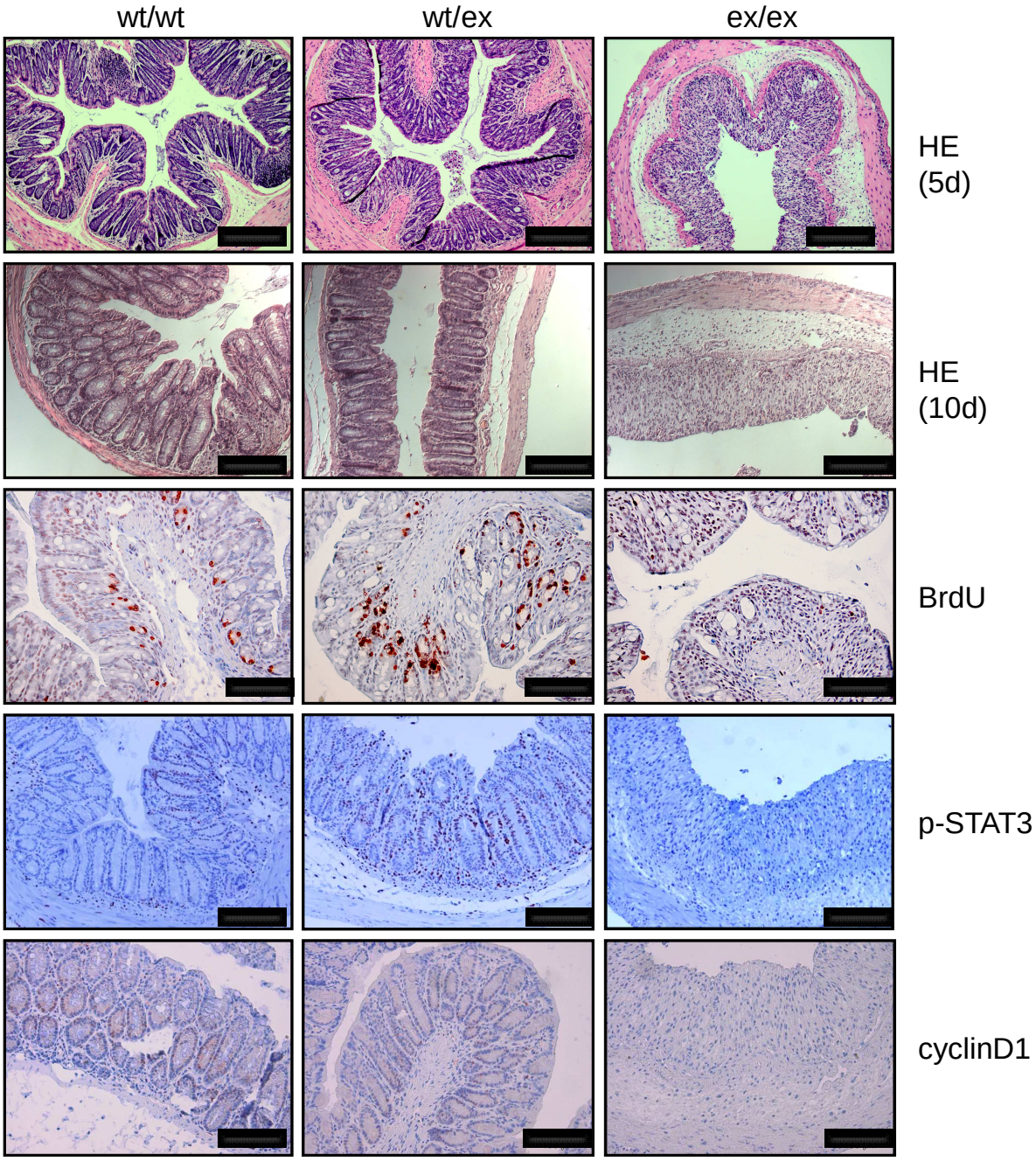

Fig. 2-7: Immunohistochemistry of the colon. HE (upper panels), BrdU (middle panels), pSTAT3 and cyclinD1 (lower panels) staining of colons from wt, ADAM17$^{wt/ex}$ and ADAM17$^{ex/ex}$ mice challenged for 5d and 10d with DSS. Scale bars denote 100µm.

The proliferative response was further analyzed by cyclinD1 expression in colon sections. CyclinD1 is a cell cycle regulator and activated in its early phase. ADAM17$^{ex/ex}$ mice showed no cyclinD1 expression in contrast to wildtype and heterozygous animals (Fig. 2-7). Taken together, these results indicate that the

regenerative response in ADAM17$^{ex/ex}$ mice is impaired due to inability to activate tyrosine kinase receptor (e.g. EGFR) mediated STAT signaling.

A coordinated regenerative response is required to maintain the intestinal barrier function. An impaired barrier integrity leads to fast and severe progression of the disease. Therefore, membrane integrity was measured by permeability for FITC-dextran (Yoshikawa et al. 1984). FITC-Dextran was administered by gavage four hours before sacrifice. Blood samples were collected and serum was analyzed for presence of FITC-Dextran. Indeed, upon DSS challenge, the intestinal barrier became permeable for FITC-Dextran in ADAM17$^{ex/ex}$ mice. FITC-Dextran levels in serum of ADAM17$^{ex/ex}$ mice were highly increased compared to wildtype and heterozygous mice (see Fig. 2-8 A). In unchallenged mice, no difference in permeability could be detected. Furthermore, MPO (marker for activated neutrophils, Breckwoldt et al. 2008) activity was measured in wildtype and ADAM17$^{wt/ex}$ mice (see Fig. 2-8 B). MPO is secreted by activated neutrophils and macrophages during inflammation and after phagocytosis of bacteria. A strong increase in MPO was detected in ADAM17$^{ex/ex}$ mice, whereas wildtype mice showed no MPO activity. Thus, these results indicate that the inflammation level was higher in homozygous ADAM17$^{ex/ex}$ than in wildtype mice.

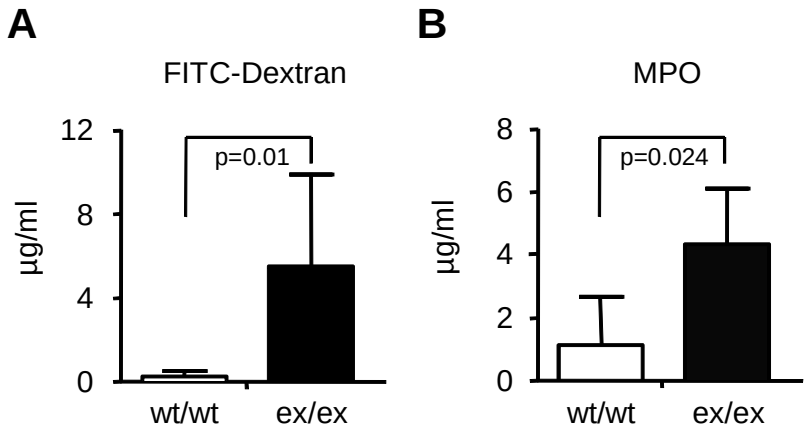

Fig. 2-8: Permeability and MPO levels in the colon of wt and ADAM17$^{ex/ex}$ mice. DSS colitis was induced as described. (A) Plasma FITC-dextran concentrations in wt (n=7) and ADAM17$^{ex/ex}$ (n=7) mice 4h after FITC-dextran administration. (B) MPO levels in the colon of ADAM17$^{ex/ex}$ mice (n=5) were increased compared to wt mice (n=4). Values are shown as means ± SD. Figure taken from Chalaris et al. accepted.

Moreover, secretion of different cytokines in colon organ cultures from DSS-treated animals was analyzed by ELISA. KC (keratinocyte chemoattractant protein) and MCP-1 (monocyte chemoattractant protein-1) are marker for activated neutrophils as well as macrophages and are released during inflammation (Luedde et al. 2002). The

levels of the inflammatory chemokines MCP-1 and KC were higher in ADAM17$^{ex/ex}$ mice compared to wt and ADAM17$^{wt/ex}$ mice (see Fig. 2-9 A, B). Furthermore, levels of the anti-inflammatory cytokine IL-10 and of the IL-6 related cytokine IL-11 were determined. Levels of both cytokines were increased in ADAM17$^{ex/ex}$ mice compared to wt and heterozygous mice (see Fig. 2-9 C, D).

Interestingly, levels of these chemo- and cytokines were also increased in DSS-challenged mice with a deletion of STAT3 in intestinal epithelial cells (Bollrath et al. 2009).

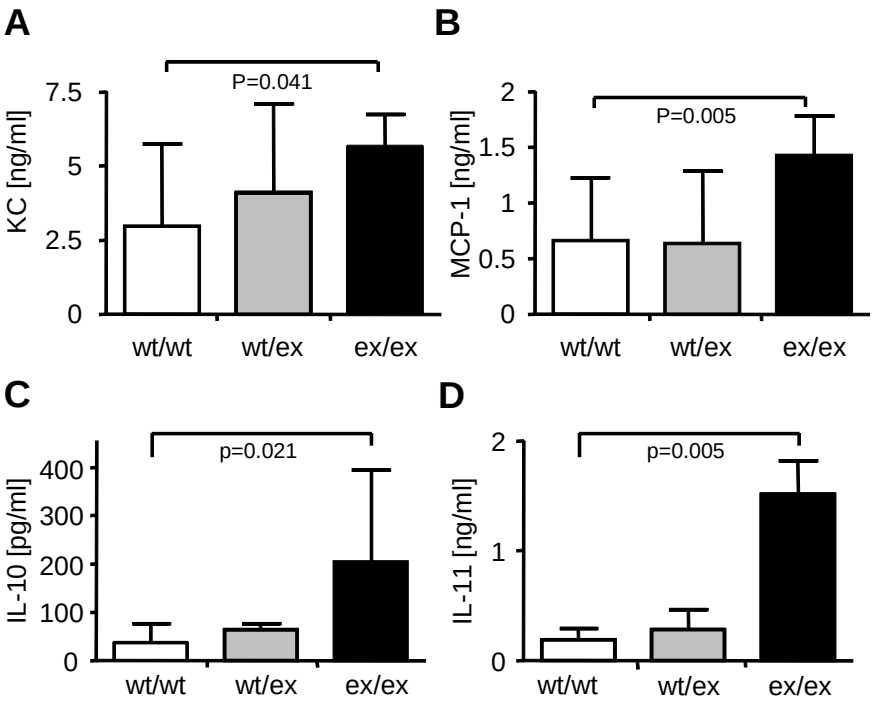

Fig. 2-9: Chemokine as well as anti-inflammatory cytokine levels in colon organ cultures. (A - D) Supernatants of colon organ cultures were assayed by ELISA for levels of the chemokines KC (A; day 10; wt/wt: n=10; wt/ex: n=5; ex/ex: n=6), MCP-1 (B; day 10; wt/wt: n=10; wt/ex: n=5; ex/ex: n=6) and of the cytokines IL-10 (C; day 10; wt/wt: n=10; wt/ex: n=5; ex/ex: n=6) and IL-11 (D; day 10; wt/wt: n=10; wt/ex: n=5; ex/ex: n=6). Values are shown as means ± SD.

Furthermore, the levels of the pro-inflammatory cytokine IFN-γ as well as of the cytokines IL-21, IL-12 and IL-17 showed slight tendency but were not significant (see Fig. 2-10).

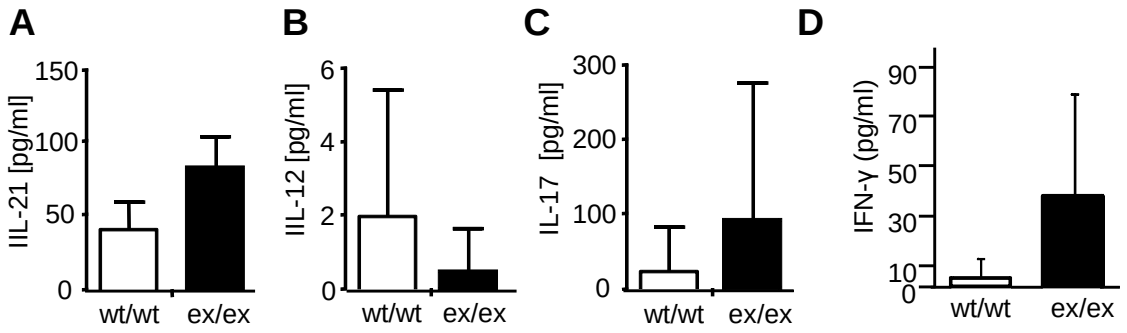

Fig. 2-10: Pro-inflammatory cytokine levels in colon organ cultures. (A - D) Supernatants of colon organ cultures were assayed by ELISA for levels of the cytokines IL-21 (A), IL-12 (B), IL-17 (C) and IFN-γ (D). Analysis was perfomed at day 10 with wt/wt: n=10; wt/ex: n=5; ex/ex: n=6. Values are shown as means ± SD.

Due to the strong inflammatory response, infiltration of different immune cells was measured. Anti-CD68 is a marker for infiltrating macrophages, whereas infiltrating T-lymphocytes can be detected by anti-CD3 antibody. As shown on Fig. 2-11 A, an increase of CD68 positive cells in intestinal tissue sections was detected in DSS-treated ADAM17$^{ex/ex}$ mice, whereas unchallenged mice exhibited no difference in CD68 positive cells. Nearly the same picture was seen in sections which were screened for CD3 positive cells. In the intestine of unchallenged mice the number of CD3 positive T cells was slightly different compared to negative control. ADAM17$^{ex/ex}$ mice treated with DSS, however, displayed a massive influx of CD3 positive T cells and macrophages (see Fig. 2-11 B).

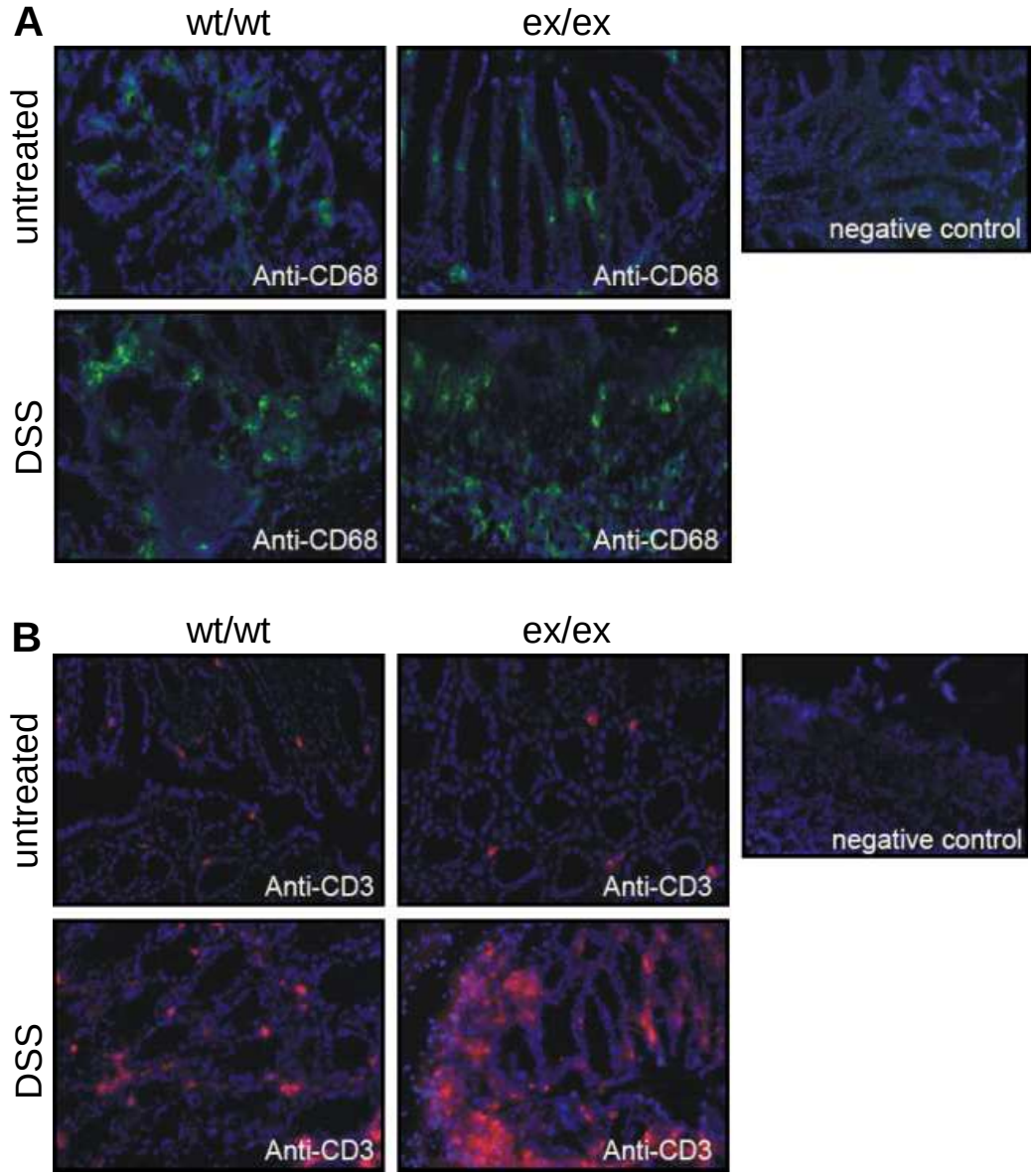

Fig. 2-11: Macrophages/Monocytes and CD3 positive T cells in intestinal tissue sections of DSS-treated ADAM17$^{wt/wt}$ or ADAM17$^{ex/ex}$ mice. (A) Colonic tissue sections of wt ADAM17 and ADAM17$^{ex/ex}$ mice stained with anti-CD68 antibody to obtain influx levels of macrophages/monocytes. (B) Colonic tissue sections of wt and ADAM17$^{ex/ex}$ mice stained with anti-CD3 antibody to visualize CD3 positive T cells.

All data suggest that activity of STAT3 which is involved in cell proliferation is impaired in ADAM17$^{ex/ex}$ mice and, therefore, leads to failure of intestinal epithelial cells to proliferate, but the role of apoptosis is still unknown. Since ADAM17$^{ex/ex}$ mice could not cleave and activate ligands of EGFR and EGFR signaling is known to be involved in STAT3 dependent cell proliferation (Sanderson et al. 2006), the influence of EGF or TGF was analyzed during DSS-induced colitis (see section 2.2).

2.2 Treatment of ADAM17$^{ex/ex}$ mice with EGFR ligands: Amelioration of disease?

The metalloprotease ADAM17 is involved in shedding of IL-6R, TNF-α, L-selectin and ligands of the EGFR (Peschon et al. 1998; Horiuchi et al. 2005; Sahin and Blobel 2007). It is known that activation of EGFR signaling induces cell proliferation and regeneration due to STAT3 phosphorylation (Sanderson et al. 2006). Hypomorphic ADAM17$^{ex/ex}$ mice lost the ability to shed TNF-α, L-selectin and ligands of the EGFR from the cell surface (see section 2.1). The downstream signaling pathway of EGFR ligands or TNF-α in ADAM17$^{ex/ex}$ mice is intact but not activated. Furthermore, it was shown that ADAM17$^{ex/ex}$ mice were highly susceptible to DSS-induced colitis due to a breakdown of the intestinal epithelial barrier (see section 2.1). Can one rescue the disease progression by treatment with EGFR ligands? Are the mice then protected from DSS-induced colitis?

To elucidate this issue, wt and ADAM17$^{ex/ex}$ mice were injected with TGF-α and EGF during DSS-induced colitis. Wt and ADAM17$^{ex/ex}$ mice daily injected with EGFR ligands lost less weight than PBS injected mice after treatment with DSS (see Fig. 2-12 A). Histological colon sections of ADAM17$^{ex/ex}$ mice treated with either EGF or TGF showed normal architecture including destroyed epithelium but less crypt loss compared to DSS-treated ADAM17$^{ex/ex}$ mice. Furthermore, proliferation of cells of the crypts was analyzed. Interestingly, crypt cell proliferation of EGF or TGF-α treated ADAM17$^{ex/ex}$ mice could be restored compared to DSS-treated ADAM17$^{ex/ex}$ mice (see Fig. 2-12 B). Hence, phosphorylation of STAT3 in homozygous ADAM17$^{ex/ex}$ mice could be detected after DSS-induced colitis and TGF-α treatment compared to DSS-treated ADAM17$^{ex/ex}$ mice. This demonstrated that activation of EGFR signaling pathway can rescue proliferation of intestinal epithelial cells to induce a regenerative response and, therefore, led to amelioration of DSS-induced colitis (Fig. 2-12).

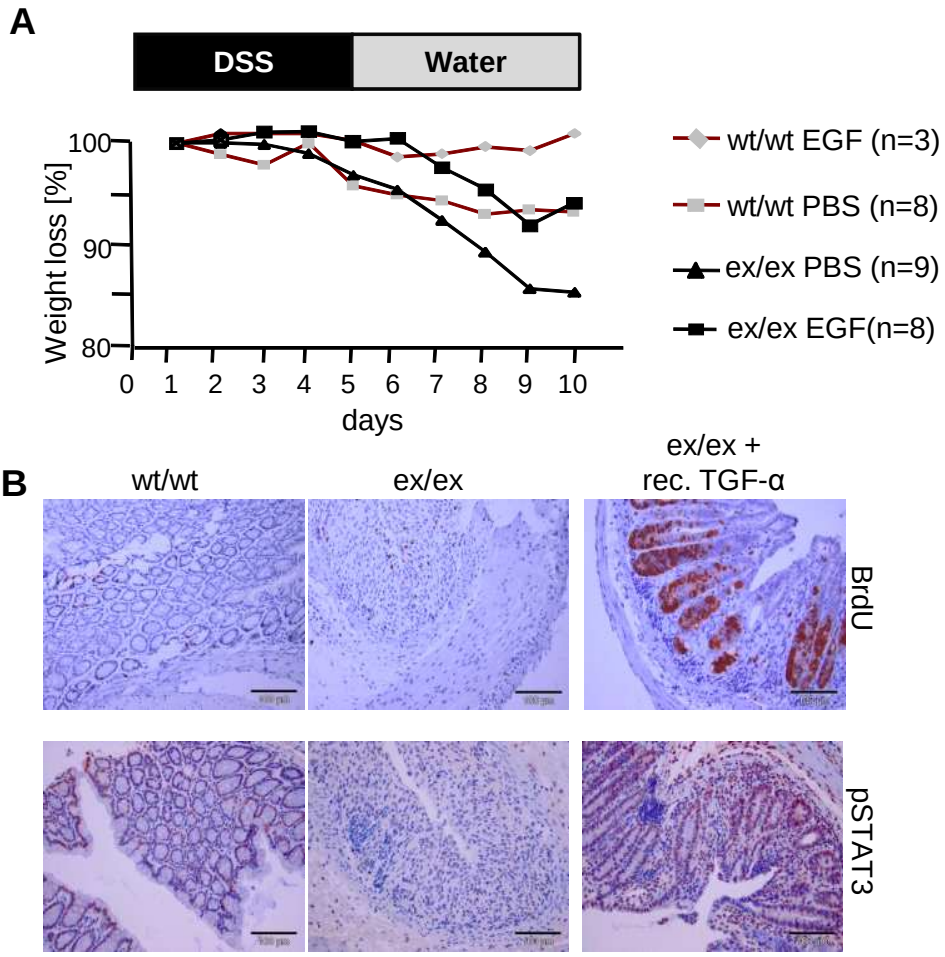

Fig. 2-12: Injection of EGFR ligands leads to amelioration of DSS-induced colitis in ADAM17$^{ex/ex}$ mice. (A) Weight progression during DSS-induced colitis of wt and ADAM17$^{ex/ex}$ mice treated with recombinant EGF. (B) Proliferation of crypt cells and phosphorylation of STAT3 in wt and ex/ex mice before and after injection of recombinant TGF-α. Bars represent 100µm. Figure taken from Chalaris et al. accepted.

2.3 Influence of sgp130Fc and anti-IL-6 antibody on DSS-induced colitis

Several signaling pathways are known to be involved in inflammatory bowel disease. As shown in section 2.1, ADAM17 mediated EGFR signaling is one signaling pathway which contributes to initiation and progression of DSS-induced colitis. This pathway induces phosphorylation of STAT3 and leads to regeneration of intestinal epithelial cells during DSS-induced colitis. Furthermore, ADAM17 is known to be involved in shedding of IL-6R from the cell surface. Soluble IL-6R binds to IL-6 and initiates IL-6 trans-signaling which is also implicated in Crohn's disease and ulcerative colitis. This pathway can be blocked using sgp130Fc or anti-IL-6R antibody. To elucidate the influence of sgp130Fc as well as anti-IL-6R antibody in IBD as potential therapeutic agents, Balb/c mice were injected with either sgp130Fc

or anti-IL-6R antibody in a TNBS-induced colitis model (Atreya et al. 2000). Interestingly, sgp130Fc as well as anti-IL-6R antibody treated mice showed less inflammation than control mice indicating that colitis can be ameliorated by interfering with IL-6 trans-signaling. The TNBS-induced colitis model is considered to reflect the pathogenesis of Crohn's disease (Maxwell and Viney 2009). To verify the role of IL-6 trans-signaling in ulcerative colitis, the DSS-induced colitis model was used. C57BL/6N mice were injected with 250µg sgp130Fc or 250µg anti-IL-6 antibody at day zero as well as day five and were treated with 2% DSS for five days followed by five days of water. Each group was comprised of six animals and weight loss was recorded daily.

As depicted in Fig. 2-13, all mice lost approximately 10% body weight during the experiment with a slight tendency for less weight loss in sgp130Fc treated mice than in anti-IL-6 antibody treated or control mice.

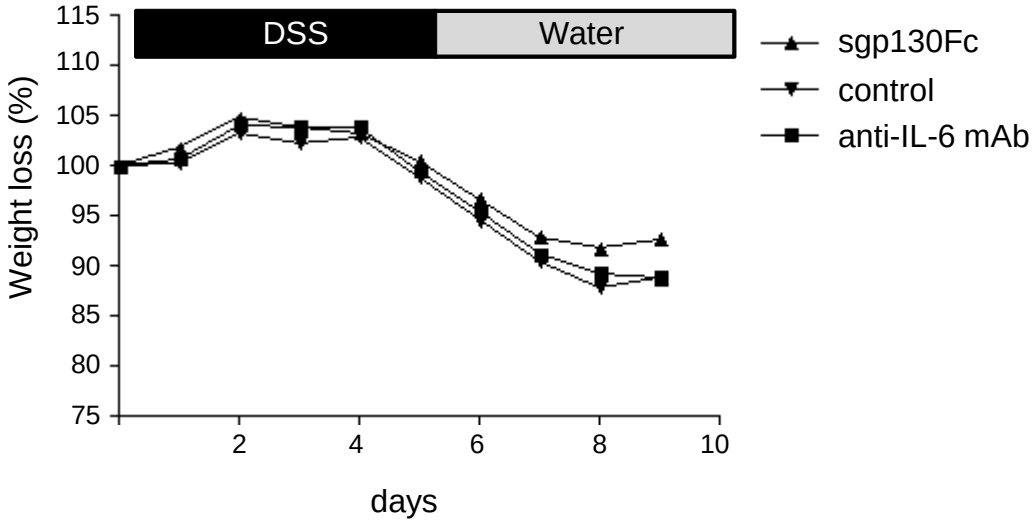

Fig. 2-13: Weight progression of mice during DSS-induced colitis treated with sg130Fc and anti-IL-6 mAb. Every group was comprised of six animals.

Furthermore, inflammation status of sgp130Fc or anti-IL-6 antibody treated mice was determined by colonoscopy (see Fig. 2-14 A). Mice treated with anti-IL-6 antibody were highly inflamed, had diarrhea, showed less luminescence and a strong increase in contact vulnerability. Control mice were also inflamed, e.g. having diarrhea and decreased luminescence, but less signs of inflammation were visible compared to anti-IL-6 antibody treated mice (see Fig. 2-14 A).

In contrast to that, sgp130Fc treated mice showed almost no signs of inflammation. The stool consistency as well as blood flow was normal and luminescence

maintained. Furthermore, disease activity index comprised of weight loss and HE staining was determined and showed that sgp130Fc treated mice were less inflamed compared to control and anti-IL-6 antibody treated mice (see Fig. 2-14 B).

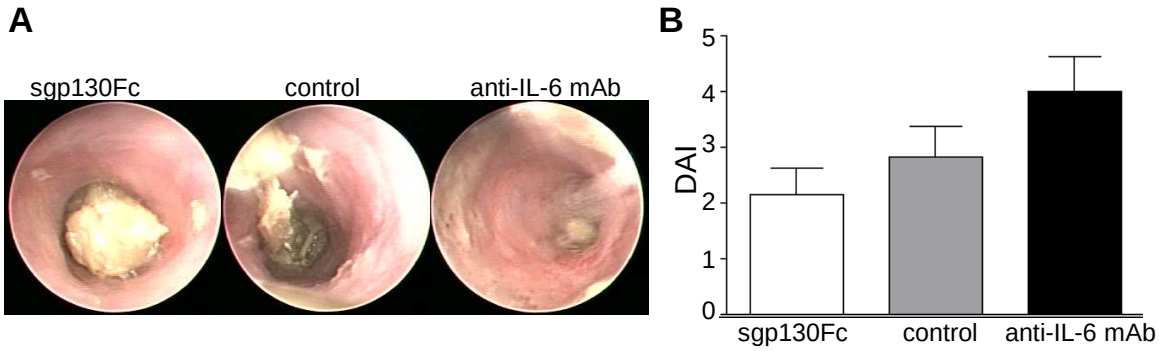

Fig. 2-14: Colonoscopy and disease activity index (DAI) of mice injected with sgp130Fc and anti-IL-6 mAb. (A) sgp130Fc treated mice showed less inflammation signs, whereas anti-IL-6 mAb treated and control mice were inflamed. (B) DAI comprised of weight loss and HE staining is increased in anti-IL-6 antibody treated mice compared to control or sgp130Fc treated mice.

Analysis of colon architecture by HE staining after DSS treatment showed that three out of six anti-IL-6 antibody treated mice were highly inflamed as seen by complete loss of intact crypts. The remaining three anti-IL-6 antibody treated mice had a destroyed epithelium caused by DSS, but the crypts were almost intact. The colon architecture of sgp130Fc treated mice showed a disrupted epithelium, but the crypts were completely intact concluding that these mice have less inflammation caused by DSS. Control mice displayed nearly the same inflammation level as sgp130Fc treated mice (see Fig. 2-15).

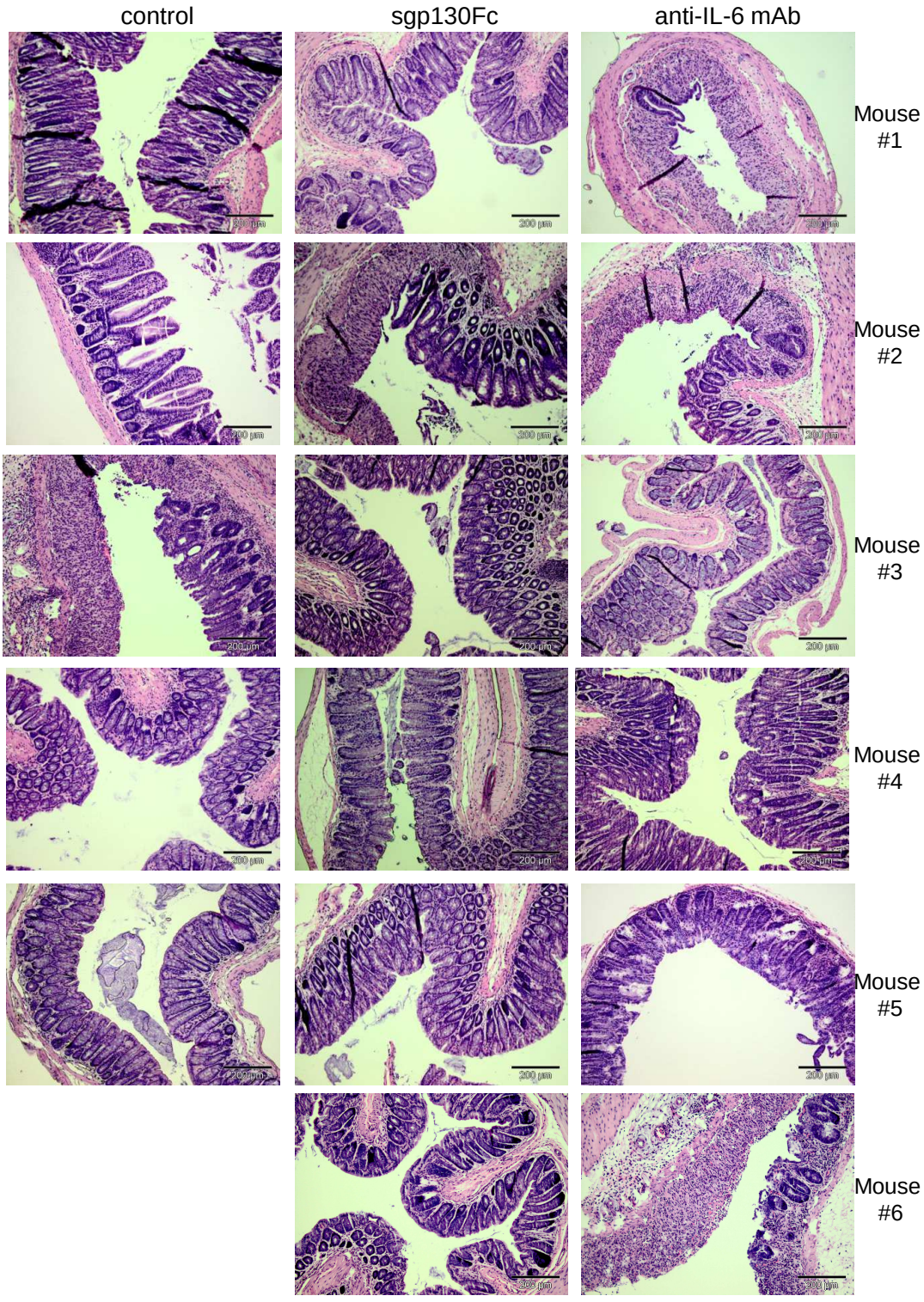

Fig. 2-15: HE staining of colon sections after anti-IL-6 mAb or sgp130Fc treatment and DSS-induced colitis. Epithelium is disrupted in all colon sections due to DSS application. sgp130Fc treated and control mice still have intact crypts, whereas anti-IL-6 mAb treatment led to a complete crypt destruction. One control mice died at day ten during colonoscopy. Bars represent 200µm.

These results are visualized by the inflammation score calculated from HE stained colon sections of each mouse. As shown on Tab. 2-1, sgp130Fc treated as well as control mice displayed an inflammation score of 1.2, whereas the level of anti-IL-6 antibody treated mice was significantly higher being 2.0.

Tab.2-1: Inflammation score of DSS-treated mice. Control mouse #6 died during colonoscopy and, therefore, no score could be calculated for this individual.1= epithelium destroyed, crypts intact; 2= epithelium disrupted, partial crypt lost; 3= epithelium destroyed, complete crypt lost.

#	control	sgp130Fc	α-IL6 mab
1	1	1	3
2	1	2	2
3	2	1	1
4	1	1	1
5	1	1	2
6	n.a.	1	3
Ø	**1.2**	**1.2**	**2.0**

Chemo- and cytokine secretion in colon organ culture was analyzed by ELISA. Levels of the chemoattractant proteins KC and MCP-1 are increased during an inflammation. As shown on Fig. 2-18, levels of KC as well as of MCP-1 showed an increased tendency in all mice after DSS-induced colitis indicating that all mice were inflamed. However, levels of KC as well as MCP-1 were higher in anti-IL-6 antibody treated mice than in sgp130Fc treated or control mice but failed to be significant (Fig. 2-16 A, B).

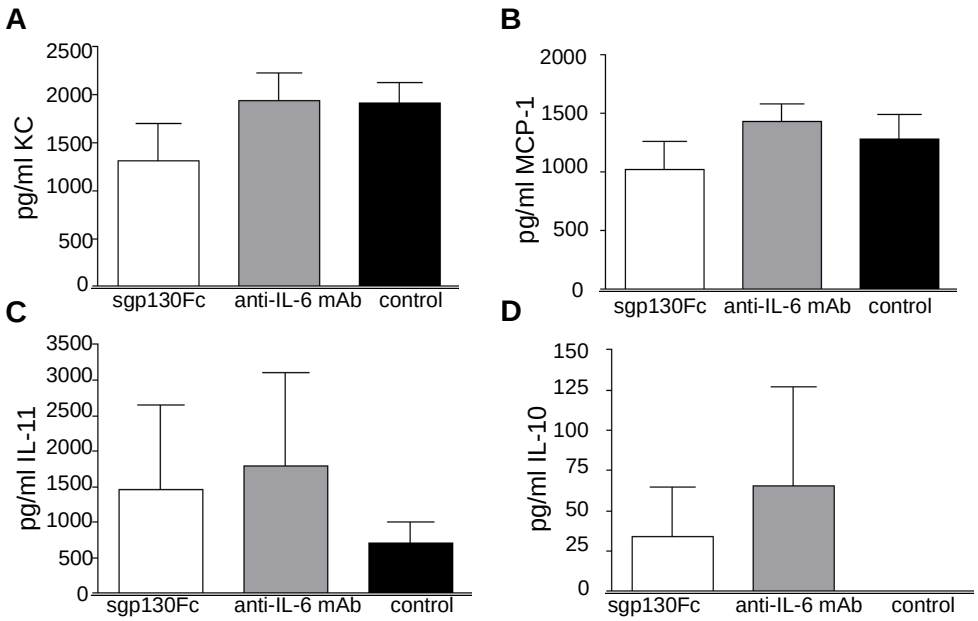

Fig. 2-16: Cytokine and chemokine secretion in colon organ cultures of treated mice. (A - D) Supernatants of colon organ cultures were harvested and analyzed by ELISA for KC (A; sgp130Fc n=6; anti-IL-6 ab n=6; control n=5), MCP-1 (B; sgp130Fc n=6; anti-IL-6 ab n=6; control n=5), IL-11 (C; sgp130Fc n=6; anti-IL-6 ab n=6; control n=5) and IL-10 (D; sgp130Fc n=6; anti-IL-6 ab n=6; control n=5).

The anti-inflammatory cytokines IL-10 as well as IL-11 are involved in prohibition of excessive inflammation reactions and IL-11 is considered to block the production of IL-6 (Walmsley et al. 1998; Murray 2005). In the latter experiment, protein levels of IL-10 and IL-11 were tendentially increased in sgp130Fc as well as in anti-IL-6

antibody treated mice showing that inflammation was tried to combat (see Fig. 2-16 C, D).

Furthermore, MPO levels in colons of treated and untreated mice were measured showing no significant differences among the three different treatments (see Fig. 2-17). MPO levels increased as a result of IBD which indicates the presence of activated neutrophils in the intestine during inflammation (Breckwoldt et al. 2008).

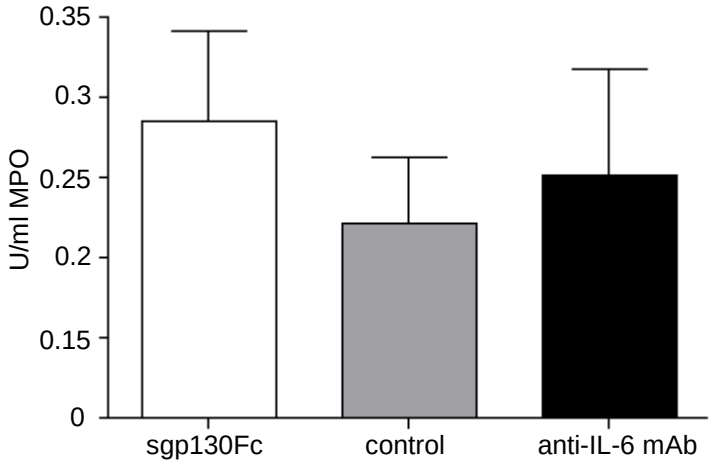

Fig. 2-17: MPO activity after DSS treatment in colon of mice injected with sgp130Fc, anti-IL-6 mAb or control mice.

Taken together, sgp130Fc has positively influenced disease progression indicating that this protein might ameliorate DSS-induced colitis. However, mice treated with anti-IL-6 antibody during DSS-induced colitis were more inflamed than sgp130Fc treated and control mice.

2.4 Which protease is responsible for the release of CD27 from the cell surface?

CD27 is a 55kDa type I transmembrane receptor protein belonging to the tumor necrosis factor (TNF) receptor family and is expressed by peripheral T cells, mature thymocytes, memory B cells and NK cells (Bigler et al. 1988). CD70, the ligand of CD27, is only transiently present on cells of the immune system upon activation (Borst et al. 2005). After interaction of CD27 with CD70, a truncated form of CD27 is released, most probably by a membrane-linked protease (Loenen et al. 1992). This interaction is important for an effective T cell response *in vivo*. However, continuous CD27-CD70 interactions may cause immune dysregulation and immunopathology in conditions of chronic immune activation (Nolte et al. 2009). Inhibiting the CD27-CD70 signaling pathway by blockade of CD70 or absence of CD27 suppresses TNBS-

induced colitis (Manocha et al. 2009). Furthermore, it was shown that CD27 is shed from the T cell surface upon stimulation with benzoyl ATP (BzATP) which is acting via P2Y purinergic receptors (Boyer and Harden 1989). Shedding of CD27 is dependent on the receptor $P2X_7$ (Moon et al. 2006), but the responsible protease remains unknown.

Members of the ADAM family, especially ADAM17, are involved in shedding of tumor necrosis factor receptors (TNFRs). CD27 is a member of the TNFR family and cleaved from the cell surface by an unidentified protease. In the absence of CD27, TNBS-induced colitis is suppressed, whereas mice with decreased levels of ADAM17, which might shed CD27 from the cell surface, exhibit severe colitis (see section 2.1). The working hypothesis was that ADAM17 may be the main sheddase for CD27 *in vivo*. Therefore, ADAM17 mediated shedding of CD27 might down-regulate CD27 signaling and, thereby, dampen disease signs in DSS-induced colitis.

To test this hypothesis, spleen cells of C57BL/6N mice were isolated and treated with 300µM BzATP to induce the release of different proteins from the cell surface. To analyze if ADAM10 or ADAM17 are involved in shedding of CD27, cells were additionally incubated with inhibitors of ADAM10 (GI, Ludwig et al. 2005) or both ADAM17 and ADAM10 (GW, Ludwig et al. 2005). Cells were analyzed by FACS for CD27 surface expression. As shown on Fig. 2-18, percentage of CD27-positive lymphocytes drastically decreases by treatment with BzATP. The decrease of CD27 from the cell surface of lymphocytes due to BzATP stimulation could be blocked to the same degree by GI (ADAM10) or GW (ADAM10/17). This indicated that ADAM10 rather than ADAM17 is involved in shedding of CD27.

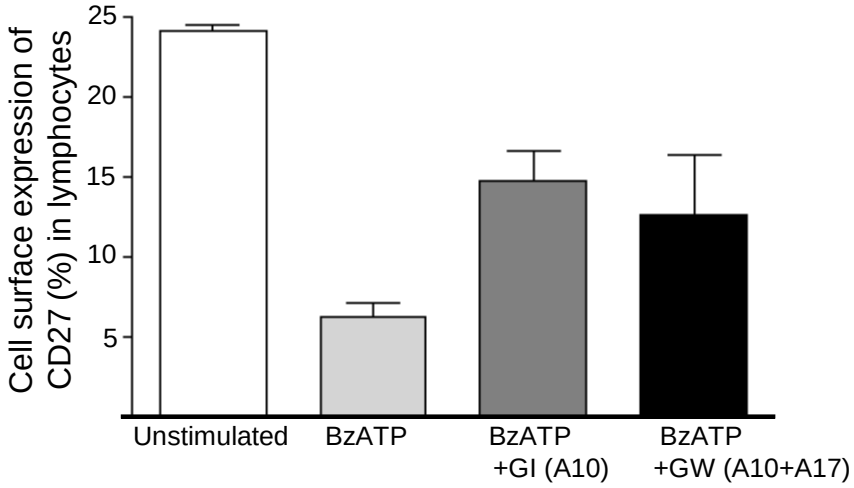

Fig. 2-18: FACS analysis of stimulated spleen cells from C57BL/6N mice. Spleen cells were isolated from C57BL/6N mice and stimulated with 300µM BzATP or BzATP and 3µM inhibitors GI or GW. Four mice were used for mean and SD. A10: ADAM10; A17: ADAM17.

To validate our *in vivo* finding data in another model, Ba/F3-gp130-IL-6R as well as MEF cells were analyzed for presence of CD27 on cell surface using FACS. As shown on Fig. 2-19, both cell lines, Ba/F3-gp130-IL-6R and MEFs, do not express CD27. Since COS7 as well as HEK cells also do not produce CD27 (Garcia et al. 2004, Akiba et al. 1998), any of the four cell lines can only be used for further shedding experiments if they are transfected with a CD27 expression construct.

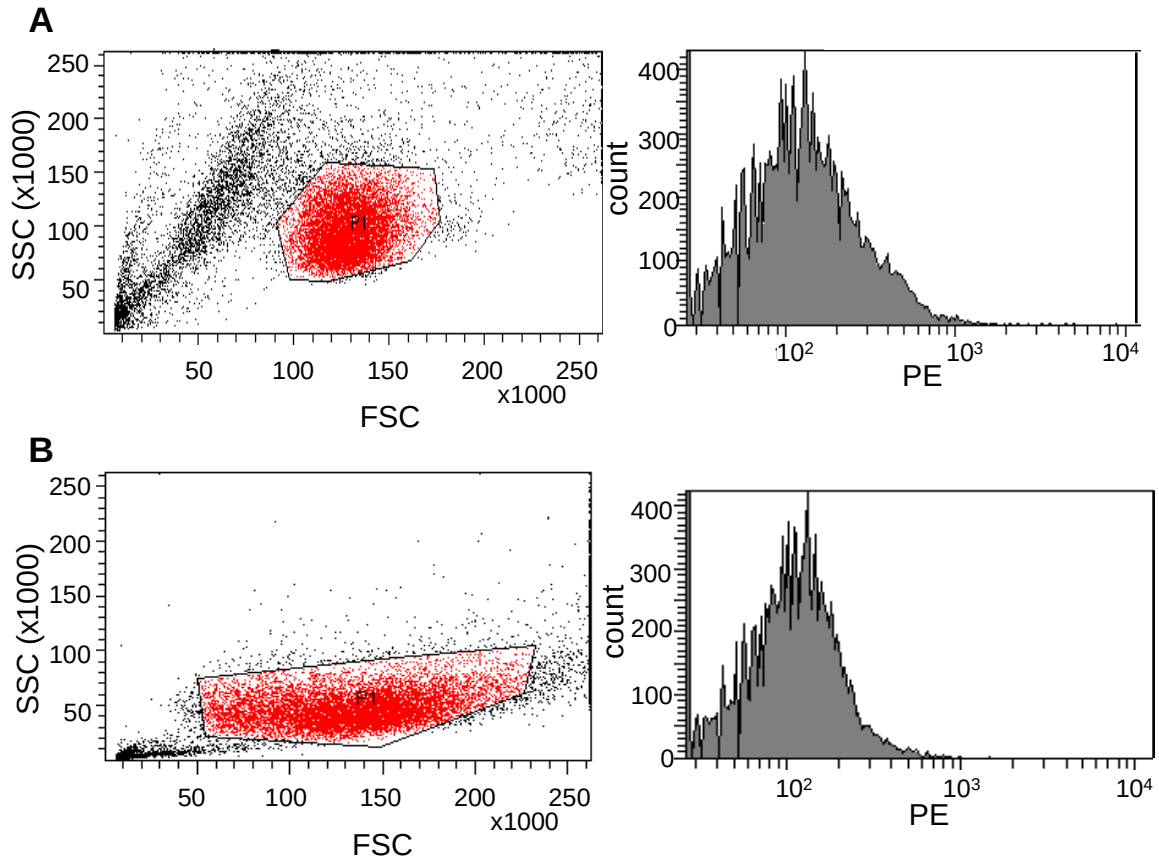

Fig. 2-19: Analysis of CD27 expression in Ba/F3-gp130-IL6R as well as MEF cells. (A) 10^6 Ba/F3-gp130-IL-6R cells were stained with PE hamster anti-mouse CD27. Cells gated in P1 (left panel) displaying Ba/F3-gp130-IL6R cells were analyzed in right panel for CD27 expression. (B) 10^6 MEF cells were stained with PE hamster anti-mouse CD27. In the left panel, P1 shows the gate for MEF cells in which the CD27 expression was determined (right panel). (A) as well as (B) shows that both cell lines are negative for CD27 expression.

For the construction of the CD27 expression plasmid, CD27 open reading frame (orf) was amplified from murine spleen cell cDNA and cloned into pcDNA3.1 containing a Flag- as well as His_6-tag. Afterwards, a cDNA encoding an alkaline phosphatase (AP) was inserted into the CD27 construct for detecting CD27 in e.g. Western blot or AP-assay (see Fig. 2-20).

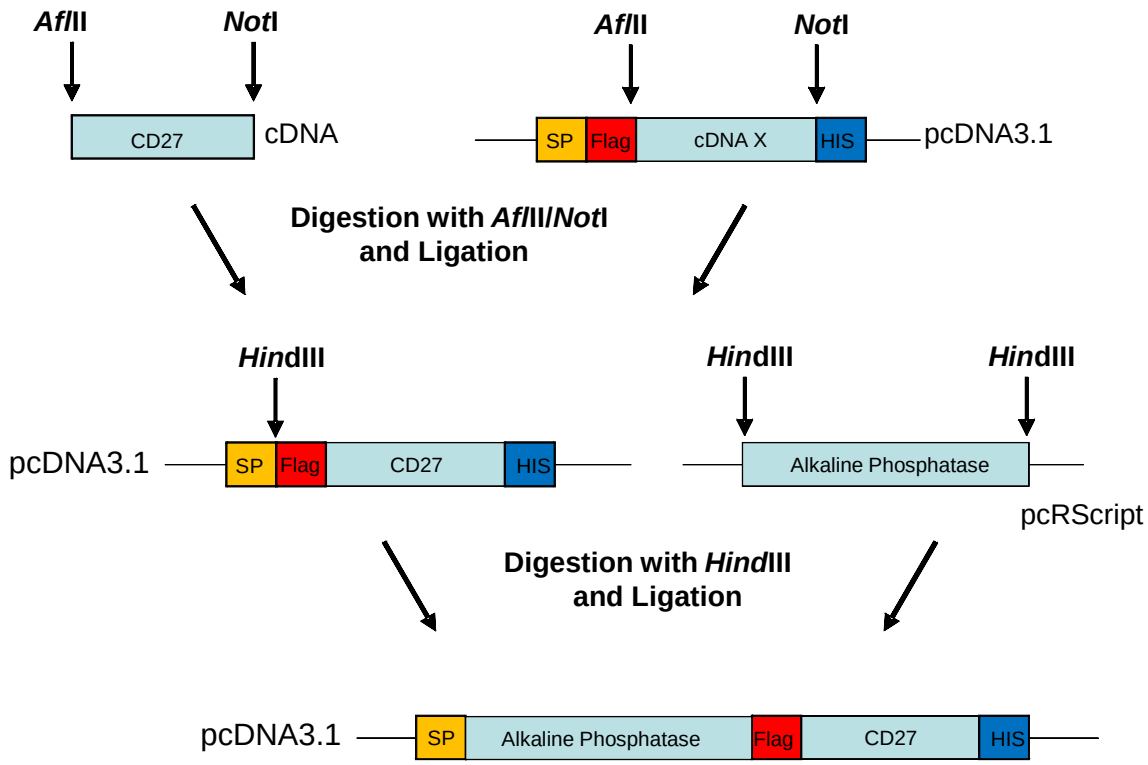

Fig. 2-20: Scheme of cloning CD27 into pcDNA3.1. CD27 orf was amplified from murine spleen cell cDNA and inserted into pcDNA3.1 containing signal peptide (SP), Flag- as well as His_6-tag. Furthermore, cDNA for human alkaline phosphatase was ligated into pcDNA3.1 between Flag-tag and SP.

COS7 as well as HEK cells were successfully transfected transiently with the expression construct encoding CD27 as revealed by Western blotting (see Fig. 2-21). The theoretically estimated size of CD27 together with AP-site and tags was 84kDa.

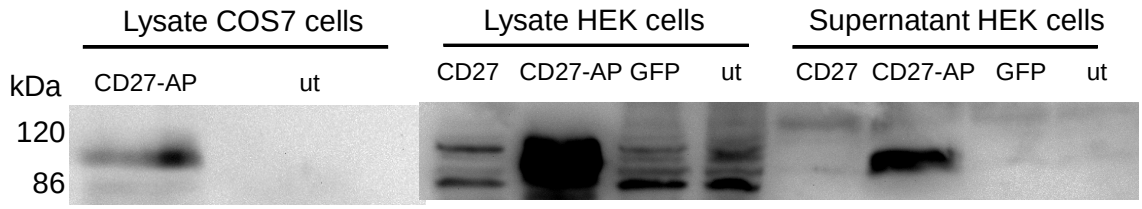

Fig. 2-21: Western blot analysis of transiently transfected COS7 and HEK cells. COS7 cells as well as HEK cells were transiently transfected with pcDNA3.1-CD27, pcDNA3.1-CD27-AP or pEGFP. Lysate and supernatant was collected and analyzed for expression of CD27. Interestingly, in supernatant of HEK cells transfected with CD27-AP, CD27 was detected 48 hours after transfection using FLAG antibody indicating that the protein is released from cell surface without stimulus. ut: untransfected.

Interestingly, 48 hours after transfection CD27 could be detected in the supernatant of HEK cells indicating that shedding occurred without any inductor. Furthermore, the release of CD27 was analyzed via AP activity. If CD27 is released into the supernatant (SN), AP activity is increased in SN and decreased in the lysate which can be measured at 405nm after coloration. As shown on Fig. 2-22, AP activity in the

supernatant of CD27-AP expressing HEK cells is increased compared to control cells without using a stimulus 48 hours after transfection.

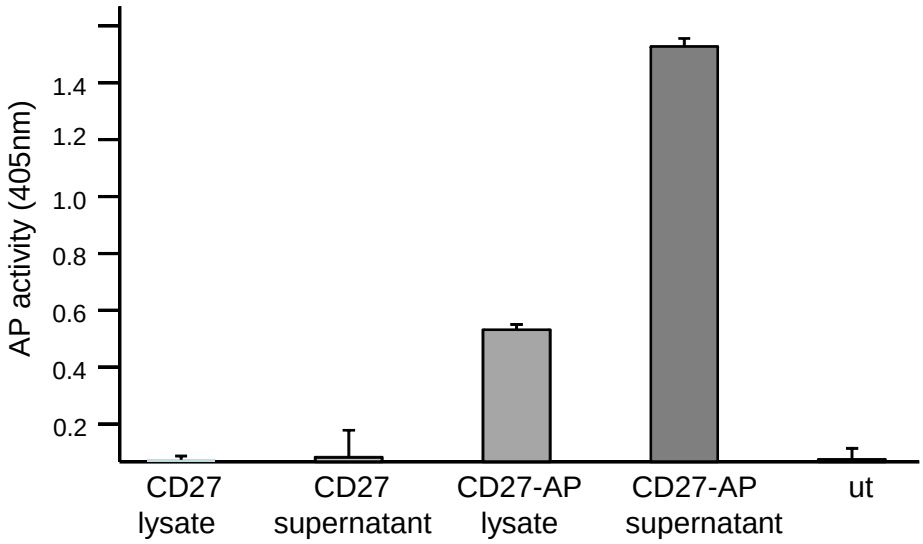

Fig. 2-22: Shedding analysis with alkaline phosphatase activity. HEK cells were transiently transfected with CD27-AP or CD27 construct**.** 48h after transfection, lysate and supernatant was collected and AP activity was measured at 405nm. Shedding occurred in HEK cells without stimulating the cells. ut: untransfected cells.

To verify if ADAM10 is involved in shedding of CD27, HEK cells were pretreated with the ADAM10 inhibitor GI for 30 minutes. Besides BzATP, other substances can also induce shedding. Therefore, cells were treated with ionomycin. Ionomycin leads to calcium influx into cells, induces apoptosis and shedding of different membrane proteins. AP activity was measured and the ratio of supernatant to lysate was calculated. As shown on Fig. 2-23, after addition of ionomycin, CD27 is released in the supernatant and this release could be inhibited by the ADAM10 inhibitor GI.

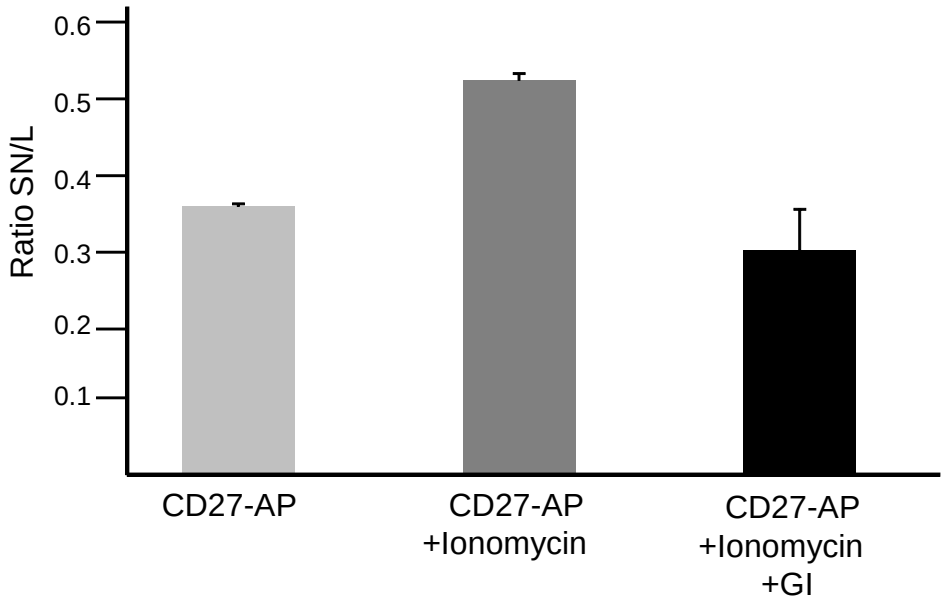

Fig. 2-23: Shedding analysis of transfected HEK cells with ionomycin and ADAM10 inhibitor GI. HEK cells were transiently transfected with CD27-AP construct. 48 hours after transfection, cells were stimulated with ionomycin to induce shedding or with ionomycin and GI to inhibit shedding. Ratio of supernatant (SN) and lysate (L) was calculated. Shedding of CD27 was diminished in presence of ADAM10 inhibitor GI.

These initial experiments showed that ADAM10 rather than ADAM17 might be involved in shedding of CD27 from the cell surface. However, these findings will be verified by using (i) MEFs deficient for ADAM10 or (ii) mice with T cell specific deletion of ADAM10. Thus, the precise role of ADAM10 in shedding of CD27 can be clarified.

3 Discussion

3.1 Role of ADAM17 in DSS-induced colitis

ADAM17 is known to be involved in shedding of different proteins from cell surface e.g. IL-6R, L-selectin and ligands of EGFR (Peschon et al. 1998; Horiuchi et al. 2005; Sahin and Blobel 2007). It is expressed by immune cells but also in most other tissues and is upregulated during inflammation and cancer (Becker et al. 2005; Kenny 2007). ADAM17 deficient mice are not viable (Peschon et al. 1998). Conditional ADAM17 knock-out mice are available, but characterization of ADAM17 is restricted mostly to one tissue or cell type. Therefore, hypomorphic ADAM17$^{ex/ex}$ mice were generated (see section 1.3). These mice are viable, but display eye, heart and skin defects. Furthermore, shedding of different substrates, such as L-selectin, TNF-α and EGFR ligands, in these mice is impaired.

Since the molecular mechanism of inflammatory bowel disease still remains unknown, it was very interesting to test if a knock-out of ADAM17 has consequences on the development of inflammatory diseases. Colitis can be induced in mice by application of DSS. ADAM17$^{ex/ex}$ mice as well as heterozygous and wildtype mice were treated with 2% DSS for five days followed by five days of water.

Under normal conditions, the colon architecture of ADAM17$^{ex/ex}$ mice is intact and cellular proliferation in the intestine was not affected by the knock-out indicating that ADAM17 activation is not needed for this process. However, ADAM17$^{ex/ex}$ mice are highly susceptible to DSS-induced colitis compared to heterozygous and wildtype mice. ADAM17$^{ex/ex}$ mice displayed severe weight loss during DSS treatment (see Fig. 2-3). DSS is directly toxic to gut epithelial cells and, therefore, affects the barrier integrity against microbial invaders. This barrier is influenced by residential commensal bacteria, rapid epithelial turnover, innate immune responses and epithelial barrier integrity. DSS-treated ADAM17$^{ex/ex}$ mice failed to maintain the barrier function as shown by colonoscopy (Fig. 2-4), HE staining (Fig. 2-7) and FITC-Dextran permeability (Fig. 2-8). HE staining also revealed that in ADAM17$^{ex/ex}$ mice the crypts are completely lost compared to wildtype and heterozygous ADAM17 mice. Thus, there are two possible causes why the crypts are destroyed: (i) apoptosis is promoted or (ii) regenerative proliferation might be impaired. Therefore, colon sections were analyzed for phosphorylation of STAT3 as well as cyclinD1 expression. Phosphorylation of STAT3 (Fig. 2-7) as well as expression of cyclinD1

(Fig. 2-7) - both are marker of proliferating cells - are impaired in DSS-treated ADAM17$^{ex/ex}$ mice. Normally, phosphorylated STAT3 induces proliferation of intestinal epithelial cells and, therefore, activates the regeneration of a destroyed epithelium. These results indicate that the regenerative response in ADAM17$^{ex/ex}$ mice is affected due to absence of the protease ADAM17. These two functions – maintaining barrier integrity and regeneration of intestinal epithelial cells – seem to be dominant towards the reduced activity of the immune system which is a consequence of impaired ADAM17 mediated shedding of substrates such as TNF-α. However, promoted apoptosis could not be excluded because after ten days of DSS treatment no crypts could be detected in colon sections. To verify that apoptosis is not involved in crypt loss, TUNEL as well well Acridin orange staining on colon tissues has to be performed. Moreover, to analyze the timing when the regenerative response is established, phosphorylation of STAT3 as well as CyclinD1 expression has to be analyzed at earlier time points when crypts are not completely absent during DSS-induced colitis.

Furthermore, ADAM17 is the main sheddase for TNF-α (Black et al. 1997) and also for several ligands of EGFR (Sunnarborg et al. 2002). Thus, it was suggested that blocking ADAM17 might be used as therapeutic strategy during different inflammatory diseases (Moss and Bartsch 2004) and cancer (Kenny 2007). Anti-TNF-α mAbs such as infliximab were generated and used successfully for treatment against rheumatoid arthritis (Elliott et al. 1993). Since antibody production is expensive, other therapeutic agents which are less costly and have a better safety profile might prove to be useful (Moss et al. 2008). However, inhibitors of metalloproteases as therapeutic drugs often failed as they caused many side effects (Moss and Bartsch 2004). Nevertheless, inhibitors of ADAM17 are available and currently in clinical trials (Moss et al. 2008). As shown in this work, deletion of ADAM17 caused a lack of stress-induced tissue regeneration and underlines that this acts dominantly over the anti-inflammatory property of this protease. Targeting ADAM17 during DSS-induced colitis, therefore, could not ameliorate disease progression but might be a helpful target in other diseases e.g. cancer. ADAM17 is known to be involved in breast cancer progression (McGowan et al. 2007; Zheng et al. 2009) and contributes to cancer progression through activation of EGFR-PI3K-AKT signaling pathway (Zheng et al. 2009). Involvement in cancer progression, therefore, provides further impetus for exploiting ADAM17 as a new target for cancer treatment.

Interestingly, mice lacking TGF-α also develop a severe colitis induced by DSS compared to wildtype mice (Egger et al. 1997). However, mice overexpressing TGF-α showed reduced susceptibility to DSS-induced colitis suggesting that TGF-α is a pivotal mediator of protection and/or healing mechanisms in the colon (Egger et al. 1998). Thus, ligands of the EGFR such as TGF-α and EGF were used as a potential therapeutic drug during DSS-induced colitis of ADAM17$^{ex/ex}$ mice. Interestingly, TGF-α treated ADAM17$^{ex/ex}$ mice exhibited less inflammation compared to untreated mice during colitis. Moreover, proliferation of intestinal epithelial cells could be restored in the presence of EGF or TGF-α (see Fig. 2-12).

Taken together, analysis of inflammatory bowel disease in the DSS-induced colitis model in hypomorphic ADAM17 mice showed that the metalloprotease exhibits a dual role: (i) ADAM17 sheds TNF-α from the cell surface to activate the immune system. In this case, ADAM17 has pro-inflammatory properties. (ii) Furthermore, ADAM17 is involved in shedding of EGFR ligands to activate a coordinated regenerative response, being anti-apoptotic (see Fig. 3-1). Interestingly, studying hypomorphic ADAM17$^{ex/ex}$ mice revealed both detrimal and beneficial properties of the metalloprotease ADAM17, whereas ADAM17 was shown to exhibit only desruptive functions in other conditional ADAM17 knock-out mouse models.

In this respect, the ADAM17$^{ex/ex}$ mouse model is well suited to analyze the *in vivo* functions and consequences after therapeutic blockade of ADAM17, in which 90-95% of ADAM17 function is impaired.

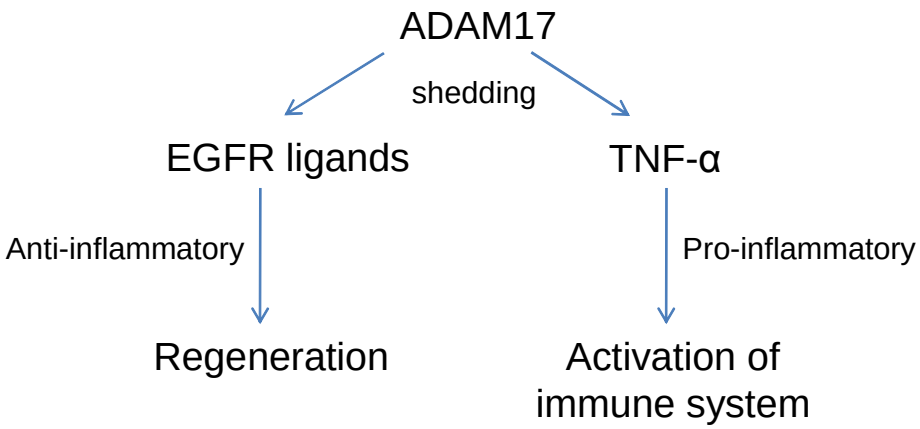

Fig. 3-1: Dual role of ADAM17 in inflammatory diseases. ADAM17 is involved in shedding of EGFR ligands as well as TNF-α and can act pro- as well as anti-inflammatory. Shedding of EGFR ligands leads to regeneration of e.g. intestinal epithelial cells, whereas shedding of TNF-α is involved in activation of the immune system.

3.2 Role of sgp130Fc and anti-IL-6 antibody in DSS-induced colitis

The mechanisms of initiation and progression of inflammatory bowel disease are not yet clarified, but it is known that different signaling pathways e.g. EGFR signaling (see above) or IL-6 trans-signaling (Atreya et al. 2000) are involved. Activation of the IL-6 trans-signaling pathway plays an important role during Crohn's disease (Rose-John and Heinrich 1994; Peters et al. 1998; Mullberg et al. 2000). This pathway can be blocked by sgp130Fc which is an inhibitor of IL-6 trans-signaling (Jostock et al. 2001).

Inflammatory bowel disease can be induced in mice by different chemical agents e.g. TNBS, oxazolone or DSS. TNBS as well as oxazolone induce a T cell mediated immune response, whereas DSS influences the barrier integrity and, therefore, is important to analyze the role of the innate immune system.

In a TNBS-induced colitis model, the IL-6 trans-signaling inhibitors sgp130Fc and anti-IL-6R antibody could ameliorate disease progression and positively influenced colitis (Atreya et al. 2000). Furthermore, anti-IL-6R antibody is used for treatment of patients with Castleman's disease, rheumatoid arthritis as well as juvenile idiopathic arthritis (Kishimoto 2010).

But which influence do sgp130Fc as well as anti-IL-6 antibody exert during DSS-induced colitis? To elucidate this issue, C57BL/6N mice were treated with sgp130Fc or anti-IL-6 antibody during DSS-induced colitis. To monitor the inflammation status, weight loss was recorded daily. sgp130Fc and anti-IL-6 antibody treated mice lost weight during the DSS cycle, but displayed no significant difference from control animals (see Fig. 2-13). Interestingly, colonoscopy and HE staining revealed that sgp130Fc treated mice had less inflammation than anti-IL-6 antibody treated and control mice (see Fig. 2-14, 2-15). These results indicate that sgp130Fc can ameliorate disease progression also in DSS-induced colitis, whereas anti-IL-6 antibody treated mice were inflamed and not protected from colitis. As mentioned above, inhibiting IL-6 trans-signaling via anti-IL-6R antibody was able to ameliorate TNBS-induced colitis (Atreya et al. 2000), whereas using anti-IL-6 antibody does not protect from DSS-induced colitis. How can this apparent contradiction be explained?

Interestingly, IL-6 knock-out mice exhibit severe colitis after DSS-treatment (Grivennikov et al. 2009), although IL-6 trans-signaling and classic signaling is blocked. IL-6 increases proliferation of intestinal epithelial cells as well as their

resistance to apoptosis and might effect tissue regeneration. In the absence of IL-6, proliferation as well as regeneration was impaired and led to disease progression. This phenotype was also seen in C57BL/6N mice treated with anti-IL-6 antibody during DSS-induced colitis. On the other hand, a permanent increase of IL-6 could lead to proliferation of intestinal epithelial cells and, therefore, disease progression is amplified. If this part of IL-6 is influenced for example by blocking the IL-6 signaling pathway with anti-IL-6R antibody or sgp130Fc, the disease could be ameliorated.

Furthermore, different colitis models were used to analyze the role of IL-6 trans-signaling. TNBS-induced colitis leads to T cell mediated immune responses and most symptoms correspond to Crohn's disease – one major inflammatory bowel disease (Wirtz et al. 2007). In contrast to this, DSS-induced colitis affects the barrier integrity and the innate immune system plays a major role in this model (Wirtz et al. 2007). Concerning on inflammatory bowel disease, it is postulated that DSS-induced colitis mimics ulcerative colitis. Therefore, blocking IL-6 trans-signaling with either anti-IL-6R antibody or anti-IL6 antibody could have different functions in Crohn's disease as well as ulcerative colitis. Thus, different inflammatory responses were analyzed although they are belonging to inflammatory bowel disease. To verify their roles each antibody has to be tested in both colitis models. Furthermore, anti-IL-6R antibody was used in clinical trials against Castleman's disease and different kinds of arthritis but not for Crohn's disease or ulcerative colitis until now (Kishimoto 2010).

Taken together, IL-6 exerts two different functions in inflammatory bowel disease and other chronic disorders. The function of the protein is balancing between anti- and pro-inflammatory properties. Up to now it is unclear how the balance is regulated. Related to inflammatory bowel disease, mice might be protected or highly susceptible to DSS-induced colitis depending on which protein is chosen for inhibition of IL-6 trans-signaling. sgp130Fc might have protective effects on colitis and, therefore, represents a potential but powerful therapeutic agent of IBD, whereas anti-IL-6 antibody might aggravate the disease progression and, thus, does not seem to represent a useful drug.

3.3 CD27, a protein involved in IBD seems to be shed by ADAM10

CD27 is a type I transmembrane receptor protein belonging to the tumor necrosis factor (TNF) receptor family and is expressed by peripheral T cells, mature thymocytes, memory B cells and NK cells (Nolte et al. 2009). CD70, the ligand of

CD27, is only present on activated T cells (Borst et al. 2005). Interaction of CD27 with CD70 is important for an effective T cell response *in vivo.* Interestingly, CD27-CD70 signaling pathway was shown to be involved in inflammatory bowel disease (Manocha et al. 2009) and blocking this pathway may provide a potential tool for therapeutic intervention in IBD. T cells from CD27 knock-out mice were transferred into $Rag^{-/-}$ mice and wildtype T cells transferred recipient mice were treated with anti-CD70 antibody. TNBS was administered and clinical symptoms of colitis were monitored. Interestingly, blockade of CD27-CD70 pathway attenuated TNBS-induced colitis (Manocha et al. 2009). Furthermore, membrane bound CD27 can be inactivated by shedding from the cell surface. This mechanism could be induced by BzATP, but the involved protease remains unknown (Moon et al. 2006).

As shown in section 2.1, mice with a deletion of ADAM17 are highly susceptible to DSS-induced colitis. Therefore, it was hypothesized that ADAM17 might be involved in the release of CD27 from the cell surface to inhibit the CD27-CD70 pathway and, thus, protect from inflammatory bowel disease (see Fig. 3.2).

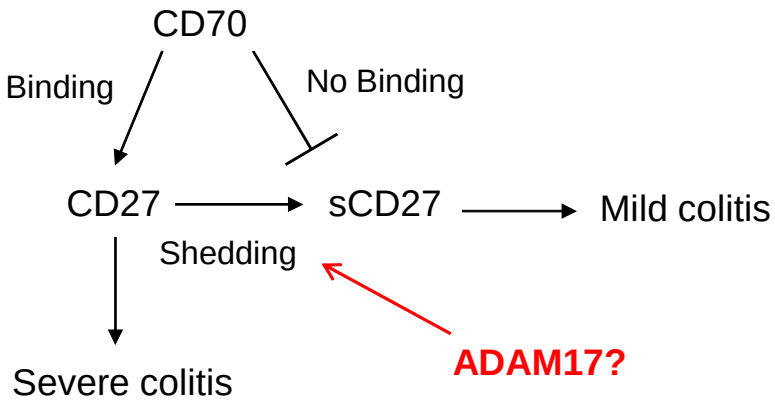

Fig. 3-2: Hypothetical model of involvement of ADAM17 in CD27 shedding. Activation of CD27-CD70 pathway leads to severe colitis, whereas blocking this pathway by inhibiting CD27 exhibits a mild form of colitis. CD27 can be inactivated by shedding, but the responsible protease is unknown suggesting that ADAM17 might be involved.

To elucidate this issue, shedding experiments were carried out using isolated spleen cells of C57BL/6N mice. Shedding was induced by administration of BzATP alone or in the presence of an inhibitor of ADAM10 (GI, Ludwig et al. 2005) or both ADAM10 and ADAM17 (GW, Ludwig et al. 2005). This *in vitro* analysis suggests that CD27 might be shed by ADAM10 and not ADAM17. To verify these results using recombinant technology, shedding experiments were carried out in COS7 as well as HEK cells transiently transfected with constructs coding for CD27 fused to alkaline phosphatase. Interestingly, shedding of CD27 occurred without any stimulus 48

hours after transfection. Furthermore, cells were treated with the ADAM10 inhibitor GI. Shedding of CD27 could be blocked by GI (see Fig. 2-23) pointing out that ADAM10 is involved in release of CD27 as already shown in spleen cells.

To clearify the release of CD27 from the cell surface *in vivo*, ADAM10KO mice could prove useful. Unfortunately, ADAM10KO mice are not viable (Hartmann et al. 2002). Therefore, it is difficult to analyze CD27 shedding *in vivo*. To overcome this problem, mouse embryonic fibroblasts deleted in ADAM10 or conditional ADAM10KO mice could be used to underline the *in vitro* experiments.

Conditional ADAM10KO mice are being generated at the moment using a $CD4^+$-Cre promoter (Jürgen Scheller, Institute of Biochemistry, Kiel, personal communication). By expressing Cre recombinase under the control of the $CD4^+$ promoter in mice, deletion of floxed ADAM10 segments will be induced in CD4-positive T cells. However, these mice first have to be characterized, e.g. if ADAM10 is indeed down-regulated or even absent in T-lymphocytes. Then these mice can be used for shedding analyses *in vivo*.

Furthermore, it would be interesting to analyze conditional ADAM10KO mice during TNBS- or DSS-induced colitis. If ADAM10 indeed is involved in CD27 shedding, mice with a deletion of this protease might be more susceptible to TNBS-induced colitis because the CD27-CD70 pathway is not inactivated and induces progression of the disease.

All initial experiments point to ADAM10 as the main sheddase for CD27 and showed that inflammatory bowel disease is regulated by a complex interplay of different molecules.

3.4 Current understanding of the molecular framework of IBD

Inflammatory bowel disease is a chronic inflammatory disorder of the gastrointestinal tract that occurs in immunocompetent individuals (Manocha et al. 2009). Despite intensive study of IBD pathogenesis, the mechanisms which contribute to disease initiation and progression still largely remain unknown. Inflammatory bowel disease can be induced in a mouse model for example by administration of DSS in drinking water (Wirtz et al. 2007).

The results obtained in this work have shown that many factors are involved in the pathogenesis of DSS-induced colitis. First, the function of the metalloprotease

ADAM17 during DSS-induced colitis was analyzed (see section 2.1). Interestingly, mice with a deletion of ADAM17 exhibit severe colitis. It is postulated that ADAM17 activates EGFR signaling pathway by shedding of EGFR ligands leading to suppression of DSS-induced colitis. Furthermore, the role of IL-6 classic as well as trans-signaling in inflammatory bowel disease was determined (see section 2.3). IL-6 classic and trans-signaling exhibit a dual role during inflammatory bowel disease: (i) Inhibiting IL-6 trans-signaling pathway specifically by sgp130Fc might ameliorate disease progression. (ii) Blocking both pathways by anti-IL-6 mAb indicates high susceptibility to IBD. Another signaling pathway which is known to promote disease progression is CD27-CD70 (see Fig. 3-3). Inhibiting this pathway by ADAM10 might have a protective role for the initiation of DSS-induced colitis.

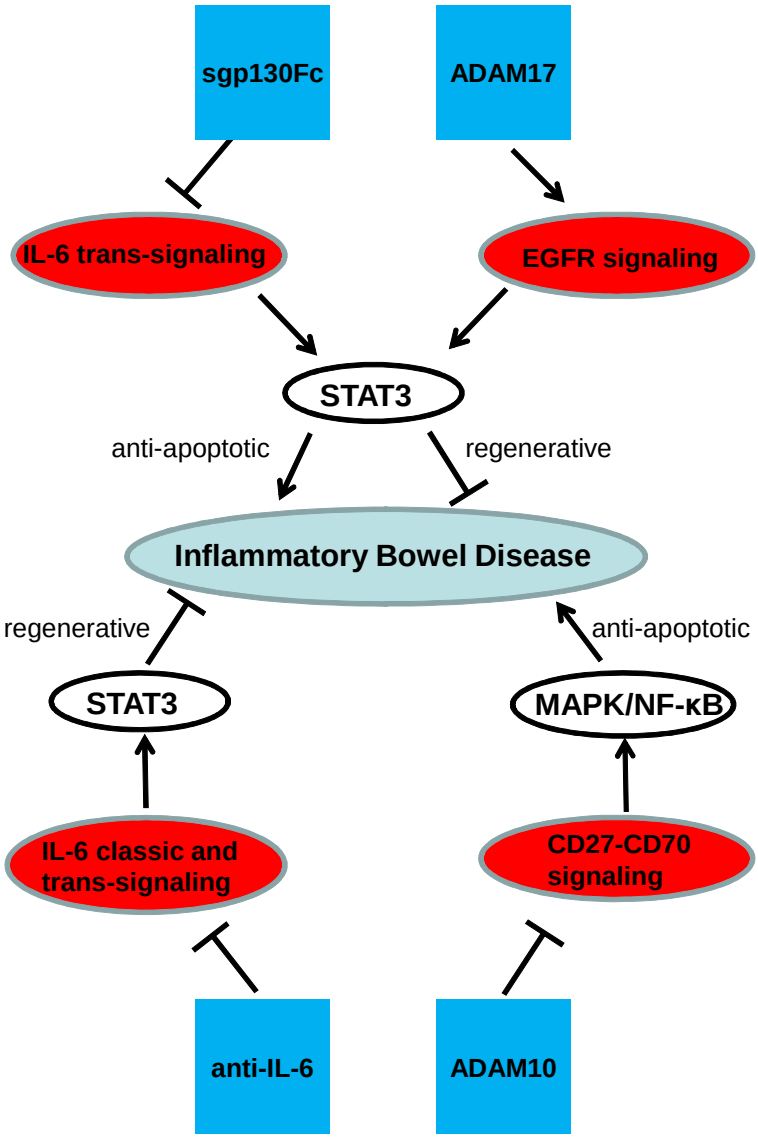

Fig. 3-3: Model of contributing pathways in inflammatory bowel disease induced by DSS. IL-6 trans-signaling promotes inflammatory bowel disease and can be inhibited by sgp130Fc. However, combined IL-6 signaling – comprised of classic and trans-signaling – as well as EGFR and CD27-CD70 signaling attenuate disease progression.

Interestingly, the major molecule, which IL-6 signaling as well as EGFR signaling share, is STAT3. STAT3 has two different functions: (i) it can act anti-apoptotic, e.g. during cancer or (ii) cell-proliferative during regeneration depending on the pathway. During IBD, STAT3 might be the decisive step. CD27/CD70 pathway signals via MAPK or NF-κB and also promotes cell survival and cell proliferation (Garcia et al. 2004; Neron et al. 2006).

Taken together, the data of this work demonstrate that inflammatory bowel disease is controlled by a complex molecular framework of at least four signal transduction pathways (see Fig. 3-3). These include IL-6 classic- and trans-signaling, ADAM17 mediated EGFR-signaling as well as suggested ADAM10 controlled CD27-CD70 signaling. Moreover, this network is even more complex, as these pathways are also interconnected. However, further experiments are required for a full understanding of the molecular framework which then might enable to develop therapeutic drugs against IBD.

4 Summary

Inflammatory bowel diseases (IBD), such as Crohn's disease and ulcerative colitis, are chronic inflammatory disorders of the gut charaterized by bloody diarrhea, ulcerations and infiltrations of inflammatory cells. The molecular mechanisms of the disease still remain unknown. In a mouse model, IBD can be induced i.a. by administration of DSS in drinking water for several days.

The metalloprotease ADAM17 is responsible for shedding of different substrates such as TNF-α, L-selectin or ligands of EGFR. Since ADAM17 knock-out mice are not viable, hypomorphic ADAM17$^{ex/ex}$ mice have been generated by our group. Shedding of L-selectin, EGFR ligands and TNF-α is impaired in these mice. To elucidate the role of ADAM17 in IBD, mice were treated with DSS. Surprisingly, ADAM17$^{ex/ex}$ mice were highly susceptible to DSS-induced colitis. They suffered from severe weight loss, destruction of crypts and increased permeability of the intestinal epithelium. Moreover, proliferation of intestinal epithelial cells in ADAM17$^{ex/ex}$ mice is impaired and treatment of ADAM17$^{ex/ex}$ mice with TGF or EGF could restore a regenerative response.

Other signaling pathways such as IL-6 classic- and trans-signaling are also involved in IBD. It is known that blocking the IL-6 trans-signaling pathway with sgp130Fc or anti-IL-6R antibody could ameliorate disease progression during TNBS-induced colitis. To elucidate the role of IL-6 trans-signaling during DSS-induced colitis, C57BL/6N mice were injected with sgp130Fc and anti-IL-6 antibody. Although no significant difference in weight loss could be detected, colon architecture, determined by colonoscopy as well as HE staining, revealed that sgp130Fc injected mice have less inflammation than control mice or those treated with anti-IL-6 antibody. This indicates that sgp130Fc might ameliorate disease progression and, therefore, represents a potential therapeutic agent of IBD.

Taken together, all results demonstrate that different signaling pathways, e.g. EGFR signaling, IL-6 classic and trans-signaling as well as CD27-CD70 signaling are involved in inflammatory bowel disease induced by DSS.

5 Zusammenfassung

Entzündliche Darmerkrankungen, zu denen Morbus Crohn und Colitis Ulcerosa gehören, sind chronisch-entzündliche Darmerkrankungen, welche durch blutigen Durchfall, Ulzerationen und Einwanderungen von Immunzellen gekennzeichnet sind. Die molekularen Mechanismen sind jedoch bislang ungeklärt. Colitis kann im Mausmodell u.a. durch Applikation von DSS im Trinkwasser induziert werden.

Die Metalloprotease ADAM17 ist verantwortlich für die Freisetzung verschiedener Substrate wie TNF-α, L-Selectin, oder Liganden des EGFR. Da ADAM17 Knock-out Mäuse nicht lebensfähig sind, wurden hypomorphe ADAM17$^{ex/ex}$ Mäuse generiert. Die Freisetzung von L-Selectin, TNF-α sowie EGFR Liganden ist in diesen Mäusen beeinträchtigt. Um die Rolle von ADAM17 in entzündlichen Darmerkrankungen zu untersuchen, wurden ADAM17$^{ex/ex}$ Mäuse mit DSS behandelt. Überraschenderweise waren diese Mäuse stark anfällig für DSS-induzierte Colitis. Die Mäuse litten unter starkem Gewichtsverlust, Zerstörung der Krypten sowie einer erhöhten Permeabilität des Darmepithels. Proliferation der intestinalen epithelialen Zellen scheint in diesen Mäusen beeinträchtigt zu sein und eine Behandlung mit TGF-α oder EGF konnte die Regeneration dieser Zellen wiederherstellen.

Andere Signalwege wie z.B. der klassische IL-6 Signalweg oder IL-6 *trans-signaling* sind ebenfalls in chronisch-entzündlichen Darmerkrankungen involviert. Es ist bekannt, dass eine TNBS-induzierte Colitis durch Blockierung des Signalweges mit sgp130Fc oder anti-IL-6R Antikörper verbessert werden kann. Um die Rolle des IL-6 *trans-signaling* während einer DSS-induzierten Colitis zu untersuchen, wurden C57BL/6N Mäuse mit sgp130Fc und anti-IL-6 Antikörper behandelt. Die Mäuse zeigten keinen Gewichtsunterschied, jedoch verdeutlichte die Darmarchitektur, welche koloskopisch sowie an HE Schnitten untersucht wurde, dass sgp130Fc behandelte Mäuse weniger Entzündung aufwiesen als mit anti-IL-6 Antikörper behandelte. Dies deutete an, dass sgp130Fc den Verlauf der Erkrankung verbessern und somit ein potentielles Therapeutikum für entzündliche Darmerkrankungen darstellen könnte.

Zusammenfassend zeigen die Ergebnisse, dass verschiedene Signalwege wie EGFR *Signaling,* klassischer IL-6 Signalweg, IL-6 *trans-signaling* sowie der CD27-CD70 Signalweg in der DSS-induzierten Colitis eine wichtige Rolle spielen.

6 Material

6.1 Organisms and cell lines

Escherichia Coli XL1 Blue	Stratagene
sgp130Fc tg mice (C57BL/6N background)	Rabe et al. 2008
ADAM17$^{ex/ex}$ mice	Chalaris et al. accepted
IL-6 knockout mice	Charles River Laboratories
C57BL6/N mice	Charles River Laboratories
COS7 (monkey kidney fibroblast cell line)	DSMZ, German Resource Centre for Biological Material
HEK (human embryonic kidney cells)	DSMZ, German Resource Centre for Biological Material

6.2 Chemical

Acetic acid	Roth
Agar-Agar	Roth
Agarose, SeaKem LE Agarose	Cambrex BioScience Rocklan
Ammonium persulfate (APS)	Merck
Ampicillin	Roth
Azoxymethane	Sigma-Aldrich
BM Blue POD Substrat	Roche
Bovine serum albumin (BSA, Fraction V)	ICN Biomedicals Inc.
Bromphenol blue	Sigma
dNTPs	Fermentas
Dimethyl sulfoxide (DMSO)	Roth
Dextran sulfate sodium (DSS, MW 40,000 Da)	TdB Cosultancy
EDTA	Gibco
Ethanol	Roth
Ethidium bromide	Roth
Fetal calf serum (FCS)	PAA
Formaldehyde	Roth
FITC-Dextran 4000	Sigma-Aldrich
G-418-sulfate	PAA
GeneRuler DNA Ladder	Fermentas

Glycine	Roth
Glycerol	Roth
HCl	Roth
Isopropanol	Roth
2-Mercaptoethanol	Merck
Methanol	Roth
$MgCl_2$	Fermentas
Milk powder	Roth
Myeloperoxidase (MPO)	Sigma-Aldrich
Penicillin/Streptomycine (P/S)	PAA
p-Nitrophenol-Phosphate	Sigma-Aldrich
Polyacrylamide Rotiphorese Gel 30	Roth
Sodium chloride	Roth
Sodium dodecyl sulfate (SDS)	Roth
Sodium hydroxide	Roth
Sulfuric acid	Sigma-Aldrich
N,N,N',N'-tetramethylethan-1,2-diamin	Roth
Tryptone/peptone	Roth
Tween 20	Roth
Yeast extract	Roth

6.3 Media

DMEM culture medium	PAA, supplemented with 10% (v/v) FCS, 1% (v/v) P/S
RPMI-1640 culture medium	PAA, supplemented with 10% (v/v) FCS, 1% (v/v) P/S, 1% (v/v) HEPES, 1mM ß-mercaptoethanol, without L-glutamine
LB medium	10g NaCl, 10g tryptone, 5g yeast extract, ad 1l Milli-Q H_2O, autoclaved
LB agar medium	20g Agar-Agar in 1l LB medium, autoclaved
LB_{amp} Agar	20g Agar-Agar in 1l LB medium, autoclaved, afterwards supplemented with 50µg/ml Ampicillin

6.4 Buffers and solutions

6.4.1 Different solutions and buffers

Ampicillin stock solution	50mg/ml
Ammonium persulfate (APS)	10% (w/v) in Milli-Q H_2O
BM blue POD	Roche
6x DNA loading dye	Fermentas
Erythrocytes lysis buffer	150mM NH_4Cl, 10mM $KHCO_3$, 100nM EDTA
FACS buffer	1% BSA, 2mM EDTA, in 1xPBS
MPO buffer	0.05 KPO_4, 0.5% $C_{19}H_{42}BrN$
5x TBE	44.5mM Tris, 44.5mM boric acid, 10mM EDTA, pH 8.0
Trypsin/EDTA (10x)	PAA
SDS stock solution	10% (w/v) in Milli-Q H_2O
AP buffer	0.1M Glycine, 1mM $MgCl_2$, 1mM $ZnCl_2$, pH 10.8
Lysis buffer	50mM Tris, pH 7.5, 150mM NaCl, 1% (v/v) Triton X-100, one Complete pellet

6.4.2 SDS-polyacrylamide gelelectrophoresis and Western blot

10x SDS running buffer	92M glycine, 0.25M Tris-HCl, pH 8.3, 1M SDS
4x SDS loading dye	500mM Tris-HCl pH 6.8, 50% (v/v) glycerol, 10% (w/v) SDS, 2% (v/v) β-mercaptoethanol, 1% (w/v) bromphenolblue
Transfer buffer	25mM Tris, 0.2M glycine, 20% methanol, pH 8.5
10x TBS (*Tris buffered Saline*)	50mM Tris, 1.5M NaCl, pH 7.5
TBST	1x TBS, 0.1% Tween 20
Blocking solution	3% (w/v) BSA or milk powder in TBST

6.4.3 ELISA

Washing buffer	0.05% Tween 20 in 1x PBS
Reagent diluent	1% BSA, 0.05% Tween 20 in 1x PBS
Stop Solution	1.8M H_2SO_4
10x PBS (*phosphate buffer saline*)	0.1M NaH_2PO_4, 1.5M NaCl, pH 7.5

6.4.4 Immunohistochemistry

Shadon Gill III Hematoxylin	Thermo Scientific
Giemsa's azure eosin methylene blue	Merck
AEC substrate	Dako
Blocking reagent	Dako
Antibody Diluent	Dako
DAPI (20mg/ml)	Sigma-Aldrich

6.4.5 Cell stimulation

BzATP	Sigma-Aldrich
GI254023X	Ludwig et al. 2005
GW280264X	Ludwig et al. 2005
Fc-Block	BD Biosciences Pharmingen™
Rat serum	Jackson ImmunoResearch
Ionomycin calcium salt	Sigma-Aldrich

6.5 Enzymes

All used enzymes which were not included in a kit were purchased from Fermentas.

6.6 Antibodies

Goat Anti-Mouse IgG POD	Pierce
Goat Anti-Rabbit IgG POD	Pierce
Rabbit Anti-mouse IgG	Dako
Cy3-conjugated donkey Anti-mouse IgG	Jackson Immuno Research
FITC labeled donkey Anti-mouse IgG	Jackson Immuno Research
Goat Anti-CD27 (C-20) IgG	Santa Cruz Biotechnology, Inc.
Mouse Anti-BrdU IgG	Sigma-Aldrich
PE hamster Anti-mouse CD27	BD Biosciences Pharmingen™
APC hamster Anti-mouse CD3e	BD Biosciences Pharmingen™
FITC rat Anti-mouse B220	BD Biosciences Pharmingen™
FITC mouse Anti-rat CD4	BD Biosciences Pharmingen™
PE rat Anti-mouse CD62L	BD Biosciences Pharmingen™
Rabbit Anti-CD3 IgG	abcam

Mouse Anti-CD68 IgG	Santa Cruz Biotechnology
Rabbit Anti-Phospho Stat3 IgG	Cell Signaling
Rabbit Anti-CyclinD1 IgG	Cell Signaling
Rat Anti-mouse MP5-20F3	In Vivo BioTech
Rabbit Anti-FLAG	Sigma-Aldrich
Rabbit Anti-ADAM17	Chemicon

6.7 Oligonucleotides (Primer)

All oligonucleotides used were synthesized from Metabion. Sequences are shown in Tab. 6-1.

Tab. 6-1: Used primers and their sequences

Name	Sequence (5'-3')	Tm (℃)
3'floxADAM17geno	CTTATTATTCTCGTGGTCACC	54.2
5'floxADAM17geno	TATGTGATAGGTGTAATG	46.9
T7-Promotor	TAATACGACTCACTATAGGG	52
M13-reverse	CATGGTCATAGCTGTTTCC	54.5
IL-6KO-Screen- P1	TTCCATCCAGTTGCCTTCTTGG	60.6
IL-6KO-Screen- P2	TTCTCATTTCCACATTTCCCAG	55.8
IL-6KO-Screen- Pneo	CCGGAGAACCTGCGTGCAATCC	67.2
CD27_AflII_2	AAAACTTAAGACCCTAGCCCCAAACAGC TG	63.3
CD27_NotI_2	AAAAGCGGCCGCAGGGTAGAAAGCAG GCTCGG	66.4

6.8 Kits

ECL Plus Westernblotting Detection System	Amersham
NucleoSpin ExtractII	Macherey-Nagel
NucleobondAX	Macherey-Nagel
NucleoSpin RNAII	Macherey-Nagel
DuoSet Mouse KC (DY453)	R&D Systems
DuoSet Mouse JE (DY479)	R&D Systems
DuoSet Mouse IL-10 (DY417)	R&D Systems
DuoSet Mouse IL-11 (DY418)	R&D Systems
DuoSet Mouse IL-6 (DY479)	R&D Systems
DuoSet Mouse IL-17 (DY421)	R&D Systems
DuoSet Mouse TNF-α (DY410)	R&D Systems
DuoSet Mouse $sTNFR_{II}$ (DY426)	R&D Systems
DuoSet Mouse IL-12 p70 (DY419)	R&D Systems

DuoSet Mouse IL-21 (DY594)	R&D Systems
DuoSet Mouse IFN-γ (DY485)	R&D Systems
DuoSet Human sgp130 (DY228)	R&D Systems
Haemoccult Test	Beckmann Coulter
Puregene Tissue Core Kit A	Qiagen

6.9 Vectors

pcDNA3.1-DEST40	Invitrogen
pMOWS	Ketteler et al. 2002

For detailed vector descriptions see appendix.

6.10 Recombinant proteins

sgp130Fc	purified from supernatant of stably transfected CHO cells as described (Jostock et al. 2001)

6.11 Electric devices and other materials

6.11.1 Centrifuges

Centrifuge 5417R	Eppendorf
Speed-Vac Universal Vacuum System Plus UVS400A	Savant

6.11.2 Incubators

HeraCell CO_2-Incubator	Heraeus Instruments
Thermomixer compact	Eppendorf
Assistent RM5	EYDAM

6.11.3 Electrophoresis devices and power supplies

Mini-sub cell	BIO-RAD
Mini-Protein 3 Electrophoresis Cell	BIO-RAD
Trans-Blot SD Semi-Dry Transfer Cell	BIO-RAD
PowerPac 200	BIO-RAD

6.11.4 Microscopes

Microscope TELAVAL 31	ZEISS
Fluorescence microscope CKX41	Olympus

6.11.5 Other devices

Multipipette	Eppendorf
Sterile working bench Hera safe	Heraeus
Milli-Q Academic System	Millipore
GelDoc 2000	BIO-RAD
Robocycler Gradient 96	Stratagene
PeqStar 96 Universal Gradient	Peqlab
FluorChemQ	Alpha Innotech
NanoDrop ND-1000 spectrophotometer	Thermo Scientific
HOPKINS Optik 64019BA	Karl Stolz AIDA™ VET
BDFACSCanto	BD Biosciences Pharmingen™
96-well-Photometer SCT Rainbow	Tecan

6.11.6 Consumables

0.5ml, 1.5ml and 2ml micro tube	Sarstedt
Petri dishes (∅ 10cm)	Sarstedt
Pipette tips	Sarstedt
Tube 15ml and 50ml	Sarstedt
Hyperfilm	Amersham Biosciences
PVDF-membrane *Highbond P*	Amersham Biosciences
Tissue culture plate (∅ 10cm)	Sarstedt
Tissue culture dish 6/96-well	Sarstedt
Nunc-ImmunoPlate	Thermo Fisher Scientific
100 Sterican size 1/2/14/18/20	Braun
Injekt-F (1ml)	Braun
Surgical Disposable Scalpels	Braun
Nylon mesh, 40mm cell strainer	BD Biosciences Pharmingen

7 Methods

7.1 Isolation of RNA

Extraction of RNA from mouse spleen cells was performed using the NucleoSpin RNAII Kit from Macherey-Nagel according to manufacturer's protocol.

7.2 cDNA synthesis

cDNA synthesis was performed using RevertAidM-MuLV Reverse Transcriptase according to manufacturer's protocol.

7.3 Polymerase chain reaction (PCR)

Nucleic acid sequences can be amplified by using polymerase chain reaction. This method can be divided into three different steps: (i) denaturation, (ii) annealing and (iii) elongation. After DNA denaturation specific primers bind during the annealing phase to the template and the defined region of the DNA is replicated during the elongation phase. By repeated denaturation, annealing and elongation for several cycles the specific DNA sequence is amplified exponentially.

Standard PCR was performed using the components shown in Tab. 7-1. The PCR was carried out with the following PCR program: 95°C 5min, up to 35x (95℃ 1min, T_m 1min, 72℃ 1min), 72℃ 5min. T_m equals the primer annealing temperature as estimated by the program pDRAW32. PCR products were analyzed by agarose gel electrophoresis.

Tab. 7-1: Components of a standard PCR

Component	Volume [µl]
Template 1-100ng	X
DreamTaq buffer (10x)	5
$MgCl_2$ (25mM)	4
dNTP-Mix (10mM)	1
Primer A (100pM)	2.5
Primer B (100pM)	2.5
DreamTaq DNA Polymerase (1U/µl)	1
Milli Q H_2O	ad 50

7.4 Reverse-transcriptase (RT) PCR

RNA was isolated from different organs and 2 µg were reverse transcribed into cDNA using Reverse Aid M-MuLV reverse transcriptase (Fermentas). ADAM17 transcripts were subsequently amplified by PCR using the following primer pair:
3' und 5' floxADAM17geno.

7.5 Agarose gel electrophoresis

Nucleic acids were separated in 0.7% to 2% (w/v) agarose gels supplemented with 0.05% (v/v) ethidium bromide. The electrophoresis was performed in horizontal gel chambers at 90 to 120 volt. Fragment sizes were estimated using DNA ladders (Fermentas).

7.6 DNA digestion with restriction enzymes

Restriction enzymes cut DNA at specific nucleotide sequences. The recognition sequences are palindromic and vary in length between 4 and 8 nucleotides. The digestion leads, depending on the enzyme, to sticky or blunt ends. Reactions were performed according to manufacturer's protocol.

7.7 Extraction of nucleic acids from agarose gels

Bands were excised from agarose gel and purified using NucleoSpin ExtractII Kit (Macherey-Nagel) according to manufacturer's protocol.

7.8 Ligation

Purified DNA-fragments were ligated into linearized plasmids using T4-DNA-ligase (Fermentas) with five-fold molar excess of insert. The reaction was prepared according to manufacturer's protocol, incubated over night at 4℃ and used directly for transformation (see section 7.9).

7.9 Transformation of chemocompetent *E.coli* XL1-Blue

10µl of ligation reaction was mixed with 50µl of chemocompetent *E.coli* XL1-Blue, incubated for 5min on ice, heat-shocked at 42℃ for 30s and incubated once more for 5min on ice. Cells were then suspended in 1ml LB medium and incubated for 1h at

37℃ and 750rpm. Afterwards transformants were selected on LB agar plates containing appropriate antibiotics and analyzed via Colony-check PCR (see 7.10).

7.10 Colony-check PCR

Colony-check PCR was used to screen bacterial colonies for the presence of a transformed plasmid. Total DNA contained in bacterial colony served as template. PCR was carried out using standard PCR parameters (see 7.3).

7.11 Purification of plasmid DNA

Extraction of plasmid DNA was performed using the Nucleobond® AX Kit from Macherey-Nagel according to manufacturer's protocol.

7.12 Quantification of nucleic acids

Amount and purity of nucleic acids were determined using NanoDrop ND-1000 spectrophotometer (Thermo Scientific) by measuring absorbance at 230, 260 and 280nm.

7.13 Sequencing

Sequencing of plasmid DNA was performed by GATC Biotech and SeqLab using chain terminator method (Sanger et al. 1977).

7.14 Cultivation of eukaryotic COS7 or HEK cells

COS7 cells are adherent African green monkey kidney fibroblasts and HEK cells are human embryonic kidney cells. Cells were cultivated in DMEM-medium containing 10% FCS as well as 1% P/S (penicillin/streptomycin) and were grown at 37℃, 5% CO_2 and 100% humidity in a cell incubator. For passaging, cells were detached using Trypsin-EDTA and splitted 1:10 or 1:100.

7.15 Transfection of eukaryotic cells

The transfection of COS7 as well as HEK cells was performed using TurboFect™ transfection reagent (Fermentas). One day before transfection, 500,000 cells were sown on a 6-well plate and grown for 24h at 37℃, 5 % CO_2 and 100% humidity. Next

day, 1µg DNA and 2µl TurboFect™ Transfection Reagent were mixed in 200µl serum-free DMEM-medium, incubated for 15min at room temperature and distributed to the bottom of each well. The transgene expression was analyzed after 48 hours by fluorescence microscopy or western blot.

7.16 Sodium dodecyl sulfate polyacrylamide gel electrophoresis (SDS-PAGE)

SDS-PAGE is a method to separate proteins according to their electrophoretic mobility and allows the analysis of proteins via staining or Western blotting. Furthermore, molecular weight of analyzed proteins can be determined using molecular weight marker.

Proteins were separated by discontinous gel electrophoresis. Compositions of the different gels are shown in Tab. 7-2. Electrophoresis was performed in 1x SDS-running buffer. Protein samples were supplemented with 4x SDS-loading dye and loaded onto the gel. Electrophoresis was carried out at 120-180V for 90 to 120min.

Tab. 7-2: Gel components for SDS-PAGE

Component	Stacking gel [µl]	Separating gel [µl]
Milli Q H_2O	1860	750
1.5M Tris/HCl, pH 8.8	-	850
0.5M Tris/HCl, pH 6.8	310	-
10% SDS	25	33
Polyacrylamide	330	1650
10% APS	25	33
TEMED	5	3

7.17 Western Blot

Proteins separated by SDS-PAGE were transferred to PVDF-membrane using semi-dry blotting (60 min, 3-4mA/cm^2). The membrane was blocked with TBST supplemented with BSA or milk powder (dependent on the primary antibody) for 1h. After washing with TBST membrane was incubated with primary antibody over-night at 4℃. Washed membranes were incubated with second ary antibody for 1h at room temperature. Unbound antibodies were washed away with TBST. Membranes were developed using the ECL-detection solution (GE Healthcare) and signals were detected using chemiluminescent FluorChemQ imaging system (AlphaInnotech).

7.18 Animal treatment

All experiments were performed according to German guidelines for animal care and protection (V742-72 241.121-3 (20-2/04) and (76-7/00) as well as V312-72241.121-3). Mice were maintained in a 12h light-dark cycle under standard conditions and were provided with food and water ad libitum. All animals were pathogen free as assessed by regular microbiological screening and kept under barrier conditions at 21℃ ± 2℃ and 60% ± 5% humidity in individually ventilated cages.

7.19 Induction of DSS-colitis and determination of clinical scores

Colitis was induced by administration of 2% dextran sulfate sodium (DSS) in the drinking water for 5d followed by 5d of regular drinking water or by administration of 2% DSS for 7d. Groups of four to six mice were used to monitor the disease activity index (DAI, see Tab. 7-3). Body weight and fecal blood loss using the hemoccult test were recorded daily. DAI displaying the combined score of weight loss, rectal bleeding and histology was performed as previously described by Siegmund et al. 2001 and Grivennikov et al. 2009. A high resolution mouse video endoscopic system was used (HOPKINS® Optik 64019BA; KARL STOLZ AIDA^{TM} VET, Berlin, Germany) and murine endoscopic score of colitis severity (MEICS, see Tab. 7-3) were obtained as described by Fantini et al. (2006).

Tab. 7-3: Components of DAI and MEICS

Disease Activity Index	Murine Endoscopic Score of Colitis Severity (MEICS)
Weight loss	Inflammatory signs in colonoscopy
Rectal bleeding	
Histology	

7.20 Colon organ culture

A segment of the distal colon was removed, cut open longitudinally and washed in PBS. Colon segments were then further cut into pieces of 1cm^2 and incubated in 6-well culture dish containing 2ml fresh DMEM medium supplemented with penicillin and streptomycin at 37℃ for 24h. Culture supernata nts were harvested and assayed for KC, MCP-1, IL-10, IL-11, IL-12, IL-21, IL-17 and IFN-γ levels by ELISA (R&D Systems, Wiesbaden, Germany) according to the manufacturer's protocols. Optical

densities were measured at 450nm using ELISA plate reader (SLT Rainbow, Tecan, Maennedorf, Switzerland) and were evaluated using a standard curve.

7.21 Myeloperoxidase activity measurement

Myeloperoxidase (MPO) activity was measured in colon tissue taken from the distal colon. After freezing in liquid nitrogen, equal aliquots of tissue samples (30µl buffer/mg colon tissue) were homogenized in MPO buffer, incubated at 60℃ for 2h and centrifuged for 5min at 10,000rpm. 10µl of the supernatant were mixed with 50µl peroxidase substrate. After 20min 50µl of H_2SO_4 were added to stop the reaction and the absorbance was measured at 450nm on a SLT Rainbow plate reader (Tecan, Maennedorf, Switzerland) and evaluated using a standard curve.

7.22 FITC dextran and BrdU administration

Intestinal permeability was assessed by administration of the non-metabolizable macromolecule FITC-dextran 4000 (Sigma-Aldrich, Deisenhofen, Germany). FITC-dextran was administered by gavage (0.6g/kg body weight) 4h before sacrifice. Whole blood and serum were obtained by cardiac puncture and centrifugation at 5,000rpm for 15min respectively. Dilutions of FITC-dextran 4,000 in PBS were used as a standard curve and absorption of 100µl serum or standard was measured in a fluorometer at 488nm. To study proliferation of epithelial cells 50mg BrdU/kg body weight (CalBiochem, Schwalbach, Germany) was injected intraperitoneally 2h before sacrifice.

7.23 Statistical analysis

All parametric data are presented as the means ± standard deviation. Data from two groups were analyzed for significance using a student's unpaired t-test (http://www.physics.csbsju.edu/stats/t-test.html). Differences were considered as statistically significant if $p \leq 0.05$.

7.24 Immunohistochemistry (IHC)

7.24.1 Processing of tissues

Colon tissue, especially the distal part, was removed and fixed in 4% paraformaldehyde in 1xPBS for 24h. Tissues were dehydrated in an ascending

ethanol and xylol series. Samples were embedded in paraffin and dissected with 5µm using a microtome (Leica RM2165).

For cryosections the last third of the colon was frozen with tissue freezing medium (Jung) in liquid nitrogen and dissected with 6µM using cryomicrotome (Leica CM3050S).

7.24.2 HE staining

Processed tissue sections were incubated in Shadon Gill III Hematoxylin, differentiated in 0.5% acetic acid, washed and stained with Giemsa's azur eosin methylen blue solution. The stained sections were analyzed by microscopy.

7.24.3 BrdU staining

To visualize BrdU incorporation sections were stained with 1:500 dilution of mouse anti-BrdU mAb in Antibody Diluent over night. Sections were then incubated for 1h with biotinylated anti-mouse secondary antibody (1:50 in Antibody Diluent) and developed with AEC substrate. Counterstaining was performed with Shadon Gill III Hemytoxylin. Stained sections were analyzed by microscopy.

7.24.4 Immunofluorescence staining

Processed cryosections were fixed in ice-cold acetone for 10min followed by sequential incubation with blocking reagent. Slides were then incubated for 1h at room temperature with α-CD3 or α-CD68 (1:50 or 1:100 in Antibody Diluent). After washing with PBS, slides were incubated for 45min at room temperature with Cy3- or FITC-labeled secondary antibodies. Nuclei were counterstained with DAPI (20mg/ml).

7.25 Isolation of spleen cells from C57BL/6N mice

Spleen was isolated from C57BL/6N mice and passed through a nylon mash into a 50ml tube containing 10ml RPMI-medium supplemented with 25mM $NaHCO_3$, 2mM glutamine, 1% penicillin/streptomycin and 10mM HEPES. The cell suspension was centrifuged at 1,300rpm for 5min at room temperature. The cell pellet was resupended with erythrocytes lysis buffer, incubated for 3min at room temperature and centrifuged again at 1,300rpm for 5min. The supernatant was discarded and cells were resuspended in 1ml RPMI-medium and counted using Neubauer counting chamber.

7.26 Cell stimulation

7.26.1 Spleen cells

Isolated spleen cells were stimulated with BzATP (300µM), GI (ADAM10 inhibitor) or GW (ADAM10+17 inhibitor). $4x10^6$ spleen cells were sown in a 96 well plate and incubated with 3µM inhibitor at 37℃ 30min before stimulation with BzATP. Cells were centrifuged for 10min at 1,500rpm after 20min of BzATP stimulation, resuspended in FACS-buffer and used for FACS analysis.

7.26.2 COS7 or HEK cells

Transfected COS7 or HEK cells were pretreated with GI (ADAM10 inhibitor) for 30min at 37℃ and afterwards stimulated 30min with ionomycin (2,5µM) at 37℃. After stimulation, cells were detached from a 6well plate with 1ml FACS-buffer containing 2mM EDTA and counted using Neubauer counting chamber.

7.27 Fluorescence activated cell sorting (FACS)

7.27.1 Spleen cells

For FACS staining 10^6 stimulated cells were used. Cells were blocked with 0.25µl Fc-Block solution and 1µl rat serum for 30min on ice. Staining occurred with APC hamster anti-mouse CD3e, PE hamster anti-mouse CD27, FITC rat anti-mouse B220, FITC mouse anti-rat CD4 or PE rat anti-mouse CD62L (diluted 1:400 in 100µl FACS-buffer) for 30min at room temperature under dark conditions. Cells were centrifuged for 5min at 3,700rpm and 4℃, resuspended in 500µl FACS-buffer and analyzed by flow cytometry.

7.28 Alkaline phosphatase (AP) analysis

Transiently transfected COS7 or HEK cells with alkaline phosphatase (AP) constructs were analyzed 48h after transfection. Therefore, cells were stimulated with either ionomycin or ionomycin and GI as described in 7.25. Supernatant of cells was collected, centrifuged at 13,000rpm for 30min and 4℃ and afterwards used for AP analysis. Cells were harvested with 1xPBS, centrifuged (1min, 13,000rpm), resupended in 75µl lysis buffer and incubated for 1h at 4℃. Afterwards, cell lysate was centrifuged for 30min at 4℃ and the supernatant was used for AP analysis. 5µl of lysate and 50µl of supernatant was loaded on a 96well dish together with controls

and added with 50µl AP substrate. AP activity was measured at 405nm and ratio of supernatant and lysate AP activity was calculated.

7.29 Transgenic animals

7.29.1 Generation and characterization of hypomorphic ADAM17$^{ex/ex}$ mice

ADAM17$^{ex/ex}$ mice were generated in our group as described in section 2.1. DNA was isolated from mouse tails using Puregene Tissue Core Kit A according to the manufacturer's protocol. Afterwards the ADAM17 transcripts were amplified by PCR (7.3.1) using primers 3'floxADAM17geno and 5'floxADAM17geno (Tab. 6-1). PCR was performed with the following PCR program: 95℃ 5min, 35x (95℃ 1min, 52℃ 1min, 72℃ 1min), 72℃ 5min. PCR products were anal yzed by agarose gelelectrophoresis. PCR products of 550bp, 380bp or both were amplified from ADAM17$^{ex/ex}$, wildtype and heterozygous animals, respectively.

8 References

Akiba, H., H. Nakano, S. Nishinaka, M. Shindo, T. Kobata, M. Atsuta, C. Morimoto, C. F. Ware, N. L. Malinin, D. Wallach, H. Yagita and K. Okumura (1998). "CD27, a member of the tumor necrosis factor receptor superfamily, activates NF-kappaB and stress-activated protein kinase/c-Jun N-terminal kinase via TRAF2, TRAF5, and NF-kappaB-inducing kinase." J Biol Chem **273**(21): 13353-8.

Alonzi, T., I. P. Newton, P. J. Bryce, E. Di Carlo, G. Lattanzio, M. Tripodi, P. Musiani and V. Poli (2004). "Induced somatic inactivation of STAT3 in mice triggers the development of a fulminant form of enterocolitis." Cytokine **26**(2): 45-56.

Amano, A., I. Nakagawa and T. Yoshimori (2006). "Autophagy in innate immunity against intracellular bacteria." J Biochem **140**(2): 161-6.

Arribas, J., L. Coodly, P. Vollmer, T. K. Kishimoto, S. Rose-John and J. Massague (1996). "Diverse cell surface protein ectodomains are shed by a system sensitive to metalloprotease inhibitors." J Biol Chem **271**(19): 11376-82.

Atreya, R., J. Mudter, S. Finotto, J. Mullberg, T. Jostock, S. Wirtz, M. Schutz, B. Bartsch, M. Holtmann, C. Becker, D. Strand, J. Czaja, J. F. Schlaak, H. A. Lehr, F. Autschbach, G. Schurmann, N. Nishimoto, K. Yoshizaki, H. Ito, T. Kishimoto, P. R. Galle, S. Rose-John and M. F. Neurath (2000). "Blockade of interleukin 6 trans signaling suppresses T-cell resistance against apoptosis in chronic intestinal inflammation: evidence in crohn disease and experimental colitis in vivo." Nat Med **6**(5): 583-8.

Auernhammer, C. J., K. Zitzmann, F. Schnitzler, J. Seiderer, P. Lohse, G. Vlotides, D. Engelhardt, M. Sackmann, B. Goke and T. Ochsenkuhn (2005). "Role of the intracellular receptor domain of gp130 (exon 17) in human inflammatory bowel disease." World J Gastroenterol **11**(8): 1196-9.

Becker, C., M. C. Fantini, S. Wirtz, A. Nikolaev, H. A. Lehr, P. R. Galle, S. Rose-John and M. F. Neurath (2005). "IL-6 signaling promotes tumor growth in colorectal cancer." Cell Cycle **4**(2): 217-20.

Bigler, R. D., Y. Bushkin and N. Chiorazzi (1988). "S152 (CD27). A modulating disulfide-linked T cell activation antigen." J Immunol **141**(1): 21-8.

Black, R. A., C. T. Rauch, C. J. Kozlosky, J. J. Peschon, J. L. Slack, M. F. Wolfson, B. J. Castner, K. L. Stocking, P. Reddy, S. Srinivasan, N. Nelson, N. Boiani, K. A. Schooley, M. Gerhart, R. Davis, J. N. Fitzner, R. S. Johnson, R. J. Paxton, C. J. March and D. P. Cerretti (1997). "A metalloproteinase disintegrin that releases tumour-necrosis factor-alpha from cells." Nature **385**(6618): 729-33.

Blobel, C. P. (2005). "ADAMs: key components in EGFR signalling and development." Nat Rev Mol Cell Biol **6**(1): 32-43.

Bollrath, J., T. J. Phesse, V. A. von Burstin, T. Putoczki, M. Bennecke, T. Bateman, T. Nebelsiek, T. Lundgren-May, O. Canli, S. Schwitalla, V. Matthews, R. M. Schmid, T. Kirchner, M. C. Arkan, M. Ernst and F. R. Greten (2009). "gp130-

mediated Stat3 activation in enterocytes regulates cell survival and cell-cycle progression during colitis-associated tumorigenesis." Cancer Cell **15**(2): 91-102.

Borst, J., J. Hendriks and Y. Xiao (2005). "CD27 and CD70 in T cell and B cell activation." Curr Opin Immunol **17**(3): 275-81.

Boyer, J. L. and T. K. Harden (1989). "Irreversible activation of phospholipase C-coupled P2Y-purinergic receptors by 3'-O-(4-benzoyl)benzoyl adenosine 5'-triphosphate." Mol Pharmacol **36**(6): 831-5.

Breckwoldt, M. O., J. W. Chen, L. Stangenberg, E. Aikawa, E. Rodriguez, S. Qiu, M. A. Moskowitz and R. Weissleder (2008). "Tracking the inflammatory response in stroke in vivo by sensing the enzyme myeloperoxidase." Proc Natl Acad Sci U S A **105**(47): 18584-9.

Chalaris, A., N. Adam, C. Sina, P. Rosenstiel, J. Lehmann, P. Schirmacher, D. Hartmann, J. Cichy, O. Gavrilova, S. Schreiber, T. Jostock, V. Matthews, R. Häsler, C. Becker, M. F. Neurath, K. Reiß, P. Saftig, J. Scheller and S. Rose-John (accepted). "Critical Role of the Disintegrin Metalloprotease ADAM17 for Intestinal Inflammation and Regeneration in Mice." Journal of Experimental Medicine.

Cho, J. H. and C. T. Weaver (2007). "The genetics of inflammatory bowel disease." Gastroenterology **133**(4): 1327-39.

Derouet, D., F. Rousseau, F. Alfonsi, J. Froger, J. Hermann, F. Barbier, D. Perret, C. Diveu, C. Guillet, L. Preisser, A. Dumont, M. Barbado, A. Morel, O. deLapeyriere, H. Gascan and S. Chevalier (2004). "Neuropoietin, a new IL-6-related cytokine signaling through the ciliary neurotrophic factor receptor." Proc Natl Acad Sci U S A **101**(14): 4827-32.

Dieleman, L. A., B. U. Ridwan, G. S. Tennyson, K. W. Beagley, R. P. Bucy and C. O. Elson (1994). "Dextran sulfate sodium-induced colitis occurs in severe combined immunodeficient mice." Gastroenterology **107**(6): 1643-52.

Dillon, S. R., C. Sprecher, A. Hammond, J. Bilsborough, M. Rosenfeld-Franklin, S. R. Presnell, H. S. Haugen, M. Maurer, B. Harder, J. Johnston, S. Bort, S. Mudri, J. L. Kuijper, T. Bukowski, P. Shea, D. L. Dong, M. Dasovich, F. J. Grant, L. Lockwood, S. D. Levin, C. LeCiel, K. Waggie, H. Day, S. Topouzis, J. Kramer, R. Kuestner, Z. Chen, D. Foster, J. Parrish-Novak and J. A. Gross (2004). "Interleukin 31, a cytokine produced by activated T cells, induces dermatitis in mice." Nat Immunol **5**(7): 752-60.

Edwards, D. R., M. M. Handsley and C. J. Pennington (2008). "The ADAM metalloproteinases." Mol Aspects Med **29**(5): 258-89.

Egger, B., H. V. Carey, F. Procaccino, N. N. Chai, E. P. Sandgren, J. Lakshmanan, V. S. Buslon, S. W. French, M. W. Buchler and V. E. Eysselein (1998). "Reduced susceptibility of mice overexpressing transforming growth factor alpha to dextran sodium sulphate induced colitis." Gut **43**(1): 64-70.

Egger, B., F. Procaccino, J. Lakshmanan, M. Reinshagen, P. Hoffmann, A. Patel, W. Reuben, S. Gnanakkan, L. Liu, L. Barajas and V. E. Eysselein (1997). "Mice

lacking transforming growth factor alpha have an increased susceptibility to dextran sulfate-induced colitis." Gastroenterology **113**(3): 825-32.

Elliott, M. J., R. N. Maini, M. Feldmann, A. Long-Fox, P. Charles, P. Katsikis, F. M. Brennan, J. Walker, H. Bijl, J. Ghrayeb and J. N. Woody (1993). "Treatment of rheumatoid arthritis with chimeric monoclonal antibodies to tumor necrosis factor alpha." Arthritis Rheum **36**(12): 1681-90.

Franke, A., T. Balschun, T. H. Karlsen, J. Hedderich, S. May, T. Lu, D. Schuldt, S. Nikolaus, P. Rosenstiel, M. Krawczak and S. Schreiber (2008). "Replication of signals from recent studies of Crohn's disease identifies previously unknown disease loci for ulcerative colitis." Nat Genet **40**(6): 713-5.

Garcia, P., A. B. De Heredia, T. Bellon, E. Carpio, M. Llano, E. Caparros, P. Aparicio and M. Lopez-Botet (2004). "Signalling via CD70, a member of the TNF family, regulates T cell functions." J Leukoc Biol **76**(1): 263-70.

Grivennikov, S., E. Karin, J. Terzic, D. Mucida, G. Y. Yu, S. Vallabhapurapu, J. Scheller, S. Rose-John, H. Cheroutre, L. Eckmann and M. Karin (2009). "IL-6 and Stat3 are required for survival of intestinal epithelial cells and development of colitis-associated cancer." Cancer Cell **15**(2): 103-13.

Gu, H., J. C. Pratt, S. J. Burakoff and B. G. Neel (1998). "Cloning of p97/Gab2, the major SHP2-binding protein in hematopoietic cells, reveals a novel pathway for cytokine-induced gene activation." Mol Cell **2**(6): 729-40.

Hampe, J., A. Franke, P. Rosenstiel, A. Till, M. Teuber, K. Huse, M. Albrecht, G. Mayr, F. M. De La Vega, J. Briggs, S. Gunther, N. J. Prescott, C. M. Onnie, R. Hasler, B. Sipos, U. R. Folsch, T. Lengauer, M. Platzer, C. G. Mathew, M. Krawczak and S. Schreiber (2007). "A genome-wide association scan of nonsynonymous SNPs identifies a susceptibility variant for Crohn disease in ATG16L1." Nat Genet **39**(2): 207-11.

Hampe, J., H. Frenzel, M. M. Mirza, P. J. Croucher, A. Cuthbert, S. Mascheretti, K. Huse, M. Platzer, S. Bridger, B. Meyer, P. Nurnberg, P. Stokkers, M. Krawczak, C. G. Mathew, M. Curran and S. Schreiber (2002). "Evidence for a NOD2-independent susceptibility locus for inflammatory bowel disease on chromosome 16p." Proc Natl Acad Sci U S A **99**(1): 321-6.

Hartmann, D., B. de Strooper, L. Serneels, K. Craessaerts, A. Herreman, W. Annaert, L. Umans, T. Lubke, A. Lena Illert, K. von Figura and P. Saftig (2002). "The disintegrin/metalloprotease ADAM 10 is essential for Notch signalling but not for alpha-secretase activity in fibroblasts." Hum Mol Genet **11**(21): 2615-24.

Hassemer, E. L., S. M. Le Gall, R. Liegel, M. McNally, B. Chang, C. J. Zeiss, R. D. Dubielzig, K. Horiuchi, T. Kimura, Y. Okada, C. P. Blobel and D. J. Sidjanin (2010). "The waved with open eyelids (woe) Locus is a Hypomorphic Mouse Mutation in Adam17." Genetics **DOI:10.1534/genetics.109.113167**.

Heinrich, P. C., I. Behrmann, S. Haan, H. M. Hermanns, G. Muller-Newen and F. Schaper (2003). "Principles of interleukin (IL)-6-type cytokine signalling and its regulation." Biochem J **374**(Pt 1): 1-20.

Heinrich, P. C., I. Behrmann, G. Muller-Newen, F. Schaper and L. Graeve (1998). "Interleukin-6-type cytokine signalling through the gp130/Jak/STAT pathway." Biochem J **334** (Pt 2): 297-314.

Hirano, T., T. Taga, N. Nakano, K. Yasukawa, S. Kashiwamura, K. Shimizu, K. Nakajima, K. H. Pyun and T. Kishimoto (1985). "Purification to homogeneity and characterization of human B-cell differentiation factor (BCDF or BSFp-2)." Proc Natl Acad Sci U S A **82**(16): 5490-4.

Hirano, T., K. Yasukawa, H. Harada, T. Taga, Y. Watanabe, T. Matsuda, S. Kashiwamura, K. Nakajima, K. Koyama, A. Iwamatsu, S. Tsunasawa, F. Sakiyama, H. Matsui, Y. Takahara, T. Taniguchi and T. Kishimoto (1986). "Complementary DNA for a novel human interleukin (BSF-2) that induces B lymphocytes to produce immunoglobulin." Nature **324**(6092): 73-6.

Holgado-Madruga, M., D. R. Emlet, D. K. Moscatello, A. K. Godwin and A. J. Wong (1996). "A Grb2-associated docking protein in EGF- and insulin-receptor signalling." Nature **379**(6565): 560-4.

Horiuchi, K., T. Kimura, T. Miyamoto, K. Miyamoto, H. Akiyama, H. Takaishi, H. Morioka, T. Nakamura, Y. Okada, C. P. Blobel and Y. Toyama (2009). "Conditional inactivation of TACE by a Sox9 promoter leads to osteoporosis and increased granulopoiesis via dysregulation of IL-17 and G-CSF." J Immunol **182**(4): 2093-101.

Horiuchi, K., T. Kimura, T. Miyamoto, H. Takaishi, Y. Okada, Y. Toyama and C. P. Blobel (2007). "Cutting edge: TNF-alpha-converting enzyme (TACE/ADAM17) inactivation in mouse myeloid cells prevents lethality from endotoxin shock." J Immunol **179**(5): 2686-9.

Horiuchi, K., H. M. Zhou, K. Kelly, K. Manova and C. P. Blobel (2005). "Evaluation of the contributions of ADAMs 9, 12, 15, 17, and 19 to heart development and ectodomain shedding of neuregulins beta1 and beta2." Dev Biol **283**(2): 459-71.

Hugot, J. P., M. Chamaillard, H. Zouali, S. Lesage, J. P. Cezard, J. Belaiche, S. Almer, C. Tysk, C. A. O'Morain, M. Gassull, V. Binder, Y. Finkel, A. Cortot, R. Modigliani, P. Laurent-Puig, C. Gower-Rousseau, J. Macry, J. F. Colombel, M. Sahbatou and G. Thomas (2001). "Association of NOD2 leucine-rich repeat variants with susceptibility to Crohn's disease." Nature **411**(6837): 599-603.

Irie-Sasaki, J., T. Sasaki, W. Matsumoto, A. Opavsky, M. Cheng, G. Welstead, E. Griffiths, C. Krawczyk, C. D. Richardson, K. Aitken, N. Iscove, G. Koretzky, P. Johnson, P. Liu, D. M. Rothstein and J. M. Penninger (2001). "CD45 is a JAK phosphatase and negatively regulates cytokine receptor signalling." Nature **409**(6818): 349-54.

Ito, H. (2005). "Treatment of Crohn's disease with anti-IL-6 receptor antibody." J Gastroenterol **40** 32-4.

Jenkins, B. J., D. Grail, T. Nheu, M. Najdovska, B. Wang, P. Waring, M. Inglese, R. M. McLoughlin, S. A. Jones, N. Topley, H. Baumann, L. M. Judd, A. S. Giraud, A. Boussioutas, H. J. Zhu and M. Ernst (2005). "Hyperactivation of Stat3 in

gp130 mutant mice promotes gastric hyperproliferation and desensitizes TGF-beta signaling." Nat Med **11**(8): 845-52.

Jones, S. A., D. Novick, S. Horiuchi, N. Yamamoto, A. J. Szalai and G. M. Fuller (1999). "C-reactive protein: a physiological activator of interleukin 6 receptor shedding." J Exp Med **189**(3): 599-604.

Jones, S. A., P. J. Richards, J. Scheller and S. Rose-John (2005). "IL-6 transsignaling: the in vivo consequences." J Interferon Cytokine Res **25**(5): 241-53.

Jostock, T., J. Mullberg, S. Ozbek, R. Atreya, G. Blinn, N. Voltz, M. Fischer, M. F. Neurath and S. Rose-John (2001). "Soluble gp130 is the natural inhibitor of soluble interleukin-6 receptor transsignaling responses." Eur J Biochem **268**(1): 160-7.

Kaser, A., A. H. Lee, A. Franke, J. N. Glickman, S. Zeissig, H. Tilg, E. E. Nieuwenhuis, D. E. Higgins, S. Schreiber, L. H. Glimcher and R. S. Blumberg (2008). "XBP1 links ER stress to intestinal inflammation and confers genetic risk for human inflammatory bowel disease." Cell **134**(5): 743-56.

Kenny, P. A. (2007). "TACE: a new target in epidermal growth factor receptor dependent tumors." Differentiation **75**(9): 800-8.

Ketteler, R., S. Glaser, O. Sandra, U. M. Martens and U. Klingmuller (2002). "Enhanced transgene expression in primitive hematopoietic progenitor cells and embryonic stem cells efficiently transduced by optimized retroviral hybrid vectors." Gene Ther **9**(8): 477-87.

Kishimoto, T. (2010). "IL-6: from its discovery to clinical applications." Int Immunol **22**(5): 347-52.

Loenen, W. A., E. De Vries, L. A. Gravestein, R. Q. Hintzen, R. A. Van Lier and J. Borst (1992). "The CD27 membrane receptor, a lymphocyte-specific member of the nerve growth factor receptor family, gives rise to a soluble form by protein processing that does not involve receptor endocytosis." Eur J Immunol **22**(2): 447-55.

Long, C., Y. Wang, A. H. Herrera, K. Horiuchi Dagger and B. Walcheck (2010). "In vivo role of leukocyte ADAM17 in the inflammatory and host responses during E. coli-mediated peritonitis." J Leukoc Biol **DOI: 10.1189/jlb.1109763**.

Ludwig, A., C. Hundhausen, M. H. Lambert, N. Broadway, R. C. Andrews, D. M. Bickett, M. A. Leesnitzer and J. D. Becherer (2005). "Metalloproteinase inhibitors for the disintegrin-like metalloproteinases ADAM10 and ADAM17 that differentially block constitutive and phorbol ester-inducible shedding of cell surface molecules." Comb Chem High Throughput Screen **8**(2): 161-71.

Luedde, T., C. Liedtke, M. P. Manns and C. Trautwein (2002). "Losing balance: cytokine signaling and cell death in the context of hepatocyte injury and hepatic failure." Eur Cytokine Netw **13**(4): 377-83.

Lust, J. A., K. A. Donovan, M. P. Kline, P. R. Greipp, R. A. Kyle and N. J. Maihle (1992). "Isolation of an mRNA encoding a soluble form of the human interleukin-6 receptor." Cytokine **4**(2): 96-100.

Manocha, M., S. Rietdijk, A. Laouar, G. Liao, A. Bhan, J. Borst, C. Terhorst and N. Manjunath (2009). "Blocking CD27-CD70 costimulatory pathway suppresses experimental colitis." J Immunol **183**(1): 270-6.

Matsumoto, S., T. Hara, K. Mitsuyama, M. Yamamoto, O. Tsuruta, M. Sata, J. Scheller, S. Rose-John, S. Kado and T. Takada (2010). "Essential roles of IL-6 trans-signaling in colonic epithelial cells, induced by the IL-6/soluble-IL-6 receptor derived from lamina propria macrophages, on the development of colitis-associated premalignant cancer in a murine model." J Immunol **184**(3): 1543-51.

Matthews, V., B. Schuster, S. Schutze, I. Bussmeyer, A. Ludwig, C. Hundhausen, T. Sadowski, P. Saftig, D. Hartmann, K. J. Kallen and S. Rose-John (2003). "Cellular cholesterol depletion triggers shedding of the human interleukin-6 receptor by ADAM10 and ADAM17 (TACE)." J Biol Chem **278**(40): 38829-39.

Maxwell, J. R. and J. L. Viney (2009). "Overview of Mouse Models of Inflammatory bowel disease and their use in drug discovery." Current Protocols in Pharmacology **47**: 5.57.1-5.57.19.

McGowan, P. M., E. McKiernan, F. Bolster, B. M. Ryan, A. D. K. Hill, E. W. McDermott, D. Evoy, N. O'Higgins, J. Crown and M. J. Duffy (2007). "ADAM17 predicts adverse outcome in patients with breast cancer." AnnOncol **19**(6): 1070-1081.

Mitsuyama, K., S. Matsumoto, S. Rose-John, A. Suzuki, T. Hara, N. Tomiyasu, K. Handa, O. Tsuruta, H. Funabashi, J. Scheller, A. Toyonaga and M. Sata (2006). "STAT3 activation via interleukin 6 trans-signalling contributes to ileitis in SAMP1/Yit mice." Gut **55**(9): 1263-9.

Mitsuyama, K., E. Sasaki, A. Toyonaga, H. Ikeda, O. Tsuruta, A. Irie, N. Arima, T. Oriishi, K. Harada and K. Fujisaki (1991). "Colonic mucosal interleukin-6 in inflammatory bowel disease." Digestion **50**(2): 104-11.

Mitsuyama, K., A. Toyonaga, E. Sasaki, O. Ishida, H. Ikeda, O. Tsuruta, K. Harada, H. Tateishi, T. Nishiyama and K. Tanikawa (1995). "Soluble interleukin-6 receptors in inflammatory bowel disease: relation to circulating interleukin-6." Gut **36**(1): 45-9.

Moon, H., H. Y. Na, K. H. Chong and T. J. Kim (2006). "P2X7 receptor-dependent ATP-induced shedding of CD27 in mouse lymphocytes." Immunol Lett **102**(1): 98-105.

Moss, M. L. and J. W. Bartsch (2004). "Therapeutic benefits from targeting of ADAM family members." Biochemistry **43**(23): 7227-35.

Moss, M. L., S. L. Jin, M. E. Milla, D. M. Bickett, W. Burkhart, H. L. Carter, W. J. Chen, W. C. Clay, J. R. Didsbury, D. Hassler, C. R. Hoffman, T. A. Kost, M. H. Lambert, M. A. Leesnitzer, P. McCauley, G. McGeehan, J. Mitchell, M. Moyer, G. Pahel, W. Rocque, L. K. Overton, F. Schoenen, T. Seaton, J. L. Su and J.

D. Becherer (1997). "Cloning of a disintegrin metalloproteinase that processes precursor tumour-necrosis factor-alpha." Nature **385**(6618): 733-6.

Moss, M. L., L. Sklair-Tavron and R. Nudelman (2008). "Drug insight: tumor necrosis factor-converting enzyme as a pharmaceutical target for rheumatoid arthritis." Nat Clin Pract Rheumatol **4**(6): 300-9.

Mullberg, J., K. Althoff, T. Jostock and S. Rose-John (2000). "The importance of shedding of membrane proteins for cytokine biology." Eur Cytokine Netw **11**(1): 27-38.

Mullberg, J., F. H. Durie, C. Otten-Evans, M. R. Alderson, S. Rose-John, D. Cosman, R. A. Black and K. M. Mohler (1995). "A metalloprotease inhibitor blocks shedding of the IL-6 receptor and the p60 TNF receptor." J Immunol **155**(11): 5198-205.

Muller-Newen, G., A. Kuster, U. Hemmann, R. Keul, U. Horsten, A. Martens, L. Graeve, J. Wijdenes and P. C. Heinrich (1998). "Soluble IL-6 receptor potentiates the antagonistic activity of soluble gp130 on IL-6 responses." J Immunol **161**(11): 6347-55.

Murphy, G. (2008). "The ADAMs: signalling scissors in the tumour microenvironment." Nat Rev Cancer **8**(12): 929-41.

Murray, P. J. (2005). "The primary mechanism of the IL-10-regulated antiinflammatory response is to selectively inhibit transcription." Proc Natl Acad Sci U S A **102**(24): 8686-91.

Naka, T., N. Nishimoto and T. Kishimoto (2002). "The paradigm of IL-6: from basic science to medicine." Arthritis Res **4** S233-42.

Neron, S., G. Suck, X. Z. Ma, D. Sakac, A. Roy, Y. Katsman, N. Dussault, C. Racine and D. R. Branch (2006). "B cell proliferation following CD40 stimulation results in the expression and activation of Src protein tyrosine kinase." Int Immunol **18**(2): 375-87.

Nicholson, S. E., T. A. Willson, A. Farley, R. Starr, J. G. Zhang, M. Baca, W. S. Alexander, D. Metcalf, D. J. Hilton and N. A. Nicola (1999). "Mutational analyses of the SOCS proteins suggest a dual domain requirement but distinct mechanisms for inhibition of LIF and IL-6 signal transduction." Embo J **18**(2): 375-85.

Nolte, M. A., R. W. van Olffen, K. P. van Gisbergen and R. A. van Lier (2009). "Timing and tuning of CD27-CD70 interactions: the impact of signal strength in setting the balance between adaptive responses and immunopathology." Immunol Rev **229**(1): 216-31.

Ogura, Y., D. K. Bonen, N. Inohara, D. L. Nicolae, F. F. Chen, R. Ramos, H. Britton, T. Moran, R. Karaliuskas, R. H. Duerr, J. P. Achkar, S. R. Brant, T. M. Bayless, B. S. Kirschner, S. B. Hanauer, G. Nunez and J. H. Cho (2001). "A frameshift mutation in NOD2 associated with susceptibility to Crohn's disease." Nature **411**(6837): 603-6.

Okayasu, I., S. Hatakeyama, M. Yamada, T. Ohkusa, Y. Inagaki and R. Nakaya (1990). "A novel method in the induction of reliable experimental acute and chronic ulcerative colitis in mice." Gastroenterology **98**(3): 694-702.

Peschon, J. J., J. L. Slack, P. Reddy, K. L. Stocking, S. W. Sunnarborg, D. C. Lee, W. E. Russell, B. J. Castner, R. S. Johnson, J. N. Fitzner, R. W. Boyce, N. Nelson, C. J. Kozlosky, M. F. Wolfson, C. T. Rauch, D. P. Cerretti, R. J. Paxton, C. J. March and R. A. Black (1998). "An essential role for ectodomain shedding in mammalian development." Science **282**(5392): 1281-4.

Peters, M., A. M. Muller and S. Rose-John (1998). "Interleukin-6 and soluble interleukin-6 receptor: direct stimulation of gp130 and hematopoiesis." Blood **92**(10): 3495-504.

Pflanz, S., L. Hibbert, J. Mattson, R. Rosales, E. Vaisberg, J. F. Bazan, J. H. Phillips, T. K. McClanahan, R. de Waal Malefyt and R. A. Kastelein (2004). "WSX-1 and glycoprotein 130 constitute a signal-transducing receptor for IL-27." J Immunol **172**(4): 2225-31.

Podolsky, D. K. (2002). "Inflammatory bowel disease." N Engl J Med **347**(6): 417-29.

Pruessmeyer, J. and A. Ludwig (2009). "The good, the bad and the ugly substrates for ADAM10 and ADAM17 in brain pathology, inflammation and cancer." Semin Cell Dev Biol **20**(2): 164-74.

Rabe, B., A. Chalaris, U. May, G. H. Waetzig, D. Seegert, A. S. Williams, S. A. Jones, S. Rose-John and J. Scheller (2008). "Transgenic blockade of interleukin 6 transsignaling abrogates inflammation." Blood **111**(3): 1021-8.

Rose-John, S. and P. C. Heinrich (1994). "Soluble receptors for cytokines and growth factors: generation and biological function." Biochem J **300** (Pt 2): 281-90.

Rose-John, S., K. Mitsuyama, S. Matsumoto, W. M. Thaiss and J. Scheller (2009). "Interleukin-6 trans-signaling and colonic cancer associated with inflammatory bowel disease." Curr Pharm Des **15**(18): 2095-103.

Sahin, U. and C. P. Blobel (2007). "Ectodomain shedding of the EGF-receptor ligand epigen is mediated by ADAM17." FEBS Lett **581**(1): 41-4.

Sanderson, M. P., P. J. Dempsey and A. J. Dunbar (2006). "Control of ErbB signaling through metalloprotease mediated ectodomain shedding of EGF-like factors." Growth Factors **24**(2): 121-36.

Sanger, F., S. Nicklen and A. R. Coulson (1977). "DNA sequencing with chain-terminating inhibitors." Proc Natl Acad Sci U S A **74**(12): 5463-7.

Scheller, J., J. Grötzinger and S. Rose-John (2006). "Updating interleukin-6 classic- and trans-signaling." Signal Transduction **6**: 240-259.

Schiemann, W. P., J. L. Bartoe and N. M. Nathanson (1997). "Box 3-independent signaling mechanisms are involved in leukemia inhibitory factor receptor alpha- and gp130-mediated stimulation of mitogen-activated protein kinase. Evidence for participation of multiple signaling pathways which converge at Ras." J Biol Chem **272**(26): 16631-6.

Schmitz, J., M. Weissenbach, S. Haan, P. C. Heinrich and F. Schaper (2000). "SOCS3 exerts its inhibitory function on interleukin-6 signal transduction through the SHP2 recruitment site of gp130." J Biol Chem **275**(17): 12848-56.

Siegmund, B., H. A. Lehr, G. Fantuzzi and C. A. Dinarello (2001). "IL-1 beta - converting enzyme (caspase-1) in intestinal inflammation." Proc Natl Acad Sci U S A **98**(23): 13249-54.

Sunnarborg, S. W., C. L. Hinkle, M. Stevenson, W. E. Russell, C. S. Raska, J. J. Peschon, B. J. Castner, M. J. Gerhart, R. J. Paxton, R. A. Black and D. C. Lee (2002). "Tumor necrosis factor-alpha converting enzyme (TACE) regulates epidermal growth factor receptor ligand availability." J Biol Chem **277**(15): 12838-45.

Taga, T. and T. Kishimoto (1997). "Gp130 and the interleukin-6 family of cytokines." Annu Rev Immunol **15**: 797-819.

Thiel, S., H. Dahmen, A. Martens, G. Muller-Newen, F. Schaper, P. C. Heinrich and L. Graeve (1998). "Constitutive internalization and association with adaptor protein-2 of the interleukin-6 signal transducer gp130." FEBS Lett **441**(2): 231-4.

Vollmer, P., I. Walev, S. Rose-John and S. Bhakdi (1996). "Novel pathogenic mechanism of microbial metalloproteinases: liberation of membrane-anchored molecules in biologically active form exemplified by studies with the human interleukin-6 receptor." Infect Immun **64**(9): 3646-51.

Walev, I., P. Vollmer, M. Palmer, S. Bhakdi and S. Rose-John (1996). "Pore-forming toxins trigger shedding of receptors for interleukin 6 and lipopolysaccharide." Proc Natl Acad Sci U S A **93**(15): 7882-7.

Walmsley, M., D. M. Butler, L. Marinova-Mutafchieva and M. Feldmann (1998). "An anti-inflammatory role for interleukin-11 in established murine collagen-induced arthritis." Immunology **95**(1): 31-7.

Weskamp, G., K. Mendelson, S. Swendeman, S. Le Gall, Y. Ma, S. Lyman, A. Hinoki, S. Eguchi, V. Guaiquil, K. Horiuchi and C. P. Blobel (2010). "Pathological neovascularization is reduced by inactivation of ADAM17 in endothelial cells but not in pericytes." Circ Res **106**(5): 932-40.

Wirtz, S., C. Neufert, B. Weigmann and M. F. Neurath (2007). "Chemically induced mouse models of intestinal inflammation." Nat Protoc **2**(3): 541-6.

Xavier, R. J. and D. K. Podolsky (2007). "Unravelling the pathogenesis of inflammatory bowel disease." Nature **448**(7152): 427-34.

Yoshikawa, H., K. Takada and S. Muranishi (1984). "Molecular weight dependence of permselectivity to rat small intestinal blood-lymph barrier for exogenous macromolecules absorbed from lumen." J Pharmacobiodyn **7**(1): 1-6.

Zheng, X., F. Jiang, M. Katakowski, Z. G. Zhang, Q. E. Lu and M. Chopp (2009). "ADAM17 promotes breast cancer cell malignant phenotype through EGFR-PI3K-AKT activation." Cancer Biol Ther **8**(11): 1045-54.

9 Appendices

9.1 Vector maps

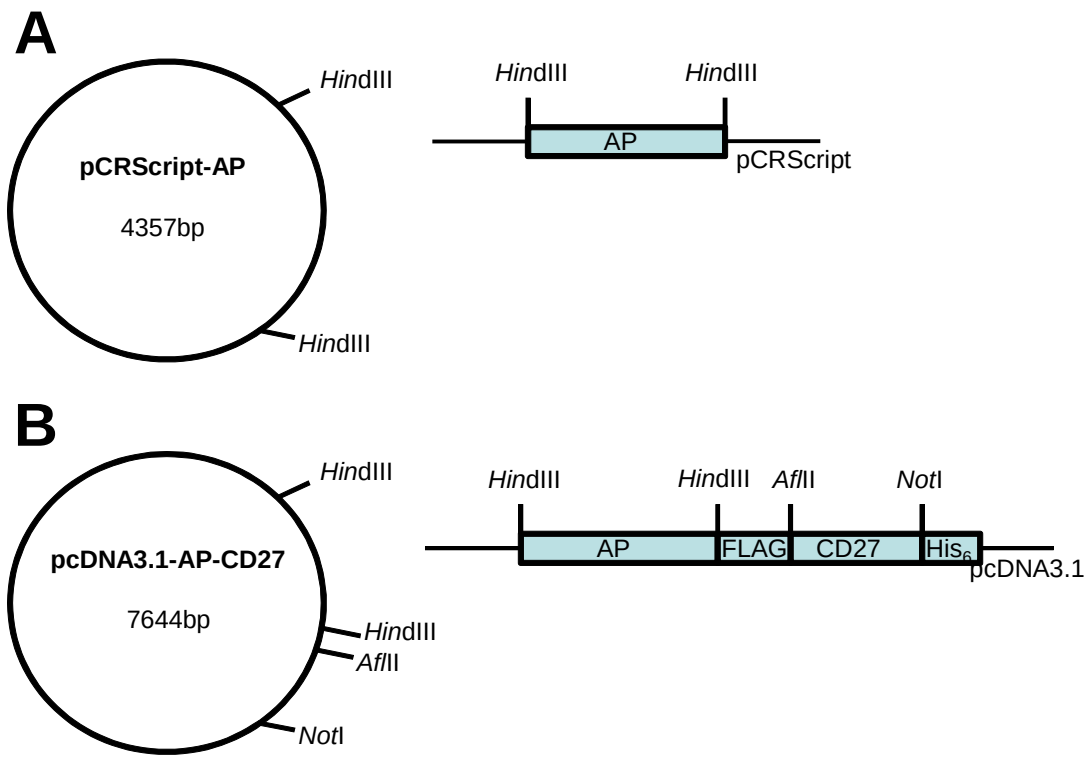

Fig. 9-1: Vector maps of pCRScript-AP and pcDNA3.1.-AP-CD27.

9.2 Sequence of pcDNA3.1-AP-CD27

GACGGATCGGGAGATCTCCCGATCCCCTATGGTGCACTCTCAGTACAATCTGCTCTGATGCCGCATAGTTAAGCC
AGTATCTGCTCCCTGCTTGTGTGTTGGAGGTCGCTGAGTAGTGCGCGAGCAAAATTTAAGCTACAACAAGGCAAG
GCTTGACCGACAATTGCATGAAGAATCTGCTTAGGGTTAGGCGTTTTGCGCTGCTTCGCGATGTACGGGCCAGAT
ATACGCGTTGACATTGATTATTGACTAGTTATTAATAGTAATCAATTACGGGGTCATTAGTTCATAGCCCATATA
TGGAGTTCCGCGTTACATAACTTACGGTAAATGGCCCGCCTGGCTGACCGCCCAACGACCCCCGCCCATTGACGT
CAATAATGACGTATGTTCCCATAGTAACGCCAATAGGGACTTTCCATTGACGTCAATGGGTGGAGTATTTACGGT
AAACTGCCCACTTGGCAGTACATCAAGTGTATCATATGCCAAGTACGCCCCCTATTGACGTCAATGACGGTAAAT
GGCCCGCCTGGCATTATGCCCAGTACATGACCTTATGGGACTTTCCTACTTGGCAGTACATCTACGTATTAGTCA
TCGCTATTACCATGGTGATGCGGTTTTGGCAGTACATCAATGGGCGTGGATAGCGGTTTGACTCACGGGGATTTC
CAAGTCTCCACCCCATTGACGTCAATGGGAGTTTGTTTTGGCACCAAAATCAACGGGACTTTCCAAAATGTCGTA
ACAACTCCGCCCCATTGACGCAAATGGGCGGTAGGCGTGTACGGTGGGAGGTCTATATAAGCAGAGCTCTCTGGC
TAACTAGAGAACCCACTGCTTACTGGCTTATCGAAATTAATACGACTCACTATAGGGAGACCCAAGCTGGCTAGC
GTTTAAACGATATCGCCACCATGGAGACAGACACACTCCTGCTATGGGTACTGCTGCTCTGGGTTCCAGGTTCCA
CTGGTGACAAGCTTATCATCCCAGTTGAGGAGGAGAACCCGGACTTCTGGAACCGCGAGGCAGCCGAGGCCCTGG
GTGCCGCCAAGAAGCTGCAGCCTGCACAGACAGCCGCCAAGAACCTCATCATCTTCCTGGGCGATGGGATGGGGG

TGTCTACGGTGACAGCTGCCAGGATCCTAAAAGGGCAGAAGAAGGACAAACTGGGGCCTGAGATACCCCTGGCCA
TGGACCGCTTCCCATATGTGGCTCTGTCCAAGACATACAATGTAGACAAACATGTGCCAGACAGTGGAGCCACAG
CCACGGCCTACCTGTGCGGGGTCAAGGGCAACTTCCAGACCATTGGCTTGAGTGCAGCCGCCCGCTTTAACCAGT
GCAACACGACACGCGGCAACGAGGTCATCTCCGTGATGAATCGGGCCAAGAAAGCAGGGAAGTCAGTGGGAGTGG
TAACCACCACACGAGTGCAGCACGCCTCGCCAGCCGGCACCTACGCCCACACGGTGAACCGCAACTGGTACTCGG
ACGCCGACGTGCCTGCCTCGGCCCGCCAGGAGGGGTGCCAGGACATCGCTACGCAGCTCATCTCCAACATGGACA
TTGACGTGATCCTAGGTGGAGGCCGAAAGTACATGTTTCGCATGGGAACCCCAGACCCTGAGTACCCAGATGACT
ACAGCCAAGGTGGGACCAGGCTGGACGGGAAGAATCTGGTGCAGGAATGGCTGGCGAAGCGCCAGGGTGCCCGGT
ATGTGTGGAACCGCACTGAGCTCATGCAGGCTTCCCTGGACCCGTCTGTGACCCATCTCATGGGTCTCTTTGAGC
CTGGAGACATGAAATACGAGATCCACCGAGACTCCACACTGGACCCCTCCCTGATGGAGATGACAGAGGCTGCCC
TGCGCCTGCTGAGCAGGAACCCCCGCGGCTTCTTCCTCTTCGTGGAGGGTGGTCGCATCGACCATGGTCATCATG
AAAGCAGGGCTTACCGGGCACTGACTGAGACGATCATGTTCGACGACGCCATTGAGAGGGCGGGCCAGCTCACCA
GCGAGGAGGACACGCTGAGCCTCGTCACTGCCGACCACTCCCACGTCTTCTCCTTCGGAGGCTACCCCCTGCGAG
GGAGCTCCATCTTCGGGCTGGCCCCTGGCAAGGCCCGGGACAGGAAGGCCTACACGGTCCTCCTATACGGAAACG
GTCCAGGCTATGTGCTCAAGGACGGCGCCCGGCCGGATGTTACCGAGAGCGAGAGCGGGAGCCCCGAGTATCGGC
AGCAGTCAGCAGTGCCCCTGGACGAAGAGACCCACGCAGGCGAGGACGTGGCGGTGTTCGCGCGCGGCCCGCAGG
CGCACCTGGTTCACGGCGTGCAGGAGCAGACCTTCATAGCGCACGTCATGGCCTTCGCCGCCTGCCTGGAGCCCT
ACACCGCCTGCGACCTGGCGCCCCCCGCCGGCACCACCGACGCCGCGCACCCGGGTAAGCTTGACTACAAAGATG
ACGATGATAAACTTAAGACCCTAGCCCCAAACAGCTGTCCAGACAAACACTACTGGACTGGGGGAGGACTCTGCT
GCCGGATGTGTGAGCCAGGTACATTCTTTGTGAAGGACTGTGAACAAGACAGAACAGCTGCTCAGTGTGATCCCT
GTATACCAGGCACCTCCTTCTCTCCAGACTACCACACCCGGCCCCACTGCGAGAGCTGCAGGCATTGTAACTCTG
GTTTTCTTATCCGCAACTGCACAGTCACTGCCAATGCTGAGTGCAGCTGTTCCAAGAACTGGCAGTGCAGGGACC
AGGAATGTACAGAGTGTGACCCTCCTCTAAACCCTGCACTGACCAGACAGCCATCTGAGACCCCGAGCCCACAGC
CACCACCCACCCACTTACCTCATGGCACAGAGAAGCCATCCTGGCCCCTACACAGGCAGCTTCCCAACTCGACTG
TCTATAGCCAGCGGTCATCCCATAGACCCCTGTGCAGCTCGGACTGCATCCGGATCTTTGTGACCTTCTCCAGCA
TGTTTCTTATCTTCGTCCTGGGTGCAATCTTGTTCTTCCATCAAAGAAGAAACCACGGGCCAAATGAAGACCGGC
AGGCAGTGCCTGAAGAGCCTTGTCCTTACAGCTGCCCCAGGGAAGAGGAGGGCAGTGCTATCCCTATCCAGGAGG
ACTACCGGAAACCCGAGCCTGCTTTCTACCCTGCGGCCGCACATCATCATCATCATCATTGAGATATCGTTTAAA
CCCGCTGATCAGCCTCGACTGTGCCTTCTAGTTGCCAGCCATCTGTTGTTTGCCCCTCCCCCGTGCCTTCCTTGA
CCCTGGAAGGTGCCACTCCCACTGTCCTTTCCTAATAAAATGAGGAAATTGCATCGCATTGTCTGAGTAGGTGTC
ATTCTATTCTGGGGGGTGGGGTGGGGCAGGACAGCAAGGGGGAGGATTGGGAAGACAATAGCAGGCATGCTGGGG
ATGCGGTGGGCTCTATGGCTTCTGAGGCGGAAAGAACCAGCTGGGGCTCTAGGGGGTATCCCCACGCGCCCTGTA
GCGGCGCATTAAGCGCGGCGGGTGTGGTGGTTACGCGCAGCGTGACCGCTACACTTGCCAGCGCCCTAGCGCCCG
CTCCTTTCGCTTTCTTCCCTTCCTTTCTCGCCACGTTCGCCGGCTTTCCCCGTCAAGCTCTAAATCGGGGGCTCC
CTTTAGGGTTCCGATTTAGTGCTTTACGGCACCTCGACCCCAAAAAACTTGATTAGGGTGATGGTTCACGTAGTG
GGCCATCGCCCTGATAGACGGTTTTTCGCCCTTTGACGTTGGAGTCCACGTTCTTTAATAGTGGACTCTTGTTCC
AAACTGGAACAACACTCAACCCTATCTCGGTCTATTCTTTTGATTTATAAGGGATTTTGCCGATTTCGGCCTATT
GGTTAAAAAATGAGCTGATTTAACAAAAATTTAACGCGAATTAATTCTGTGGAATGTGTGTCAGTTAGGGTGTGG
AAAGTCCCCAGGCTCCCCAGCAGGCAGAAGTATGCAAAGCATGCATCTCAATTAGTCAGCAACCAGGTGTGGAAA
GTCCCCAGGCTCCCCAGCAGGCAGAAGTATGCAAAGCATGCATCTCAATTAGTCAGCAACCATAGTCCCGCCCCT
AACTCCGCCCATCCCGCCCCTAACTCCGCCCAGTTCCGCCCATTCTCCGCCCCATGGCTGACTAATTTTTTTTAT
TTATGCAGAGGCCGAGGCCGCCTCTGCCTCTGAGCTATTCCAGAAGTAGTGAGGAGGCTTTTTTGGAGGCCTAGG
CTTTTGCAAAAAGCTCCCGGGAGCTTGTATATCCATTTTCGGATCTGATCAAGAGACAGGATGAGGATCGTTTCG

CATGATTGAACAAGATGGATTGCACGCAGGTTCTCCGGCCGCTTGGGTGGAGAGGCTATTCGGCTATGACTGGGC
ACAACAGACAATCGGCTGCTCTGATGCCGCCGTGTTCCGGCTGTCAGCGCAGGGGCGCCCGGTTCTTTTTGTCAA
GACCGACCTGTCCGGTGCCCTGAATGAACTGCAGGACGAGGCAGCGCGGCTATCGTGGCTGGCCACGACGGGCGT
TCCTTGCGCAGCTGTGCTCGACGTTGTCACTGAAGCGGGAAGGGACTGGCTGCTATTGGGCGAAGTGCCGGGGCA
GGATCTCCTGTCATCTCACCTTGCTCCTGCCGAGAAAGTATCCATCATGGCTGATGCAATGCGGCGGCTGCATAC
GCTTGATCCGGCTACCTGCCCATTCGACCACCAAGCGAAACATCGCATCGAGCGAGCACGTACTCGGATGGAAGC
CGGTCTTGTCGATCAGGATGATCTGGACGAAGAGCATCAGGGGCTCGCGCCAGCCGAACTGTTCGCCAGGCTCAA
GGCGCGCATGCCCGACGGCGAGGATCTCGTCGTGACCCATGGCGATGCCTGCTTGCCGAATATCATGGTGGAAAA
TGGCCGCTTTTCTGGATTCATCGACTGTGGCCGGCTGGGTGTGGCGGACCGCTATCAGGACATAGCGTTGGCTAC
CCGTGATATTGCTGAAGAGCTTGGCGGCGAATGGGCTGACCGCTTCCTCGTGCTTTACGGTATCGCCGCTCCCGA
TTCGCAGCGCATCGCCTTCTATCGCCTTCTTGACGAGTTCTTCTGAGCGGGACTCTGGGGTTCGAAATGACCGAC
CAAGCGACGCCCAACC

Coloured in green: AP-site, red: Flag-tag, blue: CD27, pink: His-tag and black: pcDNA3.1.

9.3 Sequence of inserted Exon 11a in ADAM17$^{ex/ex}$ mice

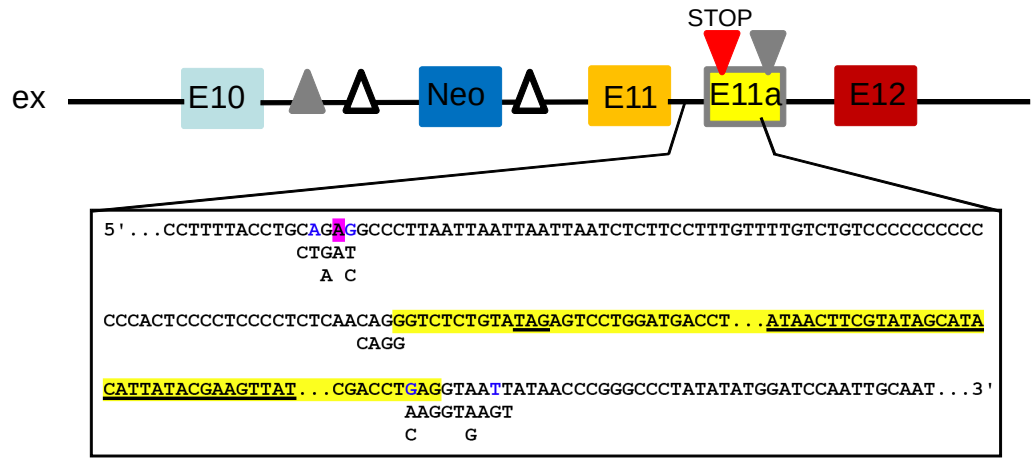

Fig. 9-2: Sequence of inserted Exon11a into ADAM17 gene. The artificial exon (highlighted in yellow) containing the stop codon is flanked by non-canonical plice donor and acceptor site.

9.4 Publications

- Adam N, Rabe B, Suthaus J, Grötzinger J, Rose-John S, Scheller J. Unraveling viral Interleukin-6 binding to gp130 and activation of STAT-signaling pathways independently of the Interleukin-6 receptor, J Virol 2009, 83 (10): 5117-26.
- Koch M, May U, Kuhns S, Drechsler H, Adam N, Hattermann N, Wirtz S, Rose-John S, Scheller J. Interleukin 27 induces differentiation of neural C6-precursor cells into astrocytes, Biochem Biophys Res. Commun 2007, 364 (3): 483-7.

- Chalaris A, Adam N, Sina C, Rosenstiel P, Lehmann-Koch J, Schirmacher P, Hartmann D, Cichy J, Gavrilova O, Schreiber S, Jostock T, Matthews V, Häsler R, Becker C, Neurath M, Reiß K, Saftig P, Scheller J, Rose-John S. Critical Role of the Disintegrin Metalloprotease ADAM17 for Intestinal Inflammation and Regeneration in Mice, JExMed, accepted.

10 Acknowledgement

Die vorliegende Doktorarbeit habe ich in der Zeit von September 2007 bis Juni 2010 in der Arbeitsgruppe von Prof. Dr. Stefan Rose-John sowie Prof. Dr. Jürgen Scheller absolviert. Beiden möchte ich für die Bereitstellung des spannenden Themas sowie für die Unterstützung während dieser Zeit danken.

Ebenso möchte ich Herrn PD Dr. Konstantin Khalturin recht herzlich danken für sein Interesse an meiner Arbeit sowie seiner Bereitschaft, das Korreferat zu übernehmen.

Weiterhin danke ich Olga Gavrilova und Christian Sina für die Hilfe in den Anfängen der DSS-Colitis sowie für die Durchführung des Koloskopierens. Ein weiterer Dank geht an Athena Chalaris für die gute Zusammenarbeit mit den ADAM17-Mäusen.

Ein besonderer Dank geht an meine engsten Mitstreiter Antje Schütt und Sven Malchow sowie meiner Lieblings-TA Steffi für die vielen lustigen, diskussionsreichen, hilfsbereiten und aufmunternden Zeiten im Labor sowie im Büro. Ohne Euch wäre die Zeit nur halb so schnell vorbeigegangen. Weiterhin danke ich Doreen Floss für die Unterstützung im Labor sowie auf unzähligen Laufstrecken in und um Kiel.

Thies Reick möchte ich für die sehr gute technische Unterstützung im Labor danken.

Der gesamten restlichen Laborcrew danke ich für die nette Arbeitsatmosphäre und Hilfsbereitschaft.

Danke Mama und Papa für die Unterstützung in allen Lebenslagen. Ihr seid immer für mich da! Ich liebe Euch.

Der größte Dank geht jedoch an Dich, lieber Felix. Vielen Dank für deine Unterstützung in den letzten Jahren. Du warst immer für mich da und hast mich in schlechten Zeiten wieder aufgebaut. Danke, für die Korrektur meiner Arbeit, die konstruktive Kritik sowie die unendliche Geduld mit mir ☺. Ich freue mich auf unsere weitere gemeinsame Zeit. Ich liebe dich sehr.

11 Erklärung

Hiermit erkläre ich, dass ich die vorliegende Dissertation nach den Regeln guter wissenschaftlicher Praxis eigenständig verfasst und keine anderen als die angegebenen Hilfsmittel und Quellen benutzt habe. Dabei habe ich keine Hilfe, außer der wissenschaftlichen Beratung durch meinen Doktorvater Prof. Dr. Stefan Rose-John in Anspruch genommen. Des Weiteren erkläre ich, dass ich noch keinen Promotionsversuch unternommen habe.

Kiel, den

_____

Nina Adam